4-2015

OPTIMIZATION OF A COMBINED APPROACH FOR THE TREATMENT OF DESALINATION REJECT BRINE AND CAPTURE OF CO_2

Ameera Fares Mohammad

United Arab Emirates University

College of Engineering

Department of Chemical and Petroleum Engineering

OPTIMIZATION OF A COMBINED APPROACH FOR THE TREATMENT OF DESALINATION REJECT BRINE AND CAPTURE OF CO_2

Ameera Fares Mohammad

This thesis is submitted in partial fulfillment of the requirements for the degree of Master of Science in Chemical Engineering

Under the Supervision of Professor Muftah Hassan El-Naas

April 2015

Declaration of Original Work

I, Ameera Fares Rasheed Mohammad, the undersigned, a graduate student at the United Arab Emirates University (UAEU) and the author of the thesis entitled "*Optimization of a combined approach for the treatment of desalination reject brine and capture of CO_2*", hereby, solemnly declare that this thesis is an original research work has been done and prepared by me under the supervision of Professor Muftah Hassan El-Naas, in the College of Engineering at UAEU. This work has not been previously formed as the basis for the award of any degree, diploma or similar title at this or any other university. The materials borrowed from other sources and included in my thesis have been properly cited and acknowledged.

Student's Signature_____ Date _____

Approval of the Master Thesis

This Master Thesis is approved by the following Examining Committee Members:

1) Advisor: Professor Muftah Hassan El-Naas

   Title: Professor

   Department of Chemical and Petroleum Engineering

   College of Engineering, UAE University

   Signature _____ Date _____

2) Member: Dr. Naeema Ibrahim Aldarmaki

   Title: Assistant Professor

   Department of Chemical and Petroleum Engineering

   College of Engineering, UAE University

   Signature _____ Date _____

3) Member (External Examiner): Professor J. Paul Chen

   Title: Professor

   Department of Civil and Environmental Engineering

   College of Engineering, National University of Singapore (NUS)

   Signature _____ Date _____

This Master Thesis is accepted by:

Dean of the College of Engineering: Professor Mohsen Sherif

Signature _____ Date _____

Dean of the College of Graduate Studies: Professor Nagi T. Wakim

Signature _____ Date _____

Copy ____ of ____

Abstract

Carbon dioxide (CO_2) is the most widespread greenhouse gas that traps heat and raises the global temperature, contributing to climate change. Existing techniques to sequester carbon dioxide have numerous environmental concerns and usually require extensive amount of energy. New technologies and methods, such as reactions with desalination reject brine according to the Solvay process, offer a new hope for the reduction of carbon dioxide concentration in the atmosphere. Brine management is another environmental concern, as many desalination plants need to find suitable approaches for the treatment or disposal of the large amounts of concentrated brine, resulting from the desalination processes. Many conventional methods are used such as disposal through deep well injection, land disposal and evaporation ponds. However these methods still suffer from many drawbacks. An alternative approach is to further process the brine to extract all the salts through reactions with carbon dioxide. This has the advantages of being environmental friendly and can produce valuable carbonate chemicals.

The present work evaluates the Solvay process where carbon dioxide is passed into ammoniated brine and reacts with sodium chloride to form a precipitate of sodium bicarbonate and a soluble ammonium chloride. The process has the dual benefit of decreasing sodium concentration in the reject brine and reducing carbon dioxide emissions to the atmosphere. Process parameters were studied in a semi-batch reactor to determine their effect on CO_2 capture efficiency and ions removal. These parameters included: ammonia to sodium chloride molar ratio, reaction time, temperature, gas flow rate, and pressure. Since ammonium bicarbonate is another

important intermediate in the formation of sodium bicarbonate, its effect on ions removal was evaluated. The optimum conditions for maximum CO_2 capture efficiency and ions removal have been determined using response surface methodology (RSM). In addition, continuous Solvay process has been studied at different liquid residence time. The optimum conditions for continuous Solvay process have also been evaluated for long experimental runs. In the semi-batch mode, the highest sodium removal of 33.0 % and the best CO_2 capture of 86.2 % were obtained under specific conditions. The optimum CO_2 capture efficiency and ions removal was found to be at temperature of 19.3^oC, gas flow rate of 1.544 L/min, and 3.3NH_3:1NaCl molar ratio. In the continuous Solvay process maximum ions removal were found at gas and liquid flow rates of 1.544 L/min and 12.5 ml/min, respectively, with a gas-to-liquid ratio of 123, and the reaction reached the steady state after 240 min; the CO_2 capture efficiency in 480 min was equal to 97.9% and maximum sodium removal was 32.5%. These results indicated the technical feasibility of the Solvay approach for the capture of CO_2 and management of desalination reject brine.

Keywords: Desalination reject brine, CO_2 capture, sodium bicarbonate, sodium removal, Solvay process.

Title and Abstract (in Arabic)

تقييم طريقة مبتكرة لتحلية المياه بالتفاعل مع ثاني أكسيد الكربون

الملخص

يعتبر غاز ثاني أكسيد الكربون (CO_2) من أكثر الغازات الدفيئة (Greenhouse Gases) تأثيرا على ارتفاع دراجات الحرارة و التغيرات المناخية .تعتبر الطرق الحالية المستخدة لحبس غاز ثاني أكسيد الكربون (CO_2 Sequester) ذات عواقب بيئية كبيرة بالإضافة لحاجتها إلى مقدار هائل من الطاقة مما ادى الى البحث عن طرق مبتكرة لحصر ثاني أكسيد الكربون عن طريق التفاعل مع المياة المالحة المطروحة (Reject Brine) من وحدات تحلية المياه إعتمادا على طريقة سولفاي (Solvay Process) والتي تعتبر من الطرق الواعدة في تقليل تركيز غاز ثاني اكسيد الكربون في الغلاف الجوي.

تشكل معالجة المياه المالحة المطروحة من وحدات تحلية المياه تحدياً بيئيا مهما , حيث تحتاج وحدات تحلية المياه لطرق مناسبة لمعالجة أو حتى طرح كميات المياه الهائلة ذات تركيز الملح العالي جداً. هناك العديد من الطرق التقليدية لمعالجة المياة المالحة مثل الحقن المباشر في الأبار(Well Injection) أو التخلص منها مباشرة عن طريق ضخها على مساحات واسعة من الأراضي (Land Disposal) أو بواسطة برك التبخير(Evaporation Ponds). ولكن هذه الطرق ما زالت تعاني من العديد من الصعوبات. وتتم الطريقة البديلة المستخدمة للإستخلاص الأملاح من هذه المياه عبر تفاعلها مع غاز ثاني أكسيد الكربون. حيث تعتبر هذه الطريقة صديقة للبيئة بالإضافة الى أنها تنتج مادة كيميائية (كربونات الصوديوم) يمكن الاستفادة منها في كثير من التطبيقات الصناعية .

الهدف من هذه الأطروحة هو تقييم عملية مبتكرة مستوحاه من عملية سولفاي والتي يتم من خلالها تمرير غاز ثاني أكسيد الكربون خلال محلول ملحي مضاف إليه الأمونيا، حيث يتفاعل كلوريد الصوديوم ليشكل راسب من بايكربونات الصوديوم و كلوريد الأمونيوم الذائب.

و تتميزهذه العملية بفائدتان وهما تقليل تركيز الصوديوم في المياه المالحة المطروحة من وحدات تحلية المياه وتقليل إنبعاث غاز ثاني اكسيد الكربون الى الغلاف الجوي. كما تتناول الاطروحة دراسة المتغيرات التي تؤثر على فعالية حصر غاز ثاني اكسيد الكربون و تقليل

تركيز الاملاح في مفاعل شبه دفعة واحدة (Semi-batch Reactor). المتغيرات التي تمت دراستها هي كالتالي : النسبة الكمية (Molar Ratio) بين الأمونيا وكلوريد الصوديوم، زمن التفاعل، درجة الحرارة، معدل تدفق الغاز، والضغط داخل المفاعل. وبما أن بيكربونات الأمونيوم تعتبر عامل وسيط مهم في إنتاج بيكربونات الصوديوم، فقد تم أيضا دراسة تاثيرها خلال العملية.

أهم نتائج هذه الدراسة تحديد الظروف الأمثل اللازمة للحصول على أعلى فعالية لحصر غاز ثاني أكسيد الكربون وتقليل تركيز الاملاح بواسطة إستخدام طريقة إستجابة السطح (Response Surface Methodology). بالإضافة إلى ذلك تمت دراسة العملية المستمرة (Continuous Process)عند معدلات تدفق سائل مختلفة. وتم تحديد الظروف الأمثل (Optimum Conditions) للعملية المستمرة بإجراء تجارب لفترة زمنية طويلة. و قد تم الحصول على أعلى إزالة للصويوديوم بنسبة % 33.0 وأفضل فعالية حصر لغاز ثاني أكسيد الكربون بنسبة % 86.2 عند درجة حرارة 19.3 مئوية، ومعدل تدفق غاز 1.544 ليتر لكل دقيقة، ونسبة كمية 3.3 أمونيا لكل 1 من كلوريد الصوديوم. وفي العملية المستمرة كانت أعلى نسبة لازالة الأملاح عند معدل تدفق سائل 12.5 مليميتر لكل دقيقة ومعدل تدفق غاز 1.544 ليتر لكل دقيقة بنسبة معدل تدفق غاز لسائل مساوية 123. حيث وصل التفاعل إلى حالة الإستقرار بعد 240 دقيقة تقريباً وكانت فعالية حصر غاز ثاني أكسيد الكربون في 480 دقيقة تساوي 97.9%. النتائج تشير إلى إمكانية إستخدام طريقة سولفاي لحصر غاز ثاني أكسيد الكربون وتحلية المياه المالحة.

أدلة البحث: تحلية المياه، ثاني أكسيد الكربون، بايكربونات الصوديوم، تفاعلات سولفاي.

Acknowledgments

Sincere thanks are expressed to my advisor Prof. Muftah El-Naas for his guidance, support and constructive feedback throughout my thesis study. I am grateful for the time he has taken to guide and support me.

My thanks extended to my husband who helped me along the way. Also, special thanks are extended to all members of the Chemical and Petroleum Engineering Department at the UAE University for assisting me during my studies and research.

Finally, I would like to acknowledge the financial support provided by Takreer research center as part of the TRC Project. I would also like to thank Dr.Kilani Ghoudi, Dr. Hussain Awad, Eng. Sami Abdulla, Eng. Filx Labata, Eng. Abudl Salam Anvarand and Eng. Essa Lwisa for their help and support.

Dedication

This thesis is dedicated to my husband, Othman Dar Saleh, who supported me all the way since I began my postgraduate study. I would like to extend this dedication to my thesis advisor whose motivation and encouragement was a great source of knowledge and experience.

Table of Contents

List of Tables

List of Figures

List of Abbreviations

AMP	2-amino-2-methylpropan-1-ol
BOD	Biochemical oxygen demand (mg/L)
CCD	Central composite design
CI	Confidence interval
DEA	Diethanolamine
DoE	Design of experiments
Exp.	Experimental result value
EOR	Enhanced oil recovery
F	Gas flow rate (L/min)
ID	Internal diameter (mm)
Kw	Ionic product for water
M	Ammonia to sodium chloride molar ratio
MDEA	N-mehyldiethanolamine
MEA	Mono ethanol amine
MED	Multiple-effect distillation
MSF	multi-stage flash distillation
OD	Outer diameter (mm)
P	Pressure (bar, kPa)
Pred.	Predicted result value
PZ	Piperazine
PTSA	Pressure and temperature swing adsorption

R	Gas constant L.kPa/(K.mole)
R^2	Determination coefficient
RO	Reverse osmosis
RSM	Response surface methodology
SSR	Stainless steel reactor
T	Temperature (^oC, K)
t	Time in minutes
VCD	Vapor compression distillation
v/v	Volume to volume ratio
w/w	Weight to weigh ratio
X_f	Final ions concentration in treated brine
X_i	Initial ions concentration in treated brine

Chapter 1: Introduction

1.1. Problem Statement

Carbon dioxide is the most widespread greenhouse gas that traps heat and raises the global temperature, contributing to climate change. There are various sources of carbon dioxide emissions, which are mainly dominated by power plants. Existing techniques to sequester carbon dioxide are ocean fertilization, mineral carbonation, forestation, underground injection, and direct ocean disposal (Huijgen et al., 2007). However there are environmental concerns, regarding the consequences of storing carbon dioxide in the ocean and in the geological formation as well as the extensive energy required. Proper use of carbon dioxide for chemical processing can add value to the carbon dioxide gas disposal by making industrially useful carbon-based products. New technologies and methods, which involve the use of the carbon dioxide in the production of carbonate materials, offer a new way to reduce the carbon dioxide concentration in the atmosphere.

Reject brine management is another environmental challenge that faces most societies, especially those depending on desalination for potable water. Desalination plants often try to find cost-effective and practical methods for reject brine disposal and, at the same time, try to comply with environmental regulations. Regulatory authorities usually do not allow direct disposal of reject brine if the concentrations of contaminants and primarily metals exceed concentration-based discharge limits (Fahim et al., 2010). Conventional methods for brine management are disposal through deep well injection, land disposal, evaporation ponds, and mechanical/thermal evaporation (El-Naas et al., 2010). In spite of their high

evaporation efficiency due high temperatures, evaporation ponds suffer from many drawbacks including the need for huge areas and the possibility of contaminant leakage into soil and groundwater (El-Naas et al., 2010). An alternative approach is to further process the brine to extract all the salts through reactions with carbon dioxide. The present work evaluates a combined approach based on the Solvay process, where carbon dioxide is passed into ammoniated brine and reacts with sodium chloride to form a precipitate of sodium bicarbonate and a soluble ammonium chloride. The process been has the dual benefit of decreasing sodium ions in the reject brine and reducing carbon dioxide emissions to the atmosphere.

1.2. Research Objectives

The main objective of this research is to optimize the desalination of the reject brine and CO_2 capture based on the Solvay process by performing the following steps:

First: Study the effect of the reaction parameters on CO_2 capture efficiency and ions removal. These parameters include: ammonia to sodium chloride molar ratio, reaction time, temperature, gas flow rate, pressure and ammonium bicarbonate to treated brine w/w percentage.

Second: Determine the optimum condition for maximum CO_2 capture efficiency and ions removal using response surface method.

Third: Conduct the continuous experiments based on the Solvay process at different liquid residence times.

Fourth: Evaluate the optimum conditions for continuous Solvay process for long experimental runs.

1.3. Organization of the Thesis

This thesis consists of six chapters. Chapter 1 includes introduction, problem statement, and research objectives. Chapter 2 presents a general review of the literature related to the study. Chapter 3 includes thermodynamic analysis for the Solvay process. Chapter 4 explains the experimental methodology followed in this study. Chapter 5 presents detailed discussion of the experimental results. Chapter 6 outlines the main conclusions drawn from the study.

Chapter 2: Literature Review

2.1. Carbon Dioxide (CO_2) Capture

Global warming is considered as one of the most serious environmental problems facing industrial societies nowadays (Bennaceur, 2014). The major cause for global warming is the emission of greenhouse gases, such as carbon dioxide, nitrous oxide and methane, into the atmosphere. Carbon dioxide (CO_2) is the largest contributor of global warming effect, in regards to its amount presence in the atmosphere which is about 60% (Hashimoto et al., 1999). In fact, the increase in the average earth surface temperature is related to the amount of carbon dioxide in the atmosphere. Approximately half of the extra carbon dioxide released to the atmosphere will dissolve in the oceans and increase the acidity which is very dangerous to the aquatic life (Carroll et al.,2013). There are several different sources of CO_2 emissions, predominately from the combustion of fossil fuels in power generation, industrial facilities, buildings and transportation (Calvo and Domingo et al ., 2014). One of the common techniques used for CO_2 capture is carbonate looping (Abanades, 2013), where the flue gas containing CO_2 is made in contact with solid material able to capture CO_2, followed by releasing the CO_2 by decarbonation at elevated temperature. The absorption of CO_2 into reactive solvents is one of the most promising technologies for capturing CO_2, because of its maturity, cost effectiveness, and capability of handling large amounts of exhaust stream (Sipöcz et al., 2013). The effective reactive solvents have high mass transfer performance, high absorption capacity, fast reaction kinetics, low degradation rate, low corrosiveness and low energy consumption for regeneration (Sema et al., 2012). Many countries have

agreed to mitigate the global warming and climate change problems by decreasing CO_2 emission by 50% in 2050. With this goal in mind, the rise of earth surface temperature will be limited at 2 °C or below. In order to accomplish this goal, the CO_2 emissions need to be reduced by at least 25% before 2020 (den Elzen et al., 2007). The CO_2 capture from fossil-fueled power plants is a potential method for controlling greenhouse gas emissions, where fossil-fueled power plants are producing about 40% of total CO_2 emissions (Holtz-Eakin and Selden, 1995). Currently, there are four major technical methods to capture CO_2 from fossil fuel power plants, including pre-combustion (Li et al., 2009), post-combustion (Chen et al., 2012; Hedin et al., 2013; Plaza et al., 2012; Song et al., 2012), oxy-fuel (Hu et al., 2012; Li et al., 2009), and chemical looping combustion (Hossain and de Lasa, 2008). All these CO_2 capture methods have drawbacks that reduce their large-scale industrial application (Kunze and Spliethoff, 2012), such method is post combustion CO_2 capture, which currently used in new fossil fuel burning power plants (Bryngelsson and Westermark, 2009). Post-combustion CO_2 capture can be divided into three categories: physical, chemical and biochemical methods. The physical method includes physical absorption, cryogenic condensation and membrane separation technology (Al-Marzouqi et al., 2008), while the chemical method includes chemical adsorption, chemical absorption and chemical looping combustion (Mattisson et al., 2001). The biological method contains the biological fixation by terrestrial vegetation and marine or freshwater microalgae (Ho et al., 2011) . Some of the possible approaches for post-combustion CO_2 capture are described in the following sections.

2.1.1. MEA scrubbing process

One of the most effective technologies for CO_2 capture is the scrubbing by reactive solvents because of its cost effectiveness and ability of handling large amounts of exhaust gas (Kohl and Nielsen, 1997). The most mature technology for the CO_2 post combustion is the amine-based absorption due to its high affinity to CO_2 (Adeosun and Abu-Zahra, 2013; Dave et al., 2009; King et al., 2011; Tarun et al., 2007). Modeling and simulation for these technologies have been carried out and several models already exist (Jayarathna et al., 2011). The MEA process is a chemical absorption process where carbon dioxide is captured from flue gases of the combustion process by using mono ethanol amine (MEA) as solvent. The MEA solutions come into contact with the flue gases and mix together in the absorber. The carbon dioxide and MEA solution is then sent to a stripper where it is reheated to release carbon dioxide. The MEA solution is then recycled to the absorber (Herzog and Golomb, 2004). Another aqueous amine solution can be used such as: diethanolamine (DEA), N-mehyldiethanolamine (MDEA), piperazine (PZ) (Liu et al., 2012), 2-amino-2-methylpropan-1-ol (AMP) (Gaspar and Cormos, 2012), or their mixtures. From the view of absorption, MEA is the most efficient solvent; where the alkanolamines performance decrease according to their reaction rate constants (MEA >AMP>DEA>MDEA) (Gaspar and Cormos, 2012). But in the case of thermodynamic limitations, AMP is the most effective solvent due to the high CO_2 solubility in its solution (Gaspar and Cormos, 2012). However, the operating cost of absorption processes using MEA is high due to its high energy consumption in regenerating and operation problems such as: corrosion, solvent loss, and solvent degradation (Afkhamipour and Mofarahi, 2014). In addition, MEA can only be loaded up to about 0.5 mol of CO_2/mol of MEA due to the stable carbamates formed;

therefore, in order to decrease the energy consumption, many researchers adopt the secondary amines, tertiary amines, hindered amines and their mixed amines as the substituted solvents. But even this does not solve the problems of the MEA process completely. Some of less energy efficient technologies that are considered to be uneconomical are membrane separation, cryogenic fractionation and adsorption using molecular sieves (Herzog and Golomb, 2004).

2.1.2. Membrane technology

Membrane technology is considered as applicable technology for selected gas separation processes such as natural gas sweetening, air separation, and hydrogen production (Brunetti et al., 2010). Some types of membrane materials used for CO_2 separation are: microporous organic polymers (Budd et al., 2005), fixed-site-carrier membranes (Qiao et al., 2015), mixed matrix membranes (Shao et al., 2009), carbon molecular sieve membranes (Singh and Koros, 2013) and inorganic membranes (Krishna and van Baten, 2010). A suitable membrane material can be selected according to the feed gas compositions, process conditions and separation requirements. For CO_2 capture from flue gas, high selectivity and high CO_2 permeance will be needed to have an effective separation process. In order to make membranes commercially viable and compete with amine absorption, the required high performance membranes should be tolerant to SO_2, NOx and other impurities which present in flue gas, have long lifetime and long-term stability (He et al., 2015). The benefits of the membrane technology are reducing the installed and operating costs (Stewart and Hessami, 2005).

2.1.3. Molecular sieve

Gel filtration or size exclusion chromatography is a specially-designed sieve that separates molecules based on their molecular weight or molecular size (Meier,

1984). The Oak Ridge National Laboratory developed an adsorbent carbon monolith named ‘‘a carbon fiber composite molecular sieve’’. Several demonstrations of separations have been performed, such as: the separation of CO_2 from CH_4, CO_2 from air and CO_2, CO, H_2S and H_2O from a mixture of gases. The main advantages of this type of separation are cost effectiveness, minimum waste production and the adaptability to many carbon capture processes. Open sieve structure allows fluid to flow freely through the material (Burchell and Judkins, 1996).

2.1.4. Desiccant adsorption

Ishibashi et al. (Ishibashi et al., 1996) described a process referred to as “ pressure and temperature swing adsorption” (PTSA) that can be applied to electric power plant flue gas. By using zeolite as desiccant, carbon dioxide can be adsorbed at near ambient pressure condition. The process starts by heating the adsorbent then the carbon dioxide regenerated under depressurization and temperature in range of 50 – 100 ^{o}C. One of the drawbacks for this process is the desiccant reaction with SO_X in the flue gas; however high removal efficiency and 90 – 95 % purity of CO_2 have been achieved by using alumina as the desiccant and 3% reduction in power consumption by recycling the desorbed gas back to the process (Ishibashi et al., 1996).

2.1.5. Disposal options by direct injection

In this process the gas is pumped into a sink capable of holding many mega-tones of gas over a period of time. There have been two major injection options identified: injection into the ocean and injection into geologic reservoirs (Herzog et al., 2001; Rai et al., 2013).

2.1.5.1. Oceanic injection

Around 80% of anthropogenic emissions of carbon dioxide will be absorbed by the ocean over a period of 100 years by direct injection (Bryngelsson and Westermark, 2009). However, around 15–20% of the carbon dioxide injected into the ocean will leak back into the atmosphere over hundreds of years (El-Naas et al., 2010). In addition, direct carbon dioxide injection does have environmental concerns due the decrease of pH level of the surrounding areas, which could affect marine organisms at depths of 1000 meter or even more (Bryngelsson and Westermark, 2009).

2.1.5.2. Geologic injection

Geologic injection is more efficient than oceanic injection, where the expected residence times in geologic injection are thousands of years comparing to that of oceanic injection of only hundreds of years. In the case of reaction between carbon dioxide and underground metal, more residence times could be achieved (Herzog and Golomb, 2004). The consideration of carbon credits should be made on the retention ability of the geologic reservoir and the amount of carbon dioxide that leaks into the atmosphere according to the relation of the amount sequestered in the geologic structure and the actual remaining quantity (Herzog et al., 2001). Enhanced oil recovery and coal seams are two forms of Geologic injection:

(a) Enhanced Oil Recovery (EOR).

By injecting carbon dioxide into an oil reservoir, the gas becomes miscible with the oil and pushes the oil through the rock reservoir and out of the wells. As the carbon dioxide is pushed out with the oil, it is recaptured and re-injected until no more oil could be extracted (Rai et al., 2013). The drawback of enhanced oil

recovery process (EOR) is the high cost of the CO_2 removal which requires large amounts of energy (Gelowitz et al., 1995).

(b) Coal seams.

In this process, carbon dioxide diffuses through the pore structure of coal and is physically adsorbed (Shu et al., 2009). Coal seams often contain large amounts of methane, where by extraction it could be a value added in the process. Carbon dioxide used instead of water to flood the coal seams, due to the higher potential for recovering the methane and higher carbon dioxide capture. Beecy et al (Beecy and Klara, 2003) reported that the "Worldwide storage capabilities for carbon dioxide in the deep coal beds are estimated to be up to 150 Gt". However further research is needed to optimize the process (Shu et al., 2009).

2.1.6. Aqueous ammonia solution

Aqueous ammonia solution considered as a promising alternative solvent (Yeh et al., 2005). The Advantages of aqueous ammonia solution are low energy consumption for CO_2 regeneration, resistance to oxidation, high CO_2 loading capacity, no absorbent degradation, and potential of capturing multiple flue gas components (SO_2, NO_2, CO_2, HCl and HF). Many researchers have studied the CO_2 capture using aqueous ammonia solution, including reaction mechanism (Choi et al., 2012), kinetics (Qin et al., 2010), removal efficiency (Diao et al., 2004) and mass transfer coefficients (Zeng et al., 2013); however, research on the aqueous ammonia based capture process at lab and pilot plant scale is still at the initial stage. Several pilot plants have been constructed and operated to test ammonia based post-combustion CO_2 capture processes (Valenti et al., 2009). Carbon dioxide can be removed by ammonia because they may react at various temperatures and operation conditions. Ammonium carbonate (NH_2COONH_4) is the main product in the dry

condition under room temperature and a pressure of 1 atm according to the following reactions (Bai and Chin, 1997):

$$2NH_3 + CO_2\,(g) \leftrightarrow NH_2COONH_4(s) \quad (2.1.1)$$

$$NH_2COONH_4(s) + H_2O\,(g) \leftrightarrow (NH_4)_2CO_3(s) \quad (2.1.2)$$

Ammonia solution is very soluble in water, and therefore, under moist air, the hydration product of ammonium carbonate $(NH_4)_2CO_3$ is produced under room temperature (Bai and Chin, 1997). Since the concentration of CO_2 in flue gas is high which can be up to 16% (v/v), a large amount of ammonia gas is required to reduce the CO_2 emission. This may lead to concern over an explosion problem with the dry CO_2–NH_3 reaction in the case of improper design. Yong et al. (Diao et al., 2004) used the wet method of ammonia scrubbing, where aqueous ammonia is sprayed into flue gas to capture CO_2, producing high quality ammonium bicarbonate. The gas–liquid chemical reactions can be expressed by the following reaction equation (Lee and Li, 2003; Yeh and Bai, 1999; Zhuang et al., 2012):

$$NH_3\,(l) + CO_2\,(g) + H_2O\,(l) \leftrightarrow NH_4HCO_3(s) \quad (2.1.3)$$

However, the actual steps of the chemical reaction include several intermediate reaction steps as follows:

$$NH_3\,(g) + CO_2\,(g) \leftrightarrow NH_2COONH_4(s) \quad (2.1.4)$$

The product NH_2COONH_4 is further hydrolyzed:

$$NH_2COONH_4\,(s) + H_2O\,(l) \leftrightarrow NH_4HCO_3\,(s) + NH_3\,(g) \quad (2.1.5)$$

Then, the NH_3 reacts with H_2O to form NH_4OH:

$$NH_3\,(g) + H_2O\,(l) \leftrightarrow NH_4OH\,(l) \quad (2.1.6)$$

The hydrolyzed product NH_4HCO_3 of reaction (2.1.5) reacts with NH_4OH to form $(NH_4)_2CO_3$:

$NH_4HCO_3\,(g) + NH_4OH\,(l) \leftrightarrow (NH_4)_2CO_3\,(s) + H_2O\,(l)$ (2.1.7)

The CO_2 is absorbed by $(NH_4)_2CO_3$ to form ammonium bicarbonate:

$(NH_4)_2CO_3\,(s) + H_2O\,(l) + CO_2\,(g) \leftrightarrow 2NH_4HCO_3\,(g)$ (2.1.8)

All the above reactions are reversible (Diao et al., 2004). CO_2 capture by aqueous ammonia has become an important method for emission control of CO_2 from post-combustion flue gases, and is receiving more attention due to its advantages over other CO_2 capture methods (Zhao et al., 2012), as shown in Table 2.1.

However, the alkaline approaches for post-combustion CO_2 capture processes belong to the chemical separation methods which demand intensive energy use to break the chemical bonds between the absorbents and the absorbed CO_2 in the solvent regeneration step (Rao et al., 2006); therefore, it is essential to find alternative solvents that combine high affinity for CO_2 and ease of solvent regeneration and reuse (Ali et al.,2014).

Table 2.1: Advantages and disadvantages of different alkaline approaches for post-combustion CO_2 capture (Zhao et al., 2012).

Method	Benefits	Drawbacks
Strong alkaline metal solution (KOH, NaOH)	•Fast reaction rate • Large absorption capability • High absorption efficiency	•Cost of absorbent •Strong corrosion to equipment •Product treatment and disposal
Weak alkaline Aqueous ammonia (NH-H_2O)	•Large absorption capability and high loading capacity • Low energy requirement for absorbent regeneration • Resourcelized utilization of products as fertilizer • Wide distribution of absorbent	•Easy to volatilize and leak •Thermal instability of products •Corrosion to equipment
Aqueous ammines (MEA, DEA, MDEA and PZ)	•Less volatile •Good stability of absorbent •Enhancement role used as additive	• Resulting in system corrosion •High energy consumption for regeneration •Easy degradation by SO_2 and O_2 in flue gas.

2.2. Desalination

Potable water production has become a worldwide concern, as population growth and associated demand exceed conventional available water resources. Over 1 billion people have no access to clean drinking water and approximately 2.3 billion people (41% of the world population) live in regions with water shortages (Morillo et al., 2014). The shortage of water supplies for drinking and irrigation purposes is already a serious problem, and severe water shortages may occur in many countries of the European Union and the northern Mediterranean by 2020 (Le Dirach et al., 2005). Within the Middle East, the United Arab Emirates is suffering from water shortage due to the fast growing population, and the expansion of industrial and agricultural activities (Mohamed et al., 2005). Desalination has become an important source of drinking water production, with thermal desalination methods developing over the past 60 years and membrane methods developing over the past 40 years (Greenlee et al., 2009). The Middle East is the leader in large-scale seawater desalination. With only 2.9 % of the world's population, it holds around 50% of the world's production capacity (Sauvet-Goichon, 2007). Between 1999 and 2001, the production of the desalination water in the UAE has increased by 30%, due to the economic and demographic development (Mohamed et al., 2005). Two of the most commercially important technologies are: Reverse Osmosis (RO) and distillation. Distillation processes include multi-stage flash (MSF) distillation, Multiple-Effect Distillation and Vapor Compression Distillation.

2.2.1. Reverse osmosis

Reverse Osmosis (RO) is a non-thermal process that involves the application of higher external pressure to overcome the osmotic pressure of the seawater. The

process involve flowing of water in the opposite direction of flow across the membrane leaving the dissolved salts in behind. Reverse Osmosis requires no heating or phase separation, and energy is only required for pressurizing the seawater feed (Greenlee et al., 2009). A large scale Reverse Osmosis process consists of: feed water pre-treatment unit, high pressure pumping unit, membrane separation unit and permeate post-treatment unit. The Reverse Osmosis process start with flowing seawater through screens to remove waste, then the seawater is passed through filters for further cleaning; the high pressure pump increases the pressure of the pretreated feed water to the suitable pressure for the membrane, and the semipermeable membrane prevents the passage of dissolved salts while permitting water to pass through. Finally the concentrated brine is discharged off site (Sauvet-Goichon, 2007; Xia et al., 2014).

2.2.2. Multi-stage flash distillation

The multi-stage flash (MSF) distillation process depends on flash evaporation, where the seawater is evaporated by reducing the pressure (Khawaji et al., 2008). Regenerative heating achieved by flashing seawater in each flash stage gives up some of its heat to the seawater going through the flashing process. The heat of condensation released by the condensing vapor at each stage increase the temperature of the feed seawater. A typical MSF plant consists of heat input unit, heat recovery unit, and heat rejection sections. MSF plants have been used since the 1950s (Morillo et al., 2014). The largest MSF unit in the United Arab Emirates is the Shuweiat plant with a capacity of 75,700 m^3/day (Khawaji et al., 2008).

2.2.3. Multiple-effect distillation

The multiple-effect distillation (MED) process is the oldest desalination method and is very efficient thermodynamically (Sayyaadi et al., 2010). The MED

process takes place in a series of evaporators called effects or “stages”, and uses the principle of reducing the ambient pressure. This process permits the seawater feed to undergo multiple boiling without supplying additional heat after the first effect. The process of evaporation and condensation is repeated from stage to stage each at a successively lower pressure and temperature. This continues for several effects, with 4 to 21 effects and performance ratio from 10 to 18 being found in a typical large plant (Chacartegui et al., 2009).

2.2.4 .Vapor compression distillation (VCD).

The heat for evaporating the seawater in the VCD process comes from the compression of vapor. The VCD plants take advantage of the principle of reducing the boiling point temperature by reducing the pressure. VCD units have been built in a variety of configurations to promote the exchange of heat to evaporate the seawater. The VCD process is generally used for small-scale desalination units. They are usually built up to the range of 3000 m^3/day. The larger unit’s power consumption is about 8 kWh/m^3 of product water. VCD units are often used for resorts, industries, and drilling sites where fresh water is not readily available (Khawaji et al., 2008).

The limitations of the desalination method are the disposal costs of the concentrated brines produced and the impact of brine on the environment. The components of reject brine are inorganic salts, small quantities of corrosion products, anti-scale additives, and other reaction products. Improper land disposal of reject brine from desalination plants pollutes the groundwater and impact soil properties (Mohamed et al., 2005). High salt concentration in reject brine with high levels of sodium, chloride, and boron can reduce plants and soil productivity and cause soil salinization (Rhoades et al., 1997).

2.3. Brine Disposal Methods

In desalination process, two streams are produced: product water stream with high purity and brine or concentrate stream (Ahmad and Baddour, 2014). The management of brine from desalination plants can be significant problem in case they are placed far from the coast. Brine disposal method should be considered, after proper feed water pretreatment, proper desalination process, and maximizing the system recovery, to minimize the brine stream, and hence reduce the cost of subsequent disposal (Breunig et al., 2013; Mohamed et al., 2005). Some of the conventional options for brine disposal from inland desalination plants are described in the next sections.

2.3.1. Disposal to surface water bodies and sewers systems

The brine stream is diluted by mixing with the water body. However many consideration should be taken into account, such as the salinity of the receiving body which might increase due to the disposal of the high salinity brine (Ahmad and Baddour, 2014). Another option is to dispose the brine to the local sewage system. This option has many advantages such as lowering the BOD of the sewage water. However the salinity of sewage water might increase which might affect the wastewater treatment facility (Mohamed et al., 2005).

2.3.2. Disposal to evaporation ponds

In evaporation ponds, the brine is discharged into a large surface area pond, where the water is naturally evaporated. Use of evaporation pond technology is practiced primarily in the arid areas (Al-Faifi et al., 2010). Evaporation pond is probably the most widespread method for brine disposal from inland desalination plants. Simple evaporation ponds have many advantages such as being easy to construct, having low maintenance and operation cost, and requiring no mechanical

equipment , making it the most appropriate method, especially in arid areas with high evaporation rates, low rainfall, and low land cost (Ahmed et al., 2000; Al-Faifi et al., 2010). The basic concern associated with use of evaporation pond for brine disposal is leakage of the brine through soil. This may result in subsequent contamination and increasing salinity of the aquifer (Al-Faifi et al., 2010; Mohamed et al., 2005).

2.3.3. Deep well injection

In deep well injection, the brine is injected back underground to depth ranges from few hundreds of meters to thousands of meters. One of the very attractive options with deep well injection is to use depleted oil and gas fields for brine disposal (Nicot and Chowdhury, 2005). Many factors should be considered with deep well injection for brine disposal which can be summarized as follows: 1) Site selection, which is performed through many geological and hydrological studies, to identify the proper area for installing the well; 2) High cost, associated with both capital and operational cost; 3) Corrosion and subsequent leakage in the well casing; 4) Uncertainty of the well life; and 5) Pollution of groundwater resources (Muniz and Skehan, 1990).

2.3.4. Land applications of brine

Land applications such as irrigation systems can be used for brine disposal. Spray irrigation is especially attractive option. Concentrate can be applied to cropland or vegetation by sprinkling or surface techniques for water conservation when lawns, parks, or golf courses are irrigated. Crops such as water-tolerant grasses with low economic return but with high salinity tolerance are chosen for this type. However soil sanlinization and groundwater contamination should be carefully considered (Khaled Elsaid et al., 2012). Advantages and disadvantages of brine disposal methods are summarized in Table 2.2.

Table 2.2: Summary of brine disposal methods and their main disadvantages.

Brine disposal method	Description	Disadvantages
Deep well injection	Brine is injected into porous subsurface rock formations	Contamination of ground water
Land application	Brine is used for irrigation of salt-tolerant crops and grasses	Salinization of soil if the method is used on large scale production
Evaporation ponds	Brine is allowed to evaporate in ponds while the remaining salts accumulate in the base of the pond	High capital costs due to high land acquisition costs. Bad impact on environment such as contamination of underlying aquifers due to leakage issues
Zero liquid discharges	Brine concentrator can reduce brine to dry solid cakes which is easy to handle for disposal	High capital and operation costs.
Sewer discharge	Discharge of brine into an existing sewage collection system.	Reduce biological treatment processes performance in case of large quantity of brine
Seawater discharge Surface discharge	Brine is discharged on the surface of seawater. The most common method for all big desalination facilities worldwide	Marine pollution due to inappropriate dilution
Seawater discharge	Brine is discharged off shore through multiport diffusers installed on the bottom of the sea	Practical due to high dilution capabilities. Proper design of diffusers required to achieve high dilution

There is an urgent need to develop a new process for the management of desalination reject brine that can be used by desalination plants, since reject brine has not been utilized and the environmental effects associated have not been sufficiently considered. The chemical reaction of reject brine with carbon dioxide is believed to be a new effective, economic and environmental friendly approach (El-Naas et al., 2010). The chemical reactions are carried out based on Solvay process to convert the reject brine into useful and reusable solid product (sodium bicarbonate). At the same time, the treated water can be used for irrigation and other industrial applications. Another advantage is capturing CO_2 gas from the industrial exhaust or flue gases. El-Naas et al (2010) (El-Naas et al., 2010) reported that the reactions of CO_2 with

ammoniated brine can be optimized at 20 °C and can achieve good conversion using different forms of carbon dioxide.

2.4. Solvay Process

The Solvay process was named after Ernest Solvay who was the first to develop the process in 1881. It is initially developed for the manufacture of sodium carbonate, where a concentrated brine solution is reacted with ammonia and carbon dioxide to form soluble ammonium bicarbonate, which reacts with the sodium chloride to form soluble ammonium chloride and a precipitate of sodium bicarbonate according to the following reactions (El-Naas, 2011):

$$NaCl + NH_3 + CO_2 + H_2O \rightarrow NaHCO_3 + NH_4Cl \quad (2.4.1)$$

$$2NaHCO_3 \rightarrow Na_2CO_3 + CO_2 + H_2O \quad (2.4.2)$$

The resulting ammonium chloride can be reacted with calcium hydroxide to recover and recycle the ammonia according to the following reaction:

$$2NH_4Cl + Ca(OH)_2 \rightarrow CaCl_2 + 2NH_3 + 2H_2O \quad (2.4.3)$$

The overall reaction can be written as:

$$2NaCl + CaCO_3 \rightarrow Na_2CO_3 + CaCl_2 \quad (2.4.4)$$

The ammonia is not involved in the overall reaction of the Solvay process, but it plays an important role in the intermediate reactions, buffers the solution at a basic pH and increase the precipitation of sodium bicarbonate from the first reaction. The sodium bicarbonate ($NaHCO_3$) is the most important intermediate product in the Solvay process, where its solubility plays an important role in the success of the process. To achieve high conversion, the solubility of $NaHCO_3$ must be as low as

possible, so it is very important to optimize the factors that can limit or reduce its solubility (El-Naas, 2011). In industrial application, the first step is passing the ammonia gas through the concentrated brine to have the ammoniated brine, and then carbon dioxide is bubbled through the ammoniated brine to form sodium bicarbonate and ammonium chloride (El-Naas, 2011).

2.4.1. Ammonium bicarbonate effect in the Solvay process

El-Nass et al reported that ammonium bicarbonate has a major effect on the possibility of using in the Solvay process, since it is an important intermediate in the formation of sodium bicarbonate and can enhance the efficiency of desalinating the reject brine according to the following reactions (El-Naas, 2011).

$$2NaCl + CaCO_3 \rightarrow Na_2CO_3 + CaCl_2 \quad (2.4.5)$$

$$NH_4OH + CO_2 \rightarrow NH_4HCO_3 \quad (2.4.6)$$

Raising the concentration of ammonium bicarbonate and hence increasing the concentration of (HCO_3^-) would force the equilibrium in the reactions below to the left and thus lower the solubility of $NaHCO_3$.

$$NH_4HCO_3\ (a) \leftrightarrow NH_4^+ + HCO_3^- \quad (2.4.7)$$

$$NaHCO_3\ (a) \leftrightarrow Na^+ + HCO_3^- \quad (2.4.8)$$

For an aqueous solution containing 8% NaCl, the solubility of $NaHCO_3$ can be reduced to 0.0 g/100g with the addition of about 13wt % ammonium bicarbonate (El-Naas, 2011).

2.5. Response Surface Method

Response surface methodology (RSM) can be defined as the collection of mathematical and statistical techniques for experimental design and modeling. The aim of RSM is determining the optimum settings for process variables that result in a

maximum or minimum response over a definite region of interest through careful design of experiments (Khuri, 2003). This requires having a good fitting model that provides an acceptable representation of the mean response because such a model is to be utilized to determine the value of the optimum. An important aspect of RSM is the design of experiments (DoE) (Ramachandran and Tsokos, 2015). These approaches were originally developed for the model fitting of physical and numerical experiments. The main objective of DoE is to select experimental points where the response should be evaluated. Then an optimal design can be found by using of a mathematical model which represents the process. The mathematical models are generally polynomials with an unknown structure, so for every particular problem a set of experiments are designed and defined as runs of the experimental design (Khuri, 2003). In a traditional DoE, screening experiments are performed in the first stage to evaluate the factors that have little or no effect on the response, in other words, the aim of the screening experiments is to identify the factors that have large effects on the response. The probable settings of each independent variable are called levels. RSM has different methodologies such as:

2.5.1. Full factorial design

To make an approximation model that can capture interactions between design variables, a full factorial approach may be essential to examine all possible combinations (Anderson-Cook et al., 2009b). A factorial experiment is an experimental scheme in which design variables are varied together, instead of one at a time. The lower and upper bounds of each variable in the optimization process needs to be defined. The acceptable range is then discretized at different levels. If each of the variables is defined at only the lower and upper bounds (two levels), the experimental design is called 2N full factorial. Similarly, if the midpoints are

included, the design is called 3N full factorial (Anderson-Cook et al., 2009a). Factorial designs can be used for fitting second-order models, which can significantly improve the optimization process when a first-order model has a lack of fit due to interaction between variables and surface curvature. A general second-order model is defined as the following model:

$$Y = \beta_o + \sum_{i=1} \beta_i X_i + \sum_{i=1} \beta_{ii} X_i^2 + \sum_{i=1} \sum_{j=i+1} \beta_{ij} X_i X_j$$

Where Y is the response function, β_o the offset term, β_i the coefficient of the linear effect, β_{ii} the coefficient of squared effect, X_i is the coded value of variable i, X_j is the coded value of variable j and β_{ij} the coefficient of interaction effect (Antony, 2014).

2.5.2. Central Composite Design

A second-order model can be constructed competently with central composite designs (CCD) (Anderson-Cook et al., 2009b). CCD is a first-order design amplified by additional central and axial points to allow evaluation of the tuning parameters of a second-order model. A CCD for 3 design variables involves 2*N* factorial points, 2*N* axial points and 1 central point. CCD presents an alternative to 3*N* designs in the construction of second-order models because the number of experiments is reduced as compared to a full factorial design (Song et al., 2014).

Chapter 3: Thermodynamic Analysis

3.1. Solvay Process Steps

The Solvay process goes through three steps as described in Reactions (3.1.1-3.1.3); however the overall reaction (3.1.4) is not spontaneous.

$$NaCl + NH_3 + CO_2 + H_2O \rightarrow NaHCO_3 + NH_4Cl \quad (3.1.1)$$

$$2NaHCO_3 \rightarrow Na_2CO_3 + CO_2 + H_2O \quad (3.1.2)$$

$$2NH_4Cl + Ca(OH)_2 \rightarrow CaCl_2 + 2NH_3 + 2H_2O \quad (3.1.3)$$

$$2NaCl + CaCO_3 \rightarrow Na_2CO_3 + CaCl_2 \quad (3.1.4)$$

The first reaction (3.1.1) involves the initial contact of the three main reactants: Carbon dioxide, sodium chloride and ammonia (El-Naas, 2011). The aim of the Solvay process is the formation of sodium carbonate, but for brine management the aim is to convert water-soluble sodium chloride into insoluble sodium bicarbonate that can be removed by filtration (El-Naas, 2011). A chemical reaction and equilibrium software, HSC Chemistry (Roine, 1989) was used to carry out a thermodynamic analysis based on sodium chloride as the main reactant in the reject brine.

3.2. Effect of Temperature

HSC software was used to determine the equilibrium composition for the first reaction at different temperatures and to evaluate the heat of reaction as a function of temperature. For a fixed temperature and pressure the number of moles present at equilibrium for any species can be determined using the Gibbs free energy

minimization method (El-Naas, 2011). The calculated thermodynamic properties for the first reaction (3.1.1) are presented in Table A.1. The analysis indicates that the first reaction is spontaneous for the whole temperature range (0 to 90 ºC) as indicated by the negative ΔG as shown in Figure 3.1, and the change in the heat of reaction from (10 to 90 ºC) is negative which indicate that the reaction is exothermic; however at temperature 20 ºC, the reaction is going to change its path to be endothermic at high temperature, this can be explained by the changing in the specific heat capacity for chemical species and hence changing in ΔH as shown in Figure 3.2. The values for ΔH and ΔG at temperature 20 ºC are - 129.1 kJ/mol and - 25.8 kJ/mol, respectively.

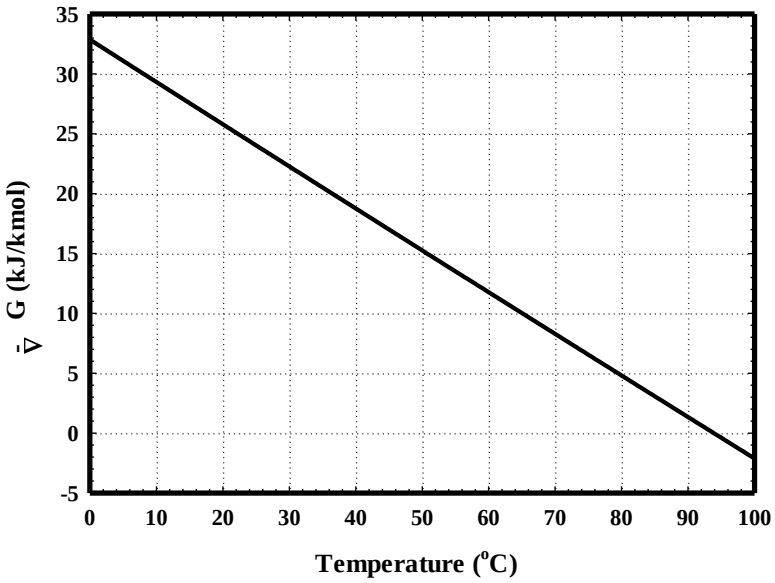

Figure 3.1: Calculated Gibbs free energy (-ΔG) versus temperature for Reaction (3.1.1) using HSC software at atmospheric pressure and stoichiometric molar ratio.

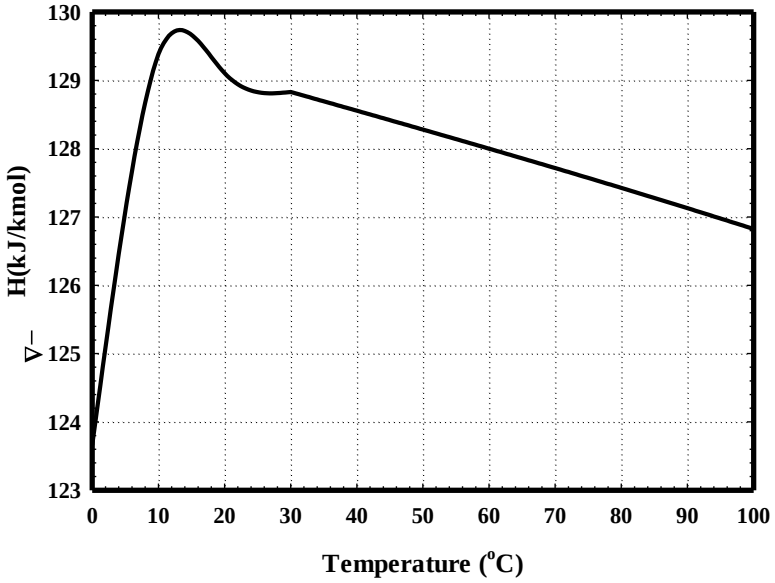

Figure 3.2: Calculated heat of reaction (-ΔH) versus temperature for Reaction (3.1.1) using HSC software at atmospheric pressure and stoichiometric molar ratio.

The temperature effect on the equilibrium composition for the first reaction (3.1.1) has been calculated. The results are presented in Table A.2 and shown in Figure 3.3. It shows that the equilibrium compositions for reactants as well as products are superimposed on each other, since they are equimolar. The optimum reaction temperature is in the range of (10-20ºC), where totally forward reaction is achieved; however, by increasing the temperature beyond 80 ^{o}C, the equilibrium compositions of the products (NH_4Cl) and ($NaHCO_3$) start decreasing and Reaction (3.1.1) becomes reversible to the left side.

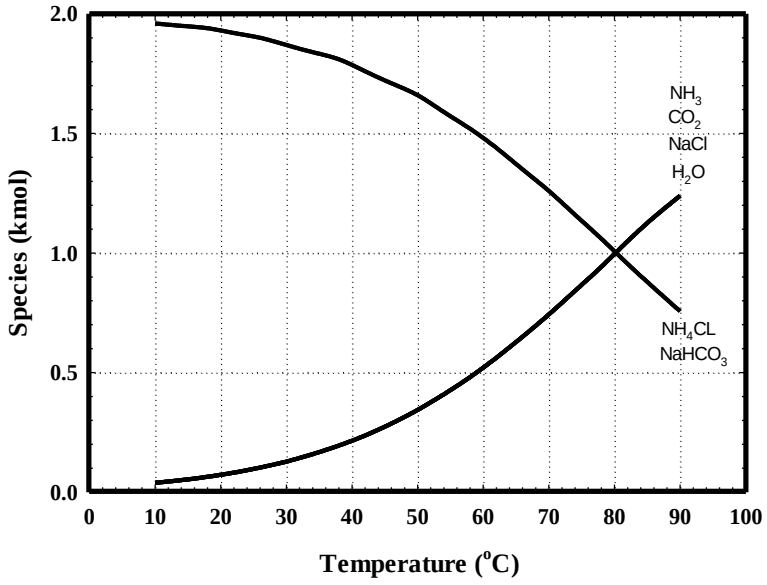

Figure 3.3: Calculated equilibrium compositions versus temperature for Reaction (3.1.1) using HSC software at atmospheric pressure.

3.3. Effect of Ammonia Molar Ratio

The effect of ammonia molar ratio on the equilibrium composition in Reaction (3.1.1) has been calculated, and the results are presented in Table A.3 and shown in Figure 3.4; it shows that a stoichiometric molar ratio of $1NH_3$: NaCl is the optimum for totally forward reaction; however, El Naas et al. (El-Naas et al., 2010) reported that the optimum molar ratio for reactions involving reject brine is $3NH_3$:1NaCl, and this higher molar ratio may be due to two reasons : the first is testing the reaction under semi-batch mode, where CO_2 gas leaves the reactor and thus stripping away some of ammonia from the solution; the second is the presence of other ions in the reaction such as magnesium which react with ammonia.

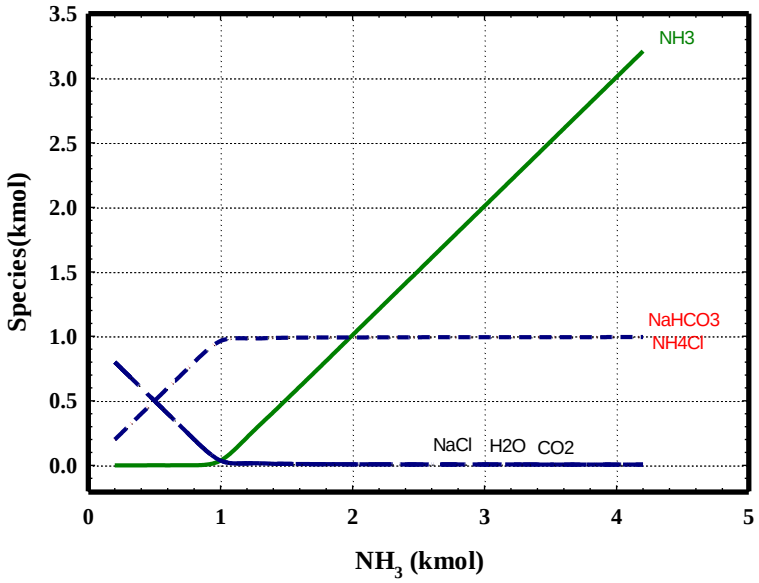

Figure 3.4: Calculated equilibrium compositions versus stoichiometric ratio of ammonia for Reaction (3.1.1) using HSC software at atmospheric pressure and temperature of 20 ^{o}C.

3.4. Effect of Pressure

The effect of pressure on the equilibrium composition in Reaction (3.1.1) has also been calculated, and the results are presented in Table A.4 and shown in Figure 3.5; they show that there is almost no effect of pressure on the equilibrium composition of reaction species; however, the software calculations neglect the effect of gas stripping phenomena which may occur in the semi-batch reaction mode, so the pressure may show some effect on the equilibrium composition in the experimental part.

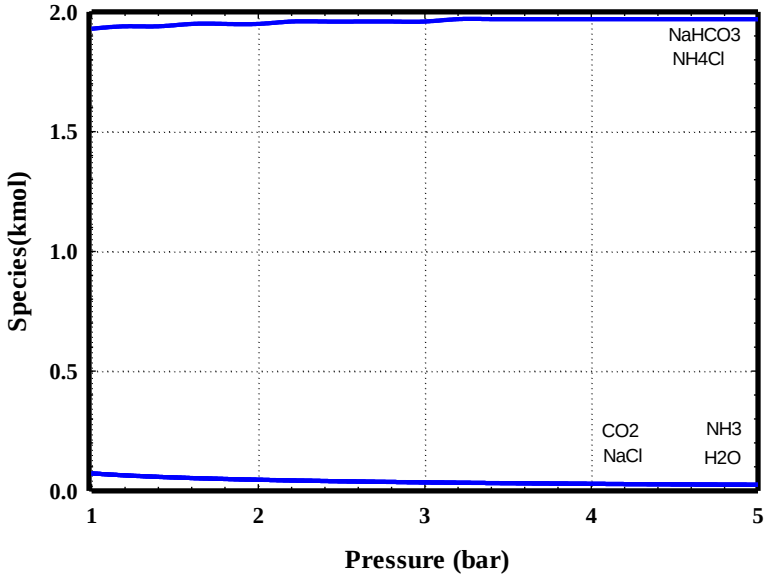

Figure 3.5: Calculated equilibrium compositions versus pressure for Reaction (3.1.1) using HSC software at temperature of 20 ^{o}C.

3.5. Thermodynamic Analysis for the Intermediate Steps in Solvay Process

In the Solvay process reaction proceeds through the following two steps:

$$NH_4OH + CO_2 \rightarrow NH_4HCO_3 \quad (3.5.1)$$

$$NaCl + NH_4HCO_3 \rightarrow NaHCO_3 + NH_4Cl \quad (3.5.2)$$

Reaction (3.5.1) has high negative ΔH and ΔG as shown in Table A.5 and Figures 3.6 & 3.7; it is an exothermic reaction that takes place as soon as the CO_2 gets in contact with the ammoniated brine. Once ammonium bicarbonate is formed, it reacts with sodium chloride according to Reaction (3.5.2). ΔG for Reaction (3.5.1) and (3.5.2) at temperature of 20 ^{o}C are -56.69 and -3 kJ/kmol respectively, so Reaction (3.5.2) is not as spontaneous as Reaction (3.5.1), and it is assumed to be the rate limiting step. The thermodynamic analysis indicates that Reaction (3.5.2) is exothermic with a negative heat of reaction up to a temperature of 40C °. Beyond

this temperature, the reaction becomes endothermic as presented in Table A.6 and shown in Figures 3.8 & 3.9.

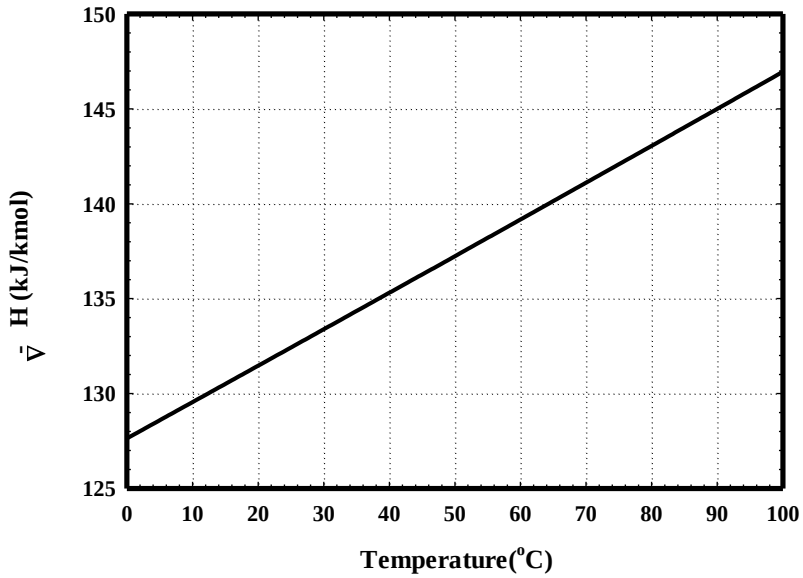

Figure 3.6: Calculated heat of reaction (-ΔH) versus temperature for Reaction (3.5.1) using HSC software at atmospheric pressure and stoichiometric molar ratio.

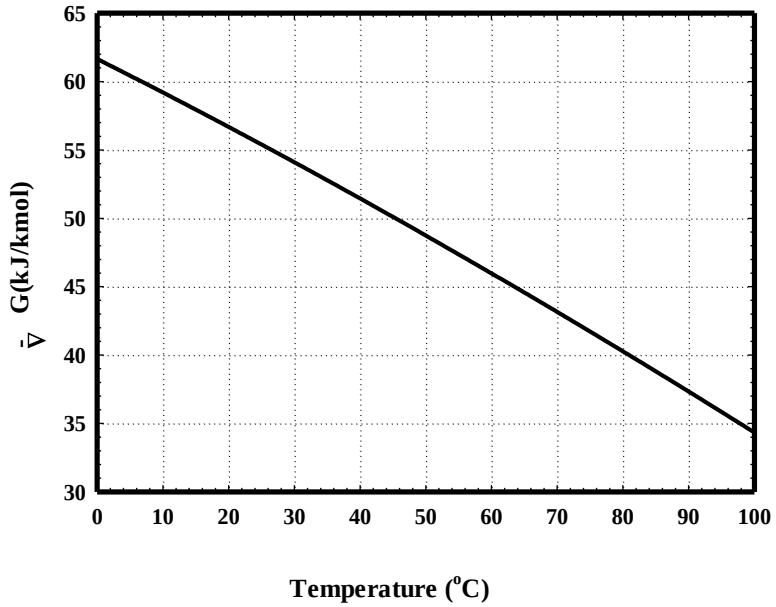

Figure 3.7: Calculated Gibbs free energy (-ΔG) versus temperature for Reaction (3.5.1) using HSC software at atmospheric pressure and stoichiometric molar ratio

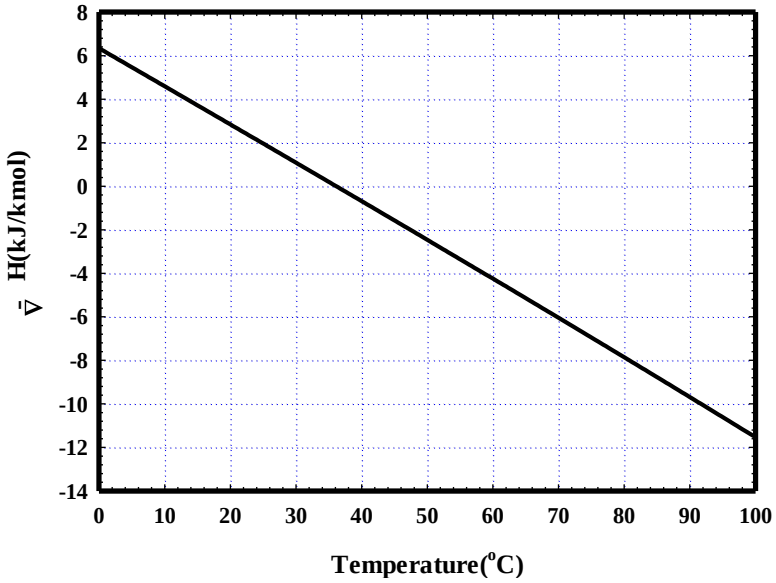

Figure 3.8: Calculated heat of reaction (-ΔH) versus temperature for Reaction (3.5.2) using HSC software at atmospheric pressure and stoichiometric molar ratio.

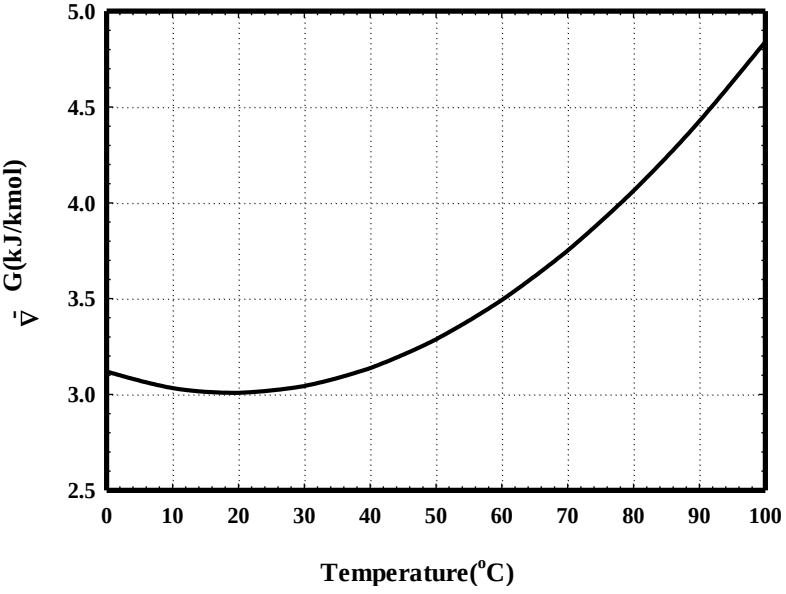

Figure 3.9: Calculated Gibbs free energy (-ΔG) versus temperature for Reaction (3.5.2) using HSC software at atmospheric pressure and stoichiometric molar ratio.

This fact was observed experimentally in a semi-batch reactor studied by El Naas et al. (El-Naas et al., 2010). The reaction temperature was measured with time and increased up to 41 ^{o}C, then dropped and stabilized at 30 ^{o}C. The change in heat of

reaction was attributed to the changes in the concentration of NH_3 in the solution as reported by Yeh and Bai (Yeh and Bai, 1999); however, El-Nass 2010 reported that the phenomenon was most likely due to the mechanisms of Reaction (3.5.2), since the heat of reaction obtained by the thermodynamic analysis was calculated per kmol of NH_3, and it was only a function of temperature (El-Naas et al., 2010).

Chapter 4: Materials and Methodology

4.1. Experimental Apparatus

The main unit of the experimental set-up is the contact reactor, which is a stainless steel jacketed, bubble column reactor (SSR) with an internal diameter of 78 mm and an overall height of 700 mm. It was specially-designed and built for this study and was operated in a semi-batch mode, where the liquid was exposed to a continuous flow of carbon dioxide mixture with air. The temperature controlled by water bath circulation through the jacket. The gas inlet at the bottom of the reactor was controlled by gas flow controller, while the liquid inlet at the top of the reactor was controlled by a piston pump. The reactor had a port for liquid sampling and can be discharged at the bottom. The gas effluent from the top was passed through moister trap then to CO_2 gas analyzer (Model 600 series, Non-Dispersive Infrared NDIR analyzers). A SCADA station was installed to control and monitor the process parameters such as: temperature, pressure, liquid level, gas flow rate and liquid flow rate. A schematic diagram and a photograph of the SSR system are shown in Figure 4.1. Specifications of the SSR system and the CO_2 gas analyzer are presented in Table A.7 and A.8, respectively.

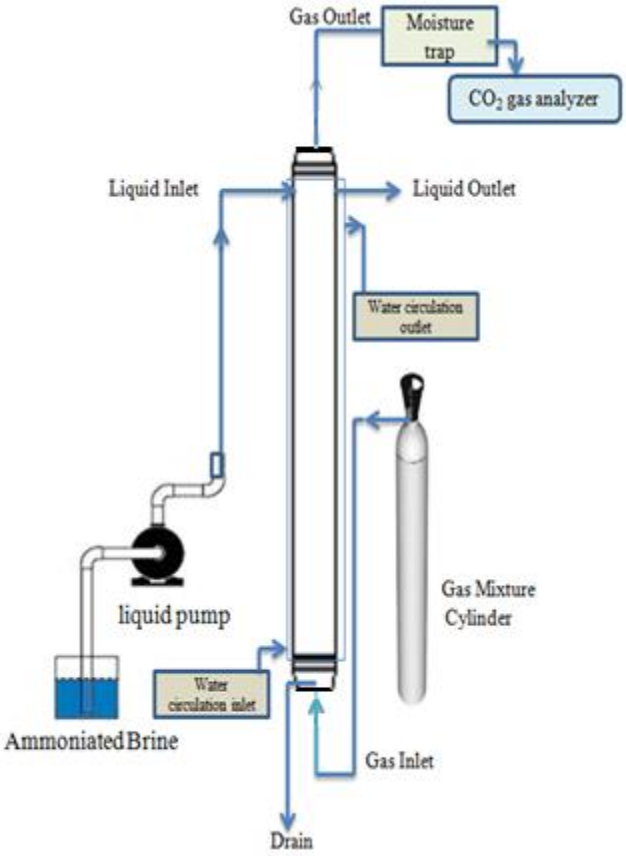

Figure 4.1: A schematic diagram & a picture of the Bubble Column Reactor

4.2. Brine Samples and other Reactants

Reject brine samples with salinity ranging from 65,000 to 75,000 ppm were obtained from a local desalination plant utilizing RO desalination process. Three brine samples were analyzed to determine pH, TDS, salinity, COD, Na^{+}, Mg^{+2}, K^{+} and Ca^{+2} concentration. The average values are presented in Table 4.1 with the standard deviation. Ammonium hydroxide (25 wt. % NH_3 and ammonium bicarbonate (purity 99.9%) was purchased from Scientific Progress medical and scientific equipment, UAE. A gas mixture of (10% CO_2 and 90% Air) was obtained from Abu Dhabi Oxygen Company, UAE.

Table 4.1: Characteristics of the reject brine

	pH	TDS	Salinity	COD	Na^{+}	Mg^{+2}	K^{+}	Ca^{+2}
Mean	9.16	73.8 g/L	71,700 ppm	1560 ppm	23,712 ppm	2,794 ppm	762 ppm	1,375 ppm
Standard deviation	0.01	0.1	5	2.5	12.2	8.7	4.6	3.1

4.3. Experimental Methods

4.3.1 Screening study

Initially, a set of screening experiments were carried out to find out the direction of the optimal domain. One factor at a time was employed in the screening step to determine the significant factors affecting ions removal and CO_2 capture. One factor at a time implies that a single factor is changed while other factors remain constant (Mohapatra et al., 2011). In all screening experiments, the reject brine samples were analyzed for sodium, magnesium, potassium and calcium ions. One liter of the reject brine was mixed for five minutes with ammonium hydroxide in the molar ratio $3NH_3$:1NaCl, and the mixture was then fed to the reactor, which was operated in a semi-batch mode (batch for liquid phase and continues for gas phase) at a controlled-temperature of 20 °C. A gas mixture CO_2 containing 10 vol. % CO_2 in

air (10% CO_2 and 90% air) was bubbled into the reactor at a flow rate of 1 L/min for 180 minutes. Two brine samples (15 ml each) were collected every 60 minutes; ammonium bicarbonate (20 w/w %) was added to one of these samples. Both samples were then tested for ions (Na^+, Mg^{+2}, K^+ and Ca^{+2}) removal using ICP (Inductively Coupled Plasma spectrometry). Meanwhile, the effluent gas was continuously passed through a moisture trap then sent to the CO_2 gas analyzer to detect the CO_2 percentage; the variation of pH with time was also measured. Factors studied in the screening step were: ammonia to sodium chloride molar ratio NH_3:NaCl, reaction time, temperature, gas flow rate, gauge pressure and ammonium bicarbonate to treated brine w/w percentage.

a) Variation of ammonia to sodium chloride molar ratio

One liter of the brine was mixed with ammonium hydroxide at different molar ratios (1, 1.5, 2, 2.5, 3 and 3.5 NH_3: 1NaCl). The mixture was reacted with CO_2 at a temperature of 20 ^oC and a gas flow rate of 1L/min for 180 minutes. Samples were collected every 60 minutes and tested for ions removal. The CO_2 composition and the pH of the reactor content were also measured with time.

b) Variation of reaction time

One liter of the real brine was mixed with ammonium hydroxide at molar ratio of $3NH_3$:1NaCl and then reacted with CO_2 for 300 minutes at a flow rate of 1 L/min and temperature of 20 ^oC. Samples were collected every 60 minutes and tested for ions removal.

c) Variation of temperature

One liter of the brine was mixed with ammonium hydroxide at molar ratio of $3NH_3$:1NaCl and then reacted with CO_2 at a gas flow rate of 1 L/min at the following temperatures (10, 20, 30, 40 and 50 °C) for 180 minutes.

d) Variation of gas flow rate

One liter of the real brine was mixed with ammonium hydroxide at molar ratio of $3NH_3$:1NaCl and reacted with CO_2 at temperature of 20 °C. The gas mixture was injected into the reactor at different flow rates (0.5, 1, 2.5, 2 and 2.5 L/min) for 180 minutes.

e) Variation of gage pressure.

One liter of the brine was mixed with ammonia solution at molar ratio of $3NH_3$:1NaCl and then reacted with CO_2 at a flow rate of 1 L/min, temperatures of 20 °C and at the following reactor gauge pressures (0, 1, 2, 3 and 4 bar).

f) Variation of ammonium bicarbonate (NH_4HCO_3) to treated brine w/w percentage

One liter of the real brine and ammonium hydroxide mixture was prepared at a molar ratio of $3NH_3$:1NaCl and then reacted with CO_2 at temperature of 20 °C and a flow rate of 1 L/min for 180 min. Samples of the effluent liquid were mixed with ammonium bicarbonate at the following weight percentages: 5, 10, 15, 20 and 25 NH_4HCO_3 to treated brine w/w % and tested for ions removal.

4.3.2 Experimental design

The CO_2 capture and ions removal (Na^+, Mg^{+2}, K^+, Ca^{+2}) based on the Solvay method was optimized using RSM (Response surface Methodology) in Minitab 17.0 application. As a fitting statistical tool, Minitab 17.0 offers multilevel factorial screening designs, and numerical optimization can be followed by analyzing the critical factors and their interactions. The design of runs was in accordance with central composite design (CCD). The reaction time was investigated in screening study and set to be three hours, since maximum ions removal was achieved at this time. The three major effect factors which affect both CO_2 capture efficiency and

ions removal were gas flow rate, temperature and ammonia to sodium chloride molar ratio; these factors were operated in the range of 0.6 to 2.3 L/min, 13.18 to 46.82 ^{o}C and 1.66 to 3.34 NH_3:1NaCl, respectively. The experimental conditions for central composite design (CCD) runs are presented in Table 4.2. The optimal temperature, gas flow rate and ammonium to sodium chloride molar ratio for CO_2 capture and ions removal have been found by response optimizer.

Table 4.2: Range and level of independent variables for central composite design runs.

				Level				
Factors	Tag	Symbol	Units	-α	-1	0	1	+α
Temperature	T	X_1	°C	13.2	20	30	40	46.8
Flow rate	F	X_2	L/min	0.659	1	1.5	2	2.341
Molar ratio	M	X_3	-	1.7	2	2.5	3	3.3

4.3.3. Continuous Solvay process

a) Effect of liquid residence time.

In this part of the study, the Solvay process was carried out in continuous mode under atmospheric pressure for 360 minutes. The solution of ammoniated brine was continuously fed at different flow rates: 50, 25, 16.7 and 12.5 ml/min, to have liquid residence times of (1, 2, 3 and 4 hours) at optimal temperature, gas flow rate, and ammonium to sodium chloride molar ratio of 19.3 ^{o}C, 1.544 L/min, 3.3 NH_3:1NaCl, respectively. Brine samples were collected every 60 minutes and tested for ions removal. The effluent gas was continuously passed through a moisture trap then sent to the CO_2 gas analyzer to detect the CO_2 percentage.

b) Steady state in continuous Solvay

The Solvay process was carried out in continuous mode under atmospheric pressure for 480 minutes using gas mixture flow rate of 1.544 L/min, temperature of 19.3 °C. The solution of ammoniated brine 3.3 NH_3:1NaCl molar ratio was

continuously fed with flow rate of 12.5 ml/min. Brine samples were collected every 60 minutes and tested for ions removal. The effluent gas was continuously passed through a moisture trap then sent to the CO_2 gas analyzer to detect the CO_2 percentage.

4.3.4. Calculations

Ions removal % $= \frac{X_i - X_f}{X_i} \times 100\%$

- X_i = initial ions concentration in the feed brine (ppm)
- X_f = final ions concentration in the treated brine (ppm)

CO_2 capture efficiency $= \frac{\text{Moles of } CO_2 \text{ captured}}{\text{Moles of } CO_2 \text{ loaded to the reactor}} \times 100\%$

- Moles of CO_2 captured $= \frac{\int_0^t \text{Volume of } CO_2 \text{ captured (L/min)} .dt}{\text{Molar volume of } CO_2 \text{ (L/mol)}}$

- Volume of CO_2 captured at time t = Gas flow rate (L/min) × CO_2 % in the feed gas × CO_2 % by the analyzer

- t = time in minutes

- Graph software was used to find the integration for the total volume of CO_2 captured within reaction time

- CO_2 % in the feed gas =10%

- Molar volume of $CO_2 = \frac{R\,T}{P}$ (L/mol)

- R = Gas constant 8.314 L.kPa/(K.mole)
- T = Temperature in (K)
- P = Pressure in kPa

- Moles of CO_2 loaded to the reactor
  $= \frac{\text{Gas flow rate(L/min)} \times CO_2\% \text{ in feed gas} \times \text{run time (min)}}{\text{Molar volume of } CO_2 \text{ (L/mol)}}$

Chapter 5: Results and Discussion

5.1. Parametric Study

5.1.1. Effect of NH_3: NaCl molar ratio on ions removal.

Figure 5.1 shows the effect of NH_3: NaCl molar ratio on ions removal. With increasing the molar ratio, the ions removal increased rapidly, for example, sodium removal reached the maximum at molar ratio of $3NH_3$:1NaCl. This can be explained by increasing the initial pH, which accordingly shifted the reaction towards bicarbonate formation. This mechanism higher pH in order to have higher concentrations of hydroxyl ions; this promotes the formation of bicarbonate ions followed by salts bicarbonate (Butler, 1982). Increasing the molar ratio (more than $3NH_3$:1NaCl) did not seem to add much to the reaction process. As a whole, the increase of the molar ratio is favorable for brine desalination, but this will increase the energy requirement of the NH_3 recovery system due to stripping of ammonia (Zhang and Guo, 2013b). The addition of 20 % w/w ammonium bicarbonate to the treated brine samples increased the ions removal in the Solvay process even at stoichiometric molar ratio. The results are presented in Table A.9.

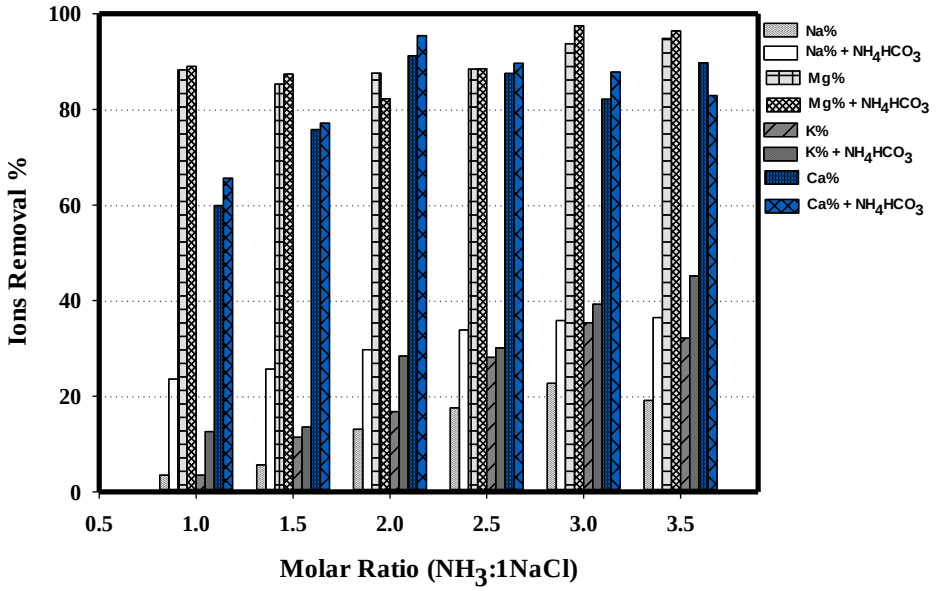

Figure 5.1: Ions removal versus NH_3: NaCl molar ratio at gas flow rate of 1L/min and temperature of 20 ^oC

5.1.2. Effect of NH_3: NaCl molar ratio on pH and CO_2 capture

With increasing ammonia to sodium chloride molar ratio, the initial pH of the solution will increase and, consequently the CO_2 capture efficiency will increase. For the chemical reaction, high NH_3:NaCl molar ratio would enhance the mass transfer and push the reaction forward according to the classic two-film theory, leading to the increase of CO_2 capture percentage. However increasing the molar ratio more than $3NH_3$:1NaCl does not seem to increase the CO_2 capture efficiency any further, indicating that the reaction is close to its limit, this is in agreement with the previous studies (Zhao et al., 2012) . Usually, using high NH_3:NaCl molar ratio may increase the risk of ammonia leakage caused by ammonia volatility (Molina and Bouallou). The results are presented in Table A.10 and A.11 and Figures 5.2, 5.3 and 5.4.

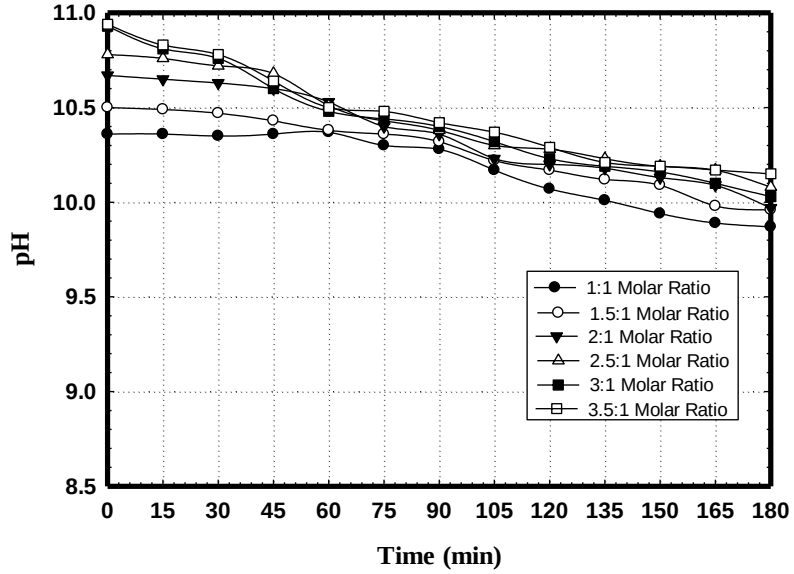

Figure 5.2: pH versus reaction time for different NH_3: NaCl molar ratios at gas flow rate of 1L/min and temperature of 20 ^oC.

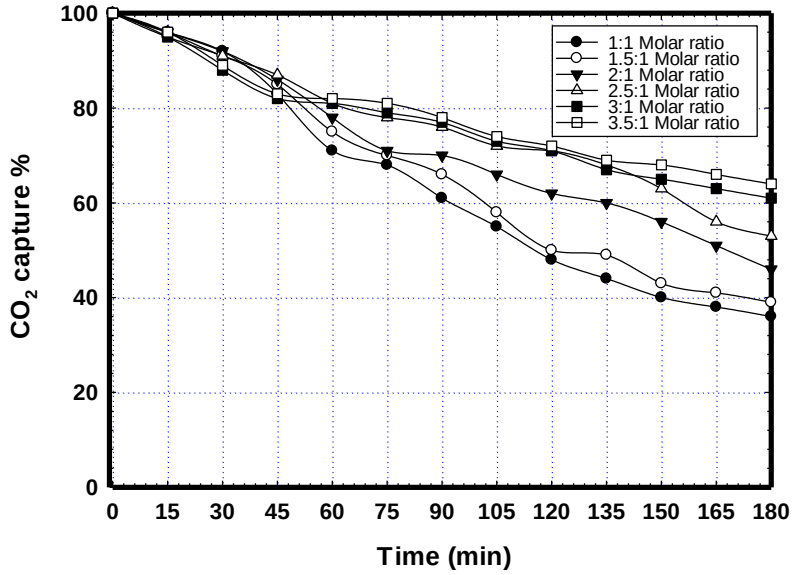

Figure 5.3: CO_2 captured versus reaction time for different NH_3: NaCl molar ratios at gas flow rate of 1L/min and temperature of 20 ^oC.

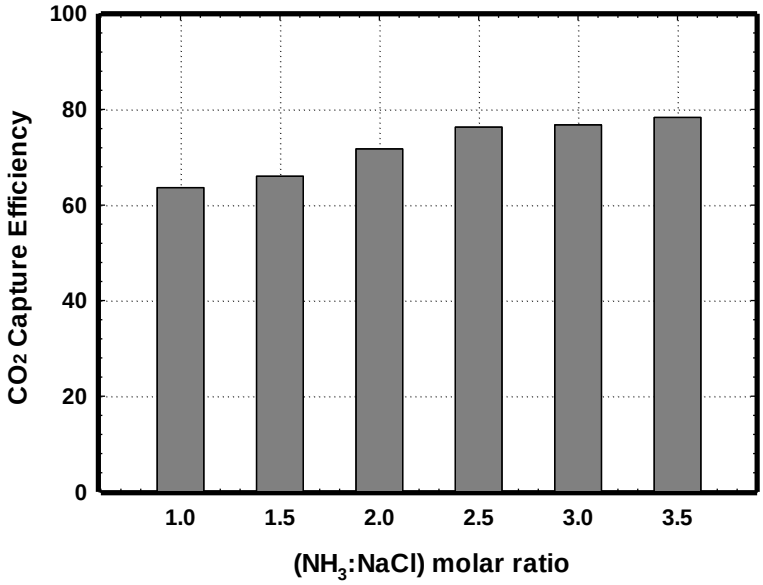

Figure 5.4: CO_2 capture efficiency versus NH_3: NaCl molar ratio at gas flow rate of 1L/min and temperature of 20 ^{o}C.

5.1.3. Effect of reaction time on ions removal

The ions removal percentage increased with increasing reaction time, reaching maximum at three hours as shown in Figure 5.5; after three hours almost no change on ions removal was observed. This may be attributed to the semi- batch mode for the reaction, where pH level decreases due to the CO_2 accumulation in the reactor, and the acidic nature of the water solution will hinder the precipitation of bicarbonate products (Nancollas, 1974). The addition of ammonium bicarbonate to the treated brine samples reduced the solubility of bicarbonate products and increased the ions removal, which seems to have a significant effect on the possibility of using ammonium bicarbonate in the Solvay process. The results are presented in Table A.12.

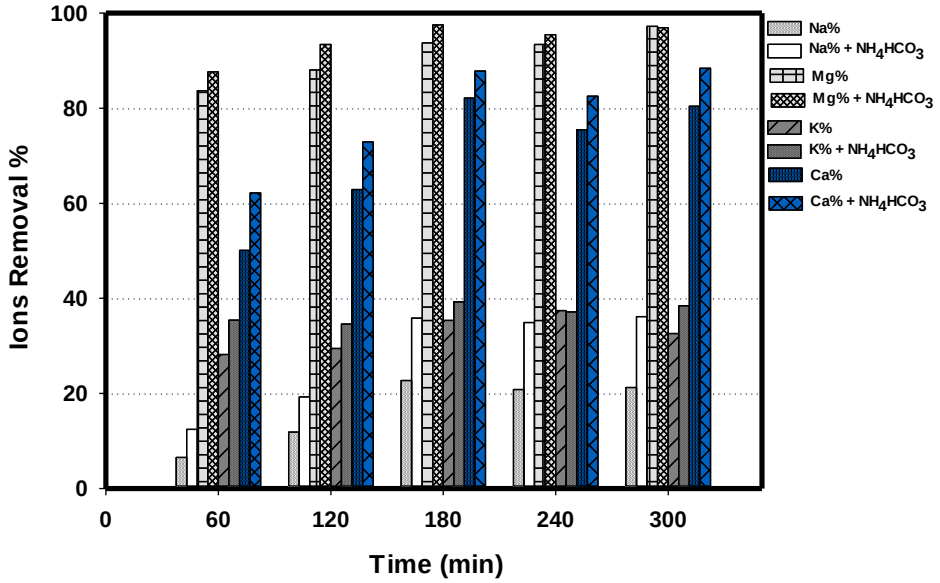

Figure 5.5: Ions removal versus reaction time at $3NH_3$:1NaCl molar ratio, gas flow rate of 1L/min and temperature of 20 ^oC.

5.1.4 Effect of reaction time on pH and CO_2 capture

The experimental results indicated that the CO_2 capture and brine pH decreased with increasing the reaction time due to the decrease in absorption capacity and the rise in acidity of the ammoniated brine, this is in agreement with the previous studies (El-Naas, 2011; Zhang and Guo, 2013b). The results are presented in Table A.13 and Figure 5.6. The maximum CO_2 capture efficiency was obtained in the first hour of the reaction due to the high basic pH level; this increased the reaction rate and accordingly CO_2 capturing efficiency (Yeh et al., 2005). The results are presented in Table A.14 and Figure 5.6 and 5.7.

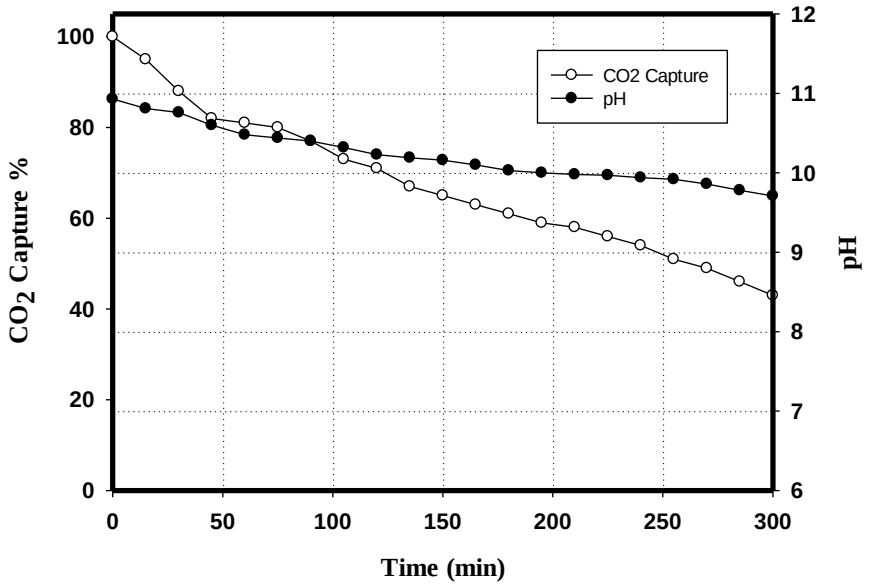

Figure 5.6: CO_2 capture and pH versus reaction time at $3NH_3$:1NaCl molar ratio, gas flow rate of 1L/min and temperature of 20 ^oC.

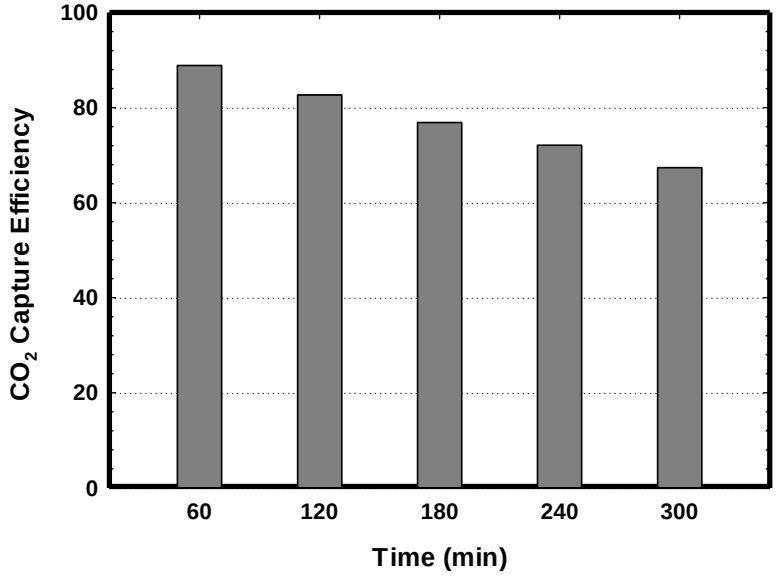

Figure 5.7: CO_2 capture efficiency versus reaction time at $3NH_3$:1NaCl molar ratio, a gas flow rate of 1L/min and temperature of 20 ^oC.

5.1.5 Effect of temperature on ions removal.

As can be seen from Figure 5.8, the ions removal increased with increasing the reaction temperature reaching a maximum at 20 ^{o}C, and no more improvement was observed when increasing the temperature above 20 ^{o}C. This can be explained by the reversibility of Solvay process reactions (Zhao et al., 2012). Previous studies suggested that the forward reactions are dominant at room temperature (Shale),while the backward reactions occur in the temperature range of 38–60 ^{o}C (Pelkie). The reduction in the sodium removal at 40-50 ^{o}C can be also related to the increase in the solubility of sodium bicarbonate (El-Naas, 2011). The addition of ammonium bicarbonate can reverse this by reducing the solubility of the sodium bicarbonate, which can definitely have significant effect on the possibility of using the Solvay process even at high temperature. The results are presented in Table A.15.

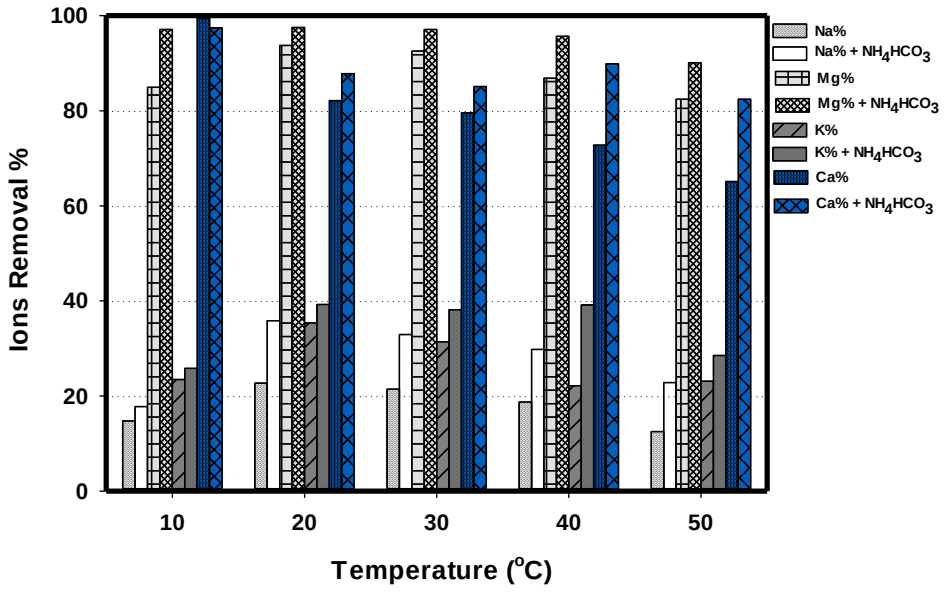

Figure 5.8: Ions removal versus temperature at $3NH_3$:1NaCl molar ratio and gas flow rate of 1L/min with.

5.1.6 Effect of temperature on the pH and CO_2 capture.

The experimental results indicated that the CO_2 capture increased with decreasing the temperature, since the solubility of CO_2 gas increases with decreasing temperature (Poling, 2000). Maximum CO_2 was captured at temperature of 10 °C. It was reported by Zhu et al. 2011 that the lower the reaction temperature is, the less stripping of Ammonia and more stable the reaction inside the reactor (Yeh et al., 2005). At high temperature, the volatility of ammonia will increase and hence increasing the concentration of CO_2 gas in the effluent gas, and as a result decreasing the CO_2 capture efficiency (Zhang and Guo, 2013a). The effect of temperature on the solution pH can be explained by Le Châtelier's Principle. When increasing the temperature, the position of equilibrium moves to counter the temperature increase by absorbing the extra heat and forming more hydrogen ions and hydroxide ions. This effect leads to increasing the value of Kw (The Ionic Product for water) and decreasing the pH as the temperature increases (Liu et al., 1996); this is in addition to the CO_2 effect in reducing the pH during the reaction as discussed in Section (5.1.4). The results are presented in Table A.16 and A.17 and shown in Figures 5.9, 5.10 and 5.11.

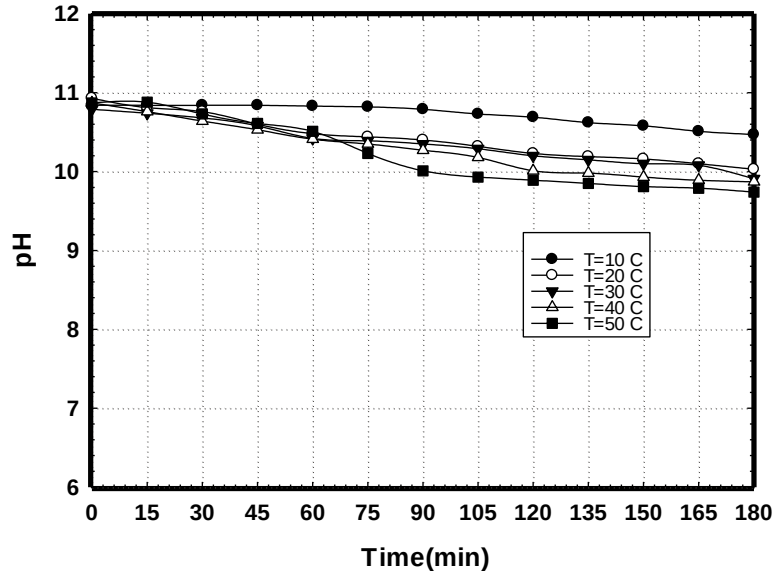

Figure 5.9: pH versus reaction time for different temperatures at $3NH_3$:1NaCl molar ratio and gas flow rate of 1L/min.

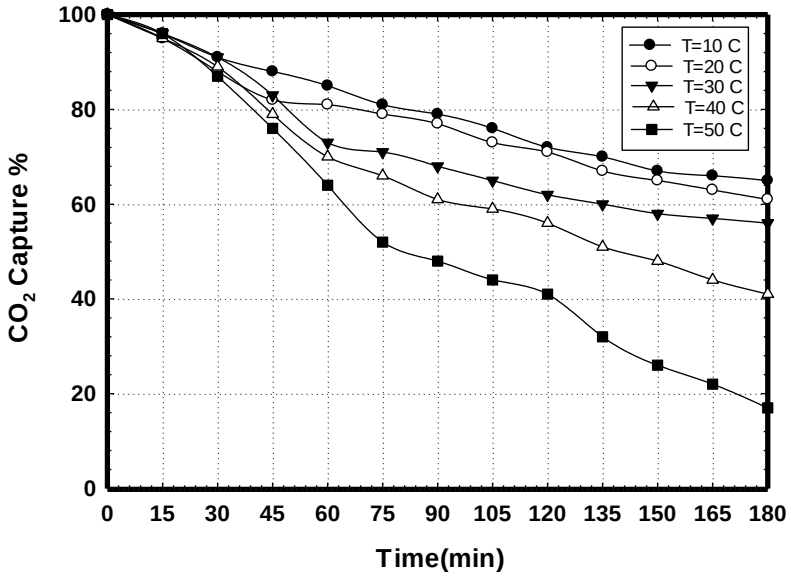

Figure 5.10: CO_2 captured versus reaction time for different temperatures at $3NH_3$:1NaCl molar ratio and gas flow rate of 1L/min.

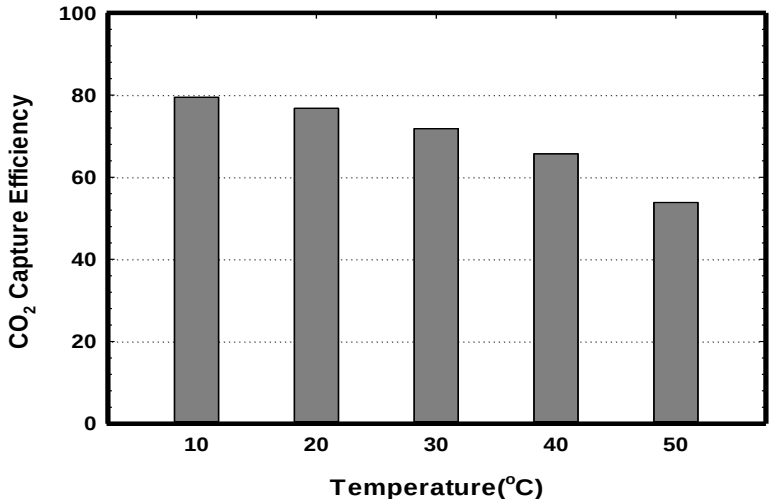

Figure 5.11: CO_2 capture efficiency versus temperature at $3NH_3$:1NaCl molar ratio and gas flow rate of 1L/min.

5.1.7 Effect of gas flow rate on ions removal.

The effect of gas flow rate on ions removal is shown in Figure 5.12. By increasing the gas flow rate to 2000 ml/min, the ions removal increase, which can be explained by enhancing the reaction rate due to increasing the CO_2 loading and hence capture by the ammoniated brine. However, higher flow rates seemed to have a slightly negative effect on some ions removal; this can be explained by two reasons: the first is decreasing the residence time for CO_2 in the reactor and hence decreasing the reaction rate (Yeh et al., 2005); the second is improving mixing in the reactor and hence increasing the solubility of ions bicarbonate. Although increasing the CO_2 gas flow rate can speed up the reaction and shorten the reaction time (Yeh et al., 2005), as shown in Figure 5.13, the time needed to reach maximum sodium removal decreased by increasing the gas flow rate. The negative effect of high gas flow rate on ions removal was reversed by using ammonium bicarbonate, which reduced the solubility of ions bicarbonate and increased the ions removal. The results are presented in Table A.18 and A.19.

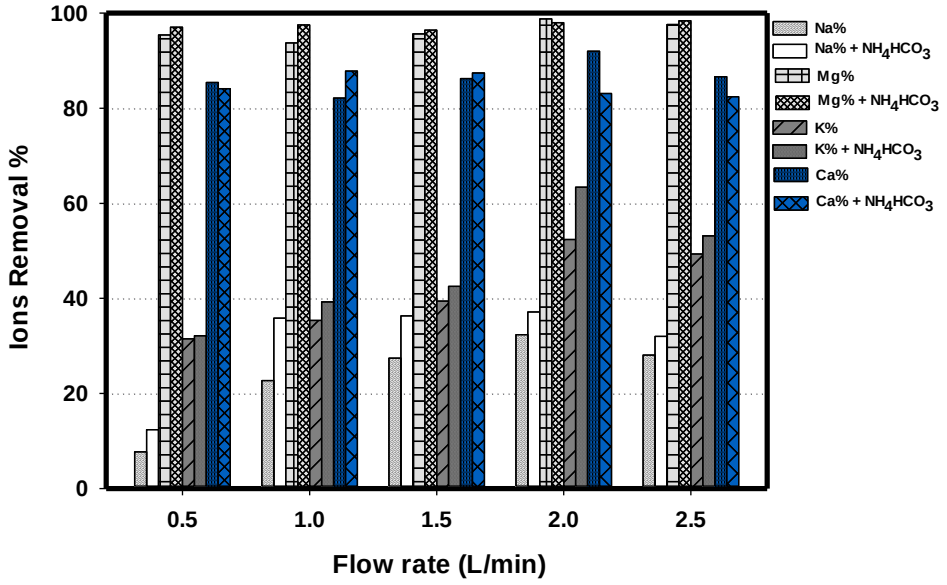

Figure 5.12: Ions removal versus gas flow rate at $3NH_3$:1NaCl molar ratio and temperature of 20 ^oC.

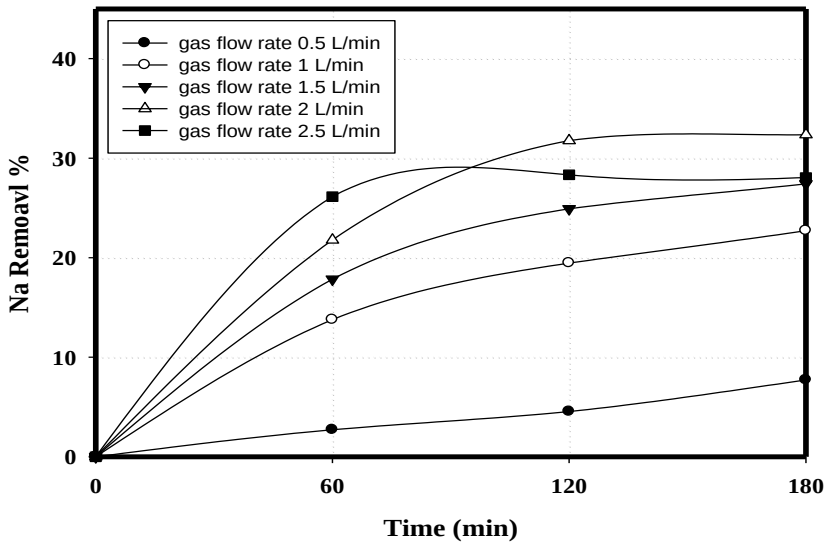

Figure 5.13: Sodium removal versus reaction time for different gas flow rates at $3NH_3$:1NaCl molar ratio and temperature of 20 ^oC.

5.1.8 Effect of gas flow rate on pH and CO_2 capture.

The effects of gas flow rate on pH and CO_2 Capture are illustrated in Figures 5.14, 5.15 and 5.16. The CO_2 capture increased with decreasing the gas flow rate, which can be attributed to the residence time of the gas in the reactor. As expected, longer

residence time results in higher reaction rate since the gas will have more contact time with the reactants in the reactor (Yeh et al., 2005). The low gas flow rate of 500 ml/ min provided the highest capture of CO_2. Zhang et al (2013) reported that by increasing the gas flow rate, the absorption capacity by the ammoniated brine decreased (Zhang and Guo, 2013a). The decline of pH during the reaction seemed to be more evident for high gas flow rates, which can be attributed to the increase in CO_2 moles entering the reactor per unit time as discussed in Section (5.1.4). The results are presented in Table A.20 and A.21.

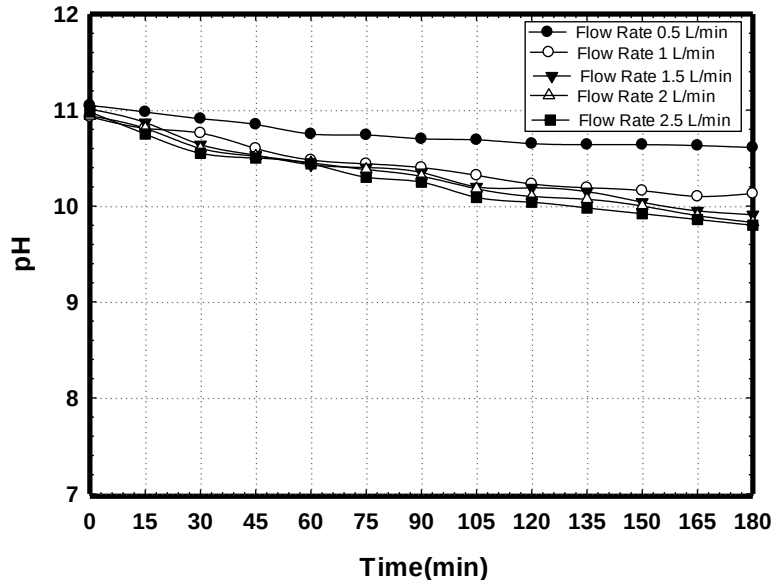

Figure 5.14: pH versus reaction time for different gas flow rates at $3NH_3$:1NaCl molar ratio and temperature of 20 ^oC.

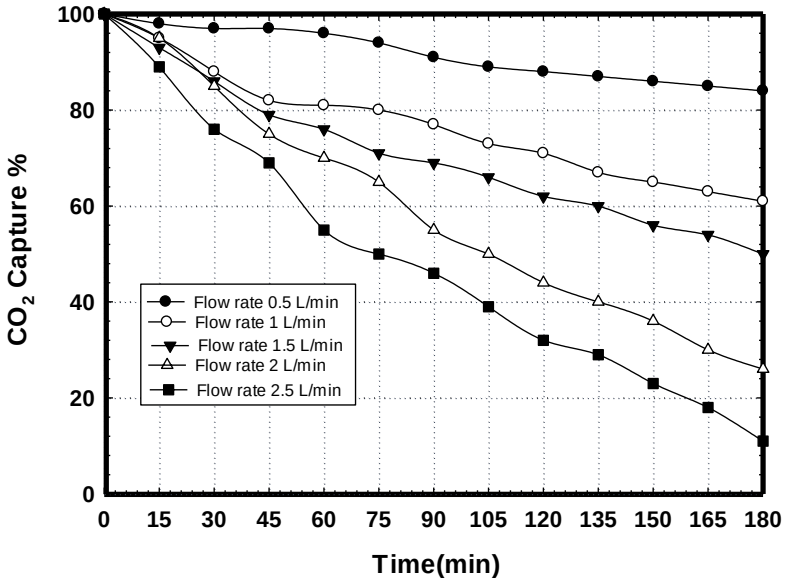

Figure 5.15: CO_2 captured versus reaction time for different gas flow rates at $3NH_3$:1NaCl molar ratio and temperature of 20 C°.

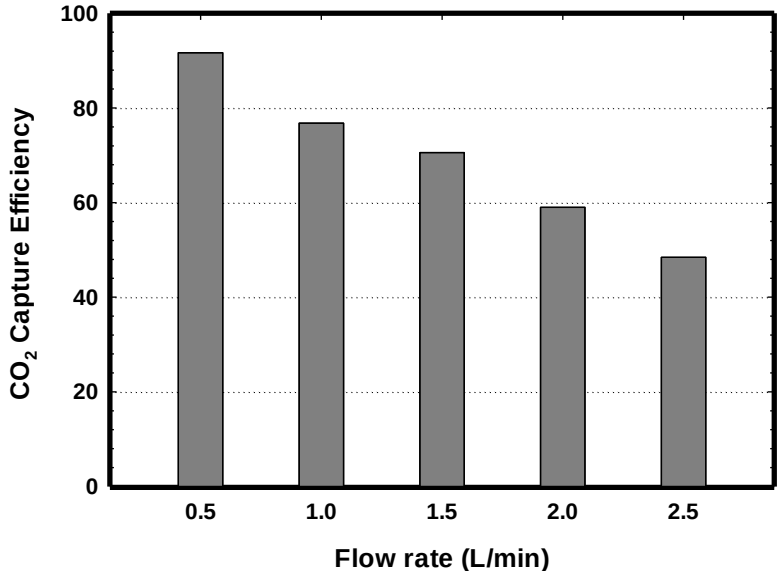

Figure 5.16: CO_2 capture efficiency versus gas flow rate at $3NH_3$:1NaCl molar ratio and temperature of 20 ^oC.

5.1.9 Effect of gauge pressure on ions removal.

Increasing the gauge pressure in the reactor up to 2 bar did not seem to have a major effect on ions removal; however, increasing the pressure more than 2 bar seemed to have negative effect on the removal of ions as shown in Figure 5.17, this can be explained by the reversibility of the process reactions, as discussed in Section (2.4.5), and by increasing the solubility of sodium bicarbonate and hence decreasing ions removal. The results are presented in Table A.22.

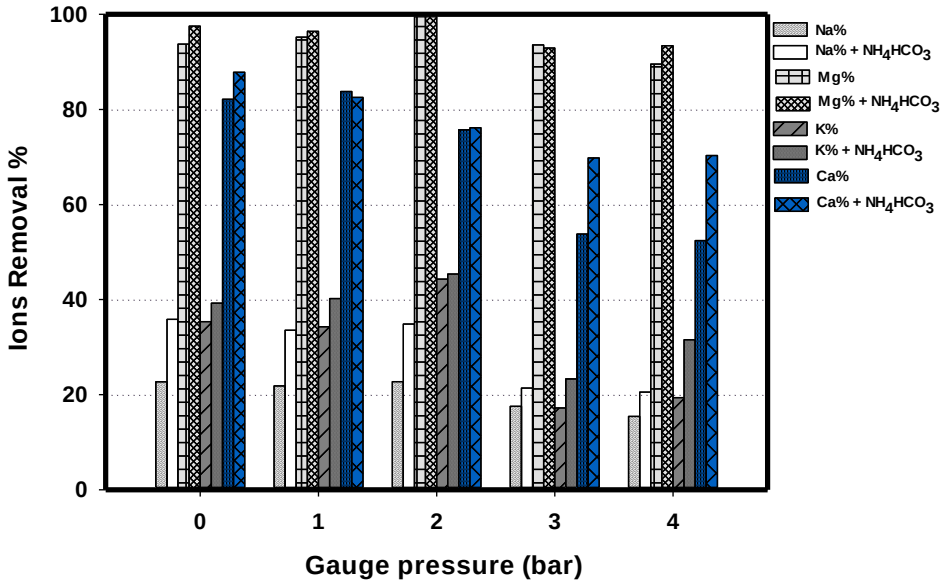

Figure 5.17: Ions removal versus gauge pressure at $3NH_3$:1NaCl molar ratio, temperature of 20 ^oC and flow rate of 1L/min.

5.1.10 Effect of gauge pressure on pH and CO_2 capture.

As expected, the experimental results indicated that CO_2 capture was improved by increasing the gauge pressure due to the increase in CO_2 solubility according to Henry's Law which states that: "the solubility of a gas in a liquid is directly proportional to the pressure of that gas above the surface of the solution (John M. Prausnitz, 1998). If the pressure is increased, the CO_2 gas molecules are forced into the solution since this will be the best option to counter the effect of the

pressure that has been applied. The effect on pH seemed to be negligible; this may be explained by reducing the amount of CO_2 gas leaving the reactor and thus reducing the stripping of ammonia. The results are presented in Table A.23 and shown in Figure 5.18 and 5.19. The CO_2 capture efficiency increased with increasing the gauge pressure to reach the maximum at 3 bar; increasing the pressure more than 3 bar seemed to have no effect on the CO_2 capture efficiency; this can be explained by the CO_2 absorption capacity for ammoniated brine (Zhang and Guo, 2013a) .The results are presented in Table A.24 and shown in Figure 5.20.

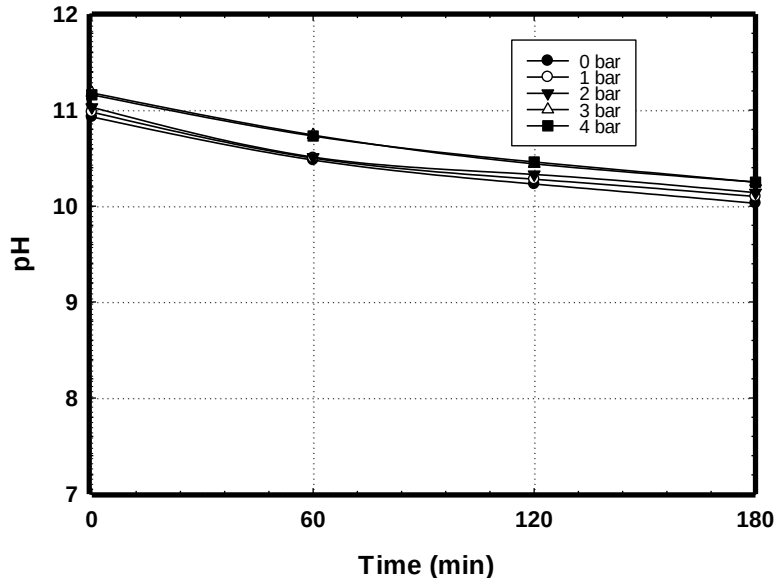

Figure 5.18: pH versus reaction time for different gauge pressures at $3NH_3$:1NaCl molar ratio, temperature of 20 ^oC and gas flow rate of 1L/min.

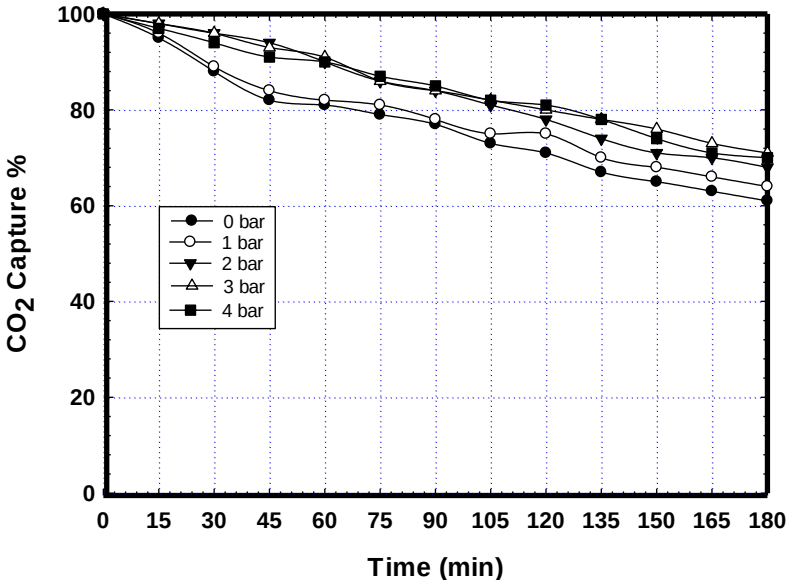

Figure 5.19: CO_2 captured versus reaction time for different gauge pressures at $3NH_3$:1NaCl molar ratio, temperature of 20 ^oC and gas flow rate of 1L/min.

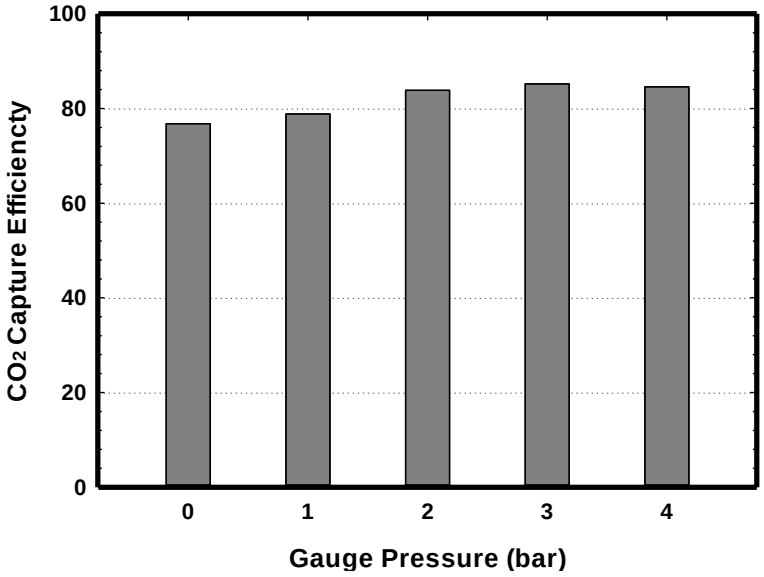

Figure 5.20: CO_2 capture efficiency versus gauge pressure at $3NH_3$:1NaCl molar ratio, temperature of 20 ^oC and gas flow rate of 1L/min.

5.1.11 Effect of ammonium bicarbonate to brine w/w% on ions removal.

The experimental results indicated that by adding ammonium bicarbonate to the treated brine the ions removal increased with increasing the percentage of ammonium bicarbonate to reach the maximum at 20 w/w %, due to increasing the

concentration of (HCO_3^-) by adding more ammonium bicarbonate, which would force the equilibrium in Reaction (2.4.8) to the left and thus lower the solubility of sodium bicarbonate (El-Naas, 2011). Increasing the ammonium bicarbonate to the treated brine w/w % more than 20 % did not have any effect on the ions removal and could be limited by the solubility of ammonium bicarbonate in water (21.6 g/100 g at 20 ^oC) (Zapp et al.). The results are presented in Table A.25 and Figure 5.21.

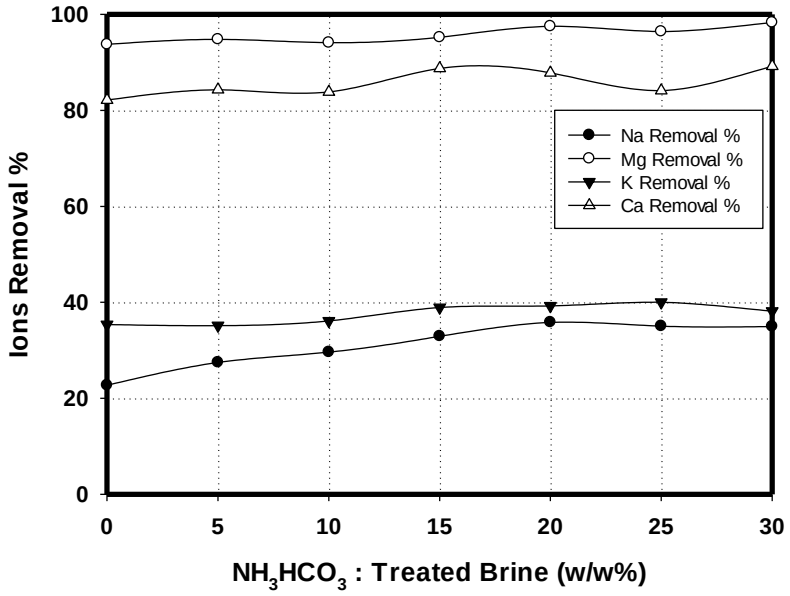

Figure 5.21: Ions removal versus NH_4HCO_3: treated brine w/w % at $3NH_3$:1NaCl molar ratio, temperature of 20^oC and gas flow rate of 1 L/min.

5.2. Statistical Analysis.

The analysis of variance in Minitab 17.0 software was used for regression analysis for the obtained data to estimate the coefficient of the regression equation. The fitted polynomial equation was expressed as 3D surface in order to visualize the relationship between the responses and experimental levels of each factor and to infer the optimum conditions. A total of 20 runs for optimizing the three individual parameters in the central composite design (CCD) were undertaken. Experimental

conditions according to the factorial design are shown in Table 5.1. CCD results show that the CO_2 capture, Na^+, Mg^{+2}, K^+ and Ca^{+2} removal varied in the range of 52.5 – 86.7 %, 12.0 – 33.5 %, 65.4 – 95.3 %, 11.6 – 54.8 % and 58.9 – 94.2 % respectively.

Table 5.1: Full factorial central composite design (CCD) for CO_2 capture and ions removal

Run #	EXP INF			Results									
	X_1 (T)	X_2 (F)	X_3 (M)	CO_2 Capture efficiency		Na^+ %		Mg^{+2} %		K^+ %		Ca^{+2} %	
				Exp	Pred	Exp	Pred	Exp	Pred	Exp	Pred	Exp	Pred
1	30.0	1.5	3.3	80.4	80.4	26.8	27.9	95.3	95.6	39.2	42.4	88.4	87.4
2	30.0	1.5	2.5	70.0	70.8	20.4	20.3	84.8	84.1	29.6	29.3	80.4	81.1
3	30.0	0.7	2.5	71.3	70.7	12.0	12.3	85.6	85.0	11.6	14.8	78.2	79.9
4	20.0	2.0	3.0	75.5	75.6	33.5	32.0	90.1	90.1	54.8	53.7	93.4	94.2
5	40.0	1.0	3.0	67.0	66.9	15.6	14.1	81.7	80.8	21.7	19.3	70.2	69.2
6	30.0	1.5	2.5	70.8	70.8	21.0	20.3	82.9	84.1	28.4	29.3	81.0	81.1
7	40.0	1.0	2.0	54.3	54.3	11.5	12.7	69.8	69.9	22.8	22.6	68.4	66.8
8	40.0	2.0	3.0	64.7	64.1	19.2	19.6	85.4	84.7	26.7	26.5	81.2	81.8
9	30.0	1.5	1.7	65.5	65.5	17.8	17.0	85.8	85.3	22.0	20.7	74.3	76.5
10	20.0	2.0	2.0	70.2	70.4	19.3	20.6	87.7	88.7	23.4	24.5	83.4	83.6
11	30.0	1.5	2.5	72.4	70.8	19.8	20.3	83.6	84.1	31.6	29.3	79.4	81.1
12	13.2	1.5	2.5	82.0	81.0	24.3	24.5	87.3	85.6	33.5	35.1	83.5	83.1
13	30.0	1.5	2.5	71.3	70.8	19.0	20.3	84.8	84.1	28.5	29.3	81.2	81.1
14	30.0	1.5	2.5	70.5	70.8	21.4	20.3	85.1	84.1	30.0	29.3	82.1	81.1
15	20.0	1.0	3.0	86.7	87.4	24.2	24.5	94.7	95.8	36.9	34.3	84.6	85.2
16	20.0	1.0	2.0	75.2	75.8	15.2	14.5	85.9	86.7	14.8	13.7	84.6	83.1
17	30.0	2.3	2.5	63.4	63.9	21.9	22.0	89.4	89.9	31.2	30.0	91.5	91.0
18	46.8	1.5	2.5	52.5	53.3	12.3	12.5	65.4	67.0	19.3	19.6	57.4	59.0
19	30.0	1.5	2.5	69.8	70.8	20.3	20.3	83.7	84.1	27.9	29.3	82.4	81.1
20	40.0	2.0	2.0	58.6	58.0	17.3	16.7	82.5	81.5	19.8	21.2	72.3	70.9

5.2.1 CO_2 capture efficiency.

RSM was undertaken to obtain the process factors and response. The statistical significance was evaluated using the P-value, and the lack-of-fit value of the model. The goodness of fit of the polynomial model was expressed by the

determination coefficient R^2, adjusted R^2 (R-sq adj), and predicted R^2 (R-sq pred). RSM results of CO_2 capture are shown in Table 5.2; the results indicate that the model is significant (P-value < 0.05). The effect of temperature, gas flow rate and molar ratio are significant (P-value < 0.05). The lack-of-fit implies that the fit is significant (P-value > 0.05). The measures of R^2, adjusted R^2 (R^2 adj), and predicted R^2 are close to 1, which implies an adequate model. The model adequacy was further verified by plotting the normal probability and residual plots for the response as shown in Figure 5.22. The residuals analysis shows that there was no evidence of outliers, as all the residuals fell within the range of -1 to + 1 and they are randomly distributed around zero, which indicates a high degree of correlation between the observed values and predicted values. The predicted model of CO_2 capture was obtained by the following second-order polynomial functions:

$$CO_2 \text{ capture} = 97.9 + 1.36\ X_1 - 49.3\ X_2 - 10.5\ X_3 - 0.0153\ X_1^2 - 8.65\ X_2^2 - 0.89\ X_3^2 + 0.127\ X_1.X_2 - 0.278\ X_1.X_3 + 21.47\ X_2.X_3$$

Table 5.2: Response surface regression. CO_2 capture efficiency versus temperature, gas flow rate, and NH_3:NaCl molar ratio

Analysis of Variance

Source	DF	Adj SS	Adj MS	F-Value	P-Value
Model	9	1368.64	152.071	183.27	0.000
Linear	3	1251.00	416.999	502.54	0.000
Temperature	1	926.88	926.885	1117.02	0.000
Flow Rate	1	55.75	55.750	67.19	0.000
Molar Ratio	1	268.36	268.363	323.41	0.000
Square	3	55.48	18.492	22.29	0.000
Temperature*Temperature	1	23.85	23.849	28.74	0.000
Flow Rate*Flow Rate	1	21.99	21.986	26.50	0.000
Molar Ratio*Molar Ratio	1	7.92	7.917	9.54	0.011
2-Way Interaction	3	62.17	20.723	24.97	0.000
Temperature*Flow Rate	1	41.09	41.087	49.52	0.000
Temperature*Molar Ratio	1	0.51	0.505	0.61	0.453
Flow Rate*Molar Ratio	1	20.58	20.576	24.80	0.001
Error	10	8.30	0.830		
Lack-of-Fit	5	3.77	0.753	0.83	0.578
Pure Error	5	4.53	0.907		
Total	19	1376.94			

Model Summary

S	R-sq	R-sq(adj)	R-sq(pred)
0.910924	99.40%	98.86%	97.45%

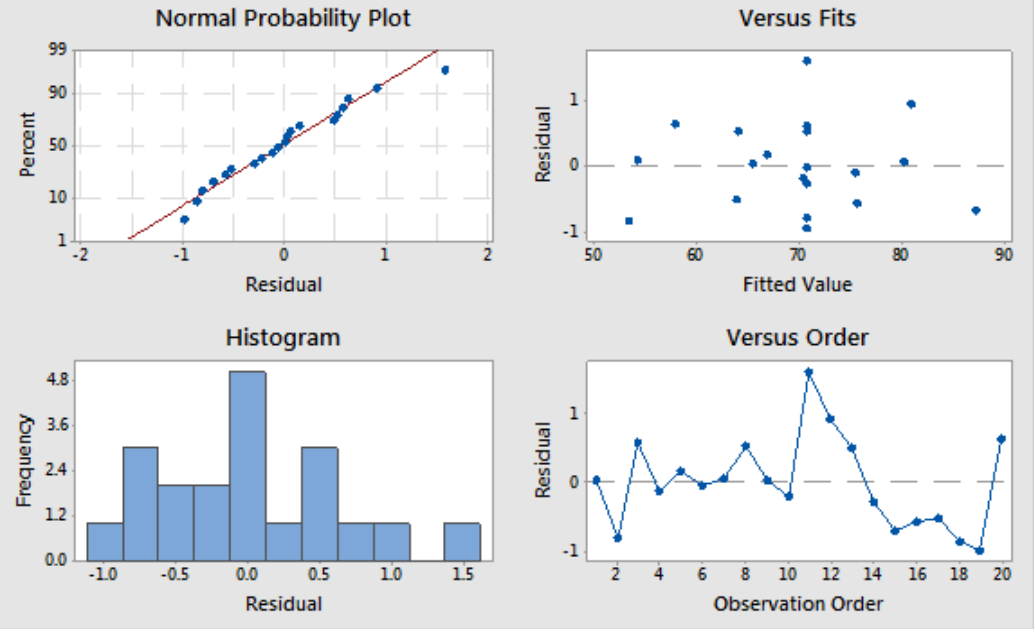

Figure 5.22: Residual plots for CO_2 capture efficiency

5.2.2. Ions removal

RSM results of the Na^+, Mg^{+2}, K^+ and Ca^{+2} removal are shown in Tables 5.3, A.26, A.27 and A.28, respectively. The results indicate the model is significant (P-value < 0.05). The effect of temperature, gas flow rate and NH_3:NaCl molar ratio are significant (P-value < 0.05) . The lack-of-fit implies that the fit is significant (P-value > 0.05). The measures of R^2, adjusted R^2, and predicted R_2 are close to 1, which implies an adequate model. The model adequacy was further verified by plotting the normal probability and residual plots for the response as shown in Figures 5.23, B.1, B.2 and B.3. The residuals analysis shows that there was no evidence of outliers as all the residuals fell within the range of -1 to + 1 and they were randomly distributed around zero, which indicates a high degree of correlation between the observed values and predicted values. The predicted model of ions removal was obtained by the following second-order polynomial functions:

$$Na^+ \text{ Removal } \% = -22.0 + 1.254\ X_1 + 18.76\ X_2 + 1.93\ X_3 - 0.00639\ X_1^2 - 4.49\ X_2^2 + 3.07\ X_3^2 - 0.1019\ X_1X_2 - 0.4296\ X_1X_3 + 1.41\ X_2X_3$$

$$Mg^{+2}\ \text{Removal \%} = 22.1 + 0.160\ X_1 - 6.29\ X_2 - 29.81\ X_3 - 0.02774\ X_1^2 + 4.67\ X_2^2 + 8.94\ X_3^2 + 0.4793\ X_1 X_2 + 0.0922\ X_1 X_3 - 7.66\ X_2 X_3$$

$$K^{+}\ \text{Removal \%} = -96.0 + 3.861\ X_1 + 35.1\ X_2 + 20.0\ X_3 - 0.00689\ X_1^2 - 9.79\ X_2^2 + 3.16\ X_3^2 - 0.613\ X_1 X_2 - 1.195\ X_1 X_3 + 8.66\ X_2 X_3$$

$$Ca^{+2}\ \text{Removal \%} = 106.9 + 1.115\ X_1 - 38.56\ X_2 - 12.76\ X_3 - 0.03555\ X_1^2 + 6.14\ X_2^2 + 1.21\ X_3^2 + 0.179\ X_1 X_2 + 0.013\ X_1 X_3 + 8.54\ X_2 X_3$$

Table 5.3: Response surface regression. Na^{+} removal % versus temperature, gas flow rate, and molar ratioNH_3:NaCl

Analysis of Variance

Source	DF	Adj SS	Adj MS	F-Value	P-Value
Model	9	505.629	56.181	39.87	0.000
Linear	3	430.893	143.631	101.93	0.000
Temperature	1	173.590	173.590	123.19	0.000
Flow Rate	1	113.791	113.791	80.75	0.000
Molar Ratio	1	143.513	143.513	101.84	0.000
Square	3	34.747	11.582	8.22	0.005
Temperature*Temperature	1	5.884	5.884	4.18	0.068
Flow Rate*Flow Rate	1	18.128	18.128	12.86	0.005
Molar Ratio*Molar Ratio	1	8.465	8.465	6.01	0.034
2-Way Interaction	3	39.989	13.330	9.46	0.003
Temperature*Flow Rate	1	2.076	2.076	1.47	0.253
Temperature*Molar Ratio	1	36.916	36.916	26.20	0.000
Flow Rate*Molar Ratio	1	0.998	0.998	0.71	0.420
Error	10	14.092	1.409		
Lack-of-Fit	5	10.398	2.080	2.82	0.140
Pure Error	5	3.693	0.739		
Total	19	519.721			

Model Summary

S	R-sq	R-sq(adj)	R-sq(pred)
1.18709	97.29%	94.85%	81.68%

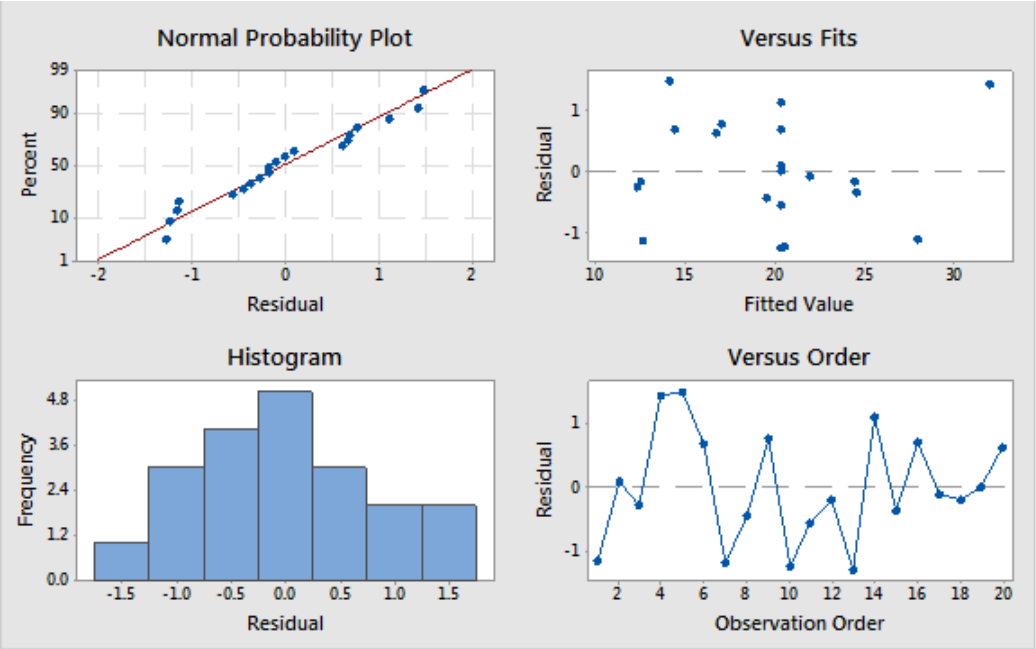

Figure 5.23: Residual Plots for Na^+ removal %

4.2.3 Models validation.

The model equations for predicting the optimum response values were tested using the selected conditions to confirm the RSM validity. Two confirmation experiments were applied with temperature, gas flow rate and NH_3:NaCl molar ratio chosen randomly from the ranges of Table 4.2 to validate the mathematical models. Table 5.4 shows the experimental values, predicted values and 95% Confidence Interval (95% CI) for CCD. Figures 5.24, 5.25, B.4, B.5 and B.6 show the actual and predicted values for CO_2 capture efficiency, Na^+, Mg^{+2}, K^+ and Ca^{+2} removal, respectively. The results demonstrate that the developed models can successfully predict the capture efficiency and ions removal using the Solvay method.

Table 5.4: Validity results by RSM for CCD

	X_1=T	X_2=F	X_3=M	Results	CO_2 capture efficiency %	Na^+ removal %	Mg^{+2} removal %	K^+ removal %	Ca^{+2} removal %
CCD	15.0	0.800	3.0	Exp.	90.0	20.0	96.6	29.0	80.3
				Pred.	92.8	22.9	99.5	28.4	84.6
				95% CI	89.9-95.7	19.2-26.7	95.6-100	21.0-35.8	79.4-89.8
	32.0	1.300	2.0	Exp.	65.9	15.0	81.2	20.5	77.9
				Pred.	65.1	16.0	80.3	22.4	76.3
				95% CI	64.1-66.0	14.8-17.3	79.0-81.7	19.9-24.9	74.5-78.0

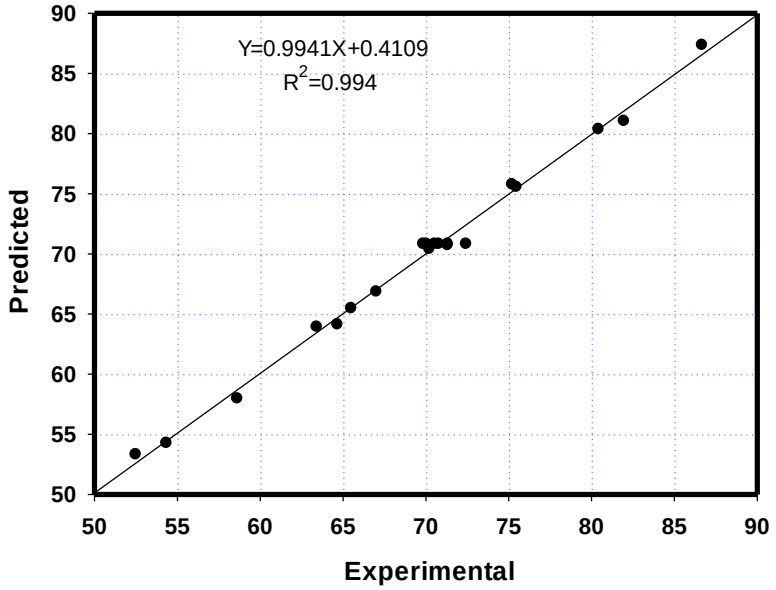

Figure 5.24: Relationship between experimental and predicted values for CO_2 capture efficiency.

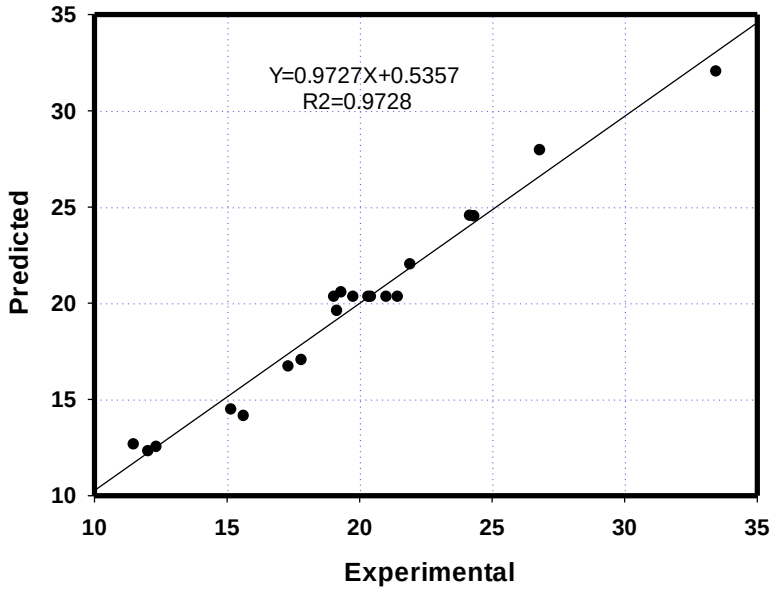

Figure 5.25: Relationship between experimental and predicted values for Na^+ removal.

5.2.4. CO_2 capture and ions removal optimization.

Process optimization was implemented to find the conditions under which maximum CO_2 capture efficiency and ions removal would be possible. The optimal values of the selected variables were obtained using response optimizer, and the optimum CO_2 capture efficiency and ions removal was found to be at a temperature of 19.3^oC, a gas flow rate of 1.544 L/min, and a molar ratio of 3.3NH_3:1NaCl as shown in Figure 5.26. The optimum conditions have been tested experimentally to find the CO_2 capture efficiency and ions removal. As shown in Table 5.5, the experimental values and predicted values are very close and within the 95% Confidence Interval.

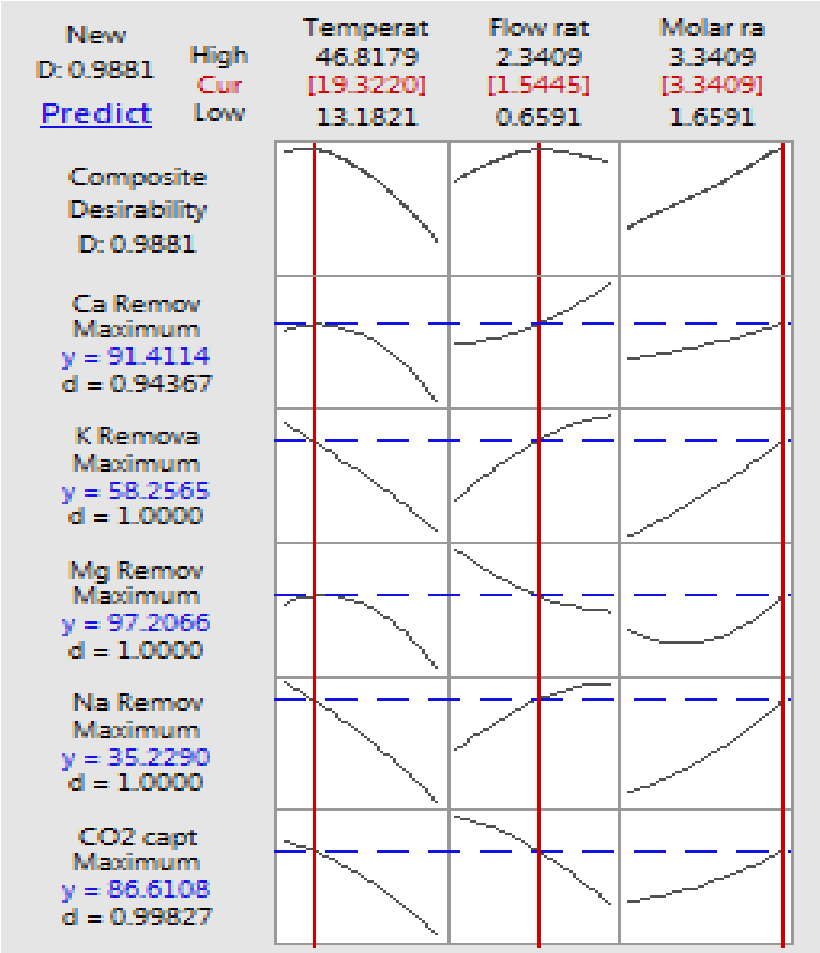

Figure 5.26: The optimum temperature, flow rate and NH_3:NaCl molar ratio to have maximum CO_2 capture efficiency and Na^+, Mg, K and Ca removal.

Table 5.5: Predicted and experimental CO_2 capture and ions removal at the optimum conditions.

X_1=T	X_2=F	X_3=M	Results	CO_2 capture efficiency	Na^+ removal %	Mg^{+2} removal %	K^+ removal %	Ca^{+2} removal %
19.3	1.544	3.3	Exp.	86.2	33.0	98.0	56.4	89.7
			Pred.	86.6	35.2	97.2	58.3	91.4
			95% CI	84.5-88.8	32.5-38.0	94.3-100.1	52.8-63.7	87.6- 95.2

5.2.5 Effect of temperature and gas flow rate

The effects of temperature on all responses and their interactions can be represented through 3D response surface plots. Figures 5.27, 5.28, B.7, B.8 and B.9 represents the maximum CO_2 capture efficiency and ions (Na^+, Mg^{+2}, K^+, Ca^{+2})

removal against temperature X_1 and flow rate X_2 while keeping the NH_3:NaCl molar ratio constant. An increase in the ions removal and CO_2 capture efficiency could be achieved when the value of temperature was decreased from 46.8 to 13.2 ^oC. The maximum CO_2 capture efficiency, and ions removal (Na^+, Mg^{+2}, K^+, Ca^{+2}) were 82.0, 24.3, 87.3, 33.5 and 83.5%, respectively. It is clear that increasing the temperature has a major effect on the CO_2 capture, Na^+ removal and K^+ removal as discussed in Sections (5.1.5 and 5.1.6); however this effect is less on the Mg^{+2} removal; since adding ammonia to the brine will precipitate magnesium hydroxide immediately out from the solution, and hence the removal of magnesium will be high even before passing CO_2 into the reactor; so the effect of increasing temperature will be only on the magnesium hydroxide part which reacts further with CO_2 to produce magnesium bicarbonate (Michael Clugston, 2000). Figures 5.29, 5.30, B.10, B.11 and B.12 show the maximum CO_2 capture efficiency and ions (Na^+, Mg^{+2}, K^+, Ca^{+2}) removal against flow rate X_2 and NH_3:NaCl molar ratio X_3, while keeping the temperature X_1 constant. A 6% to 10% increasing in ions removal could be achieved when the value of flow rate increased from 0.659 to 2.341 L/min according to the increase in the CO_2 loading as discussed in Section (5.1.7). However the CO_2 capture efficiency decreased 10% with increasing the flow rate to 2.341 L/min and this is mainly due to reducing the gas resistance time in the reactor as discussed in Section (5.1.8).

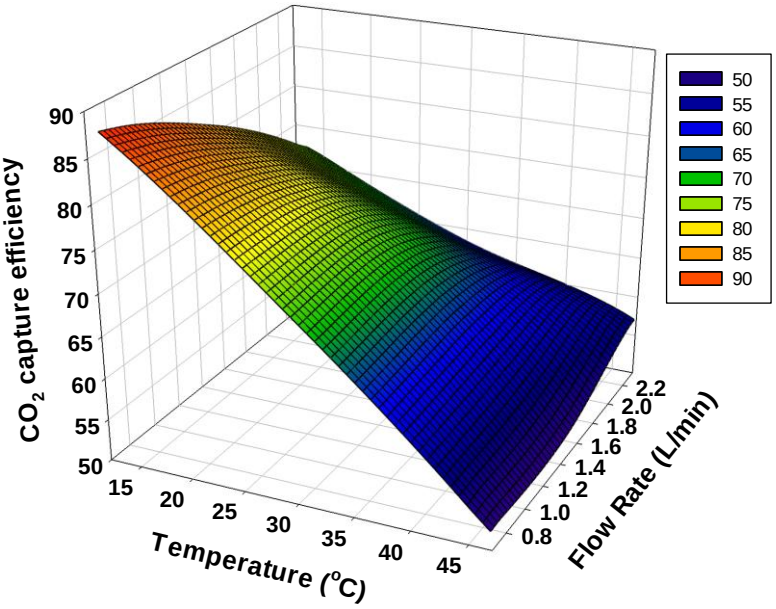

Figure 5.27: CO_2 capture efficiency on 3-D graphics for response surface optimization versus temperature and gas flow rate.

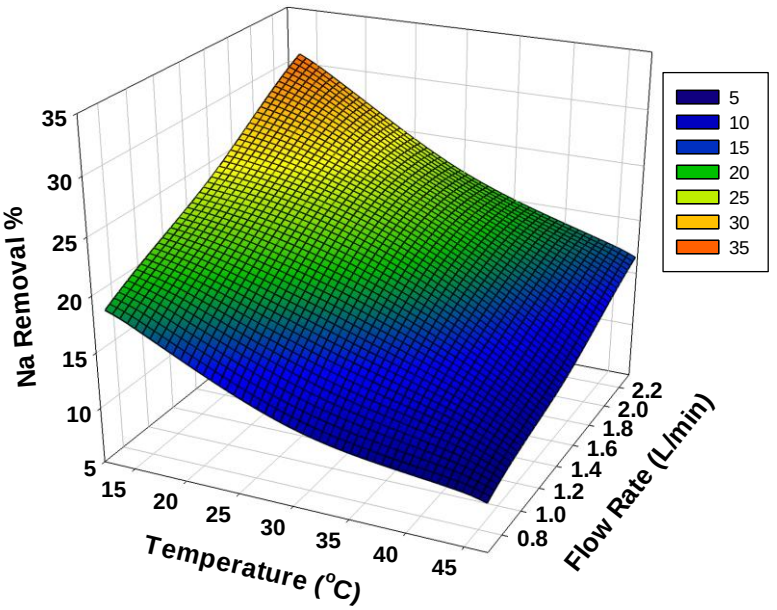

Figure 5.28: Na^+ removal % on 3-D graphics for response surface optimization versus temperature and gas flow rate.

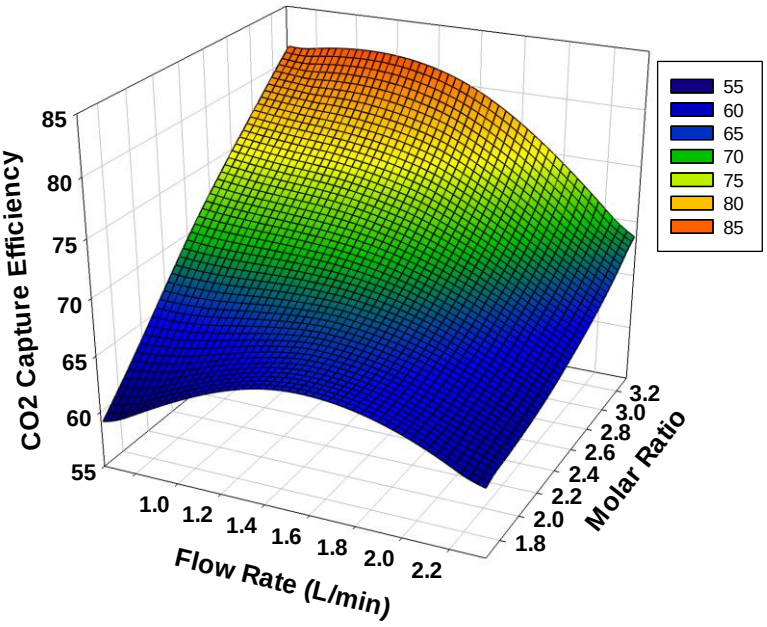

Figure 5.29: CO_2 capture efficiency on 3-D graphics for response surface optimization versus gas flow rate and NH_3:NaCl molar ratio

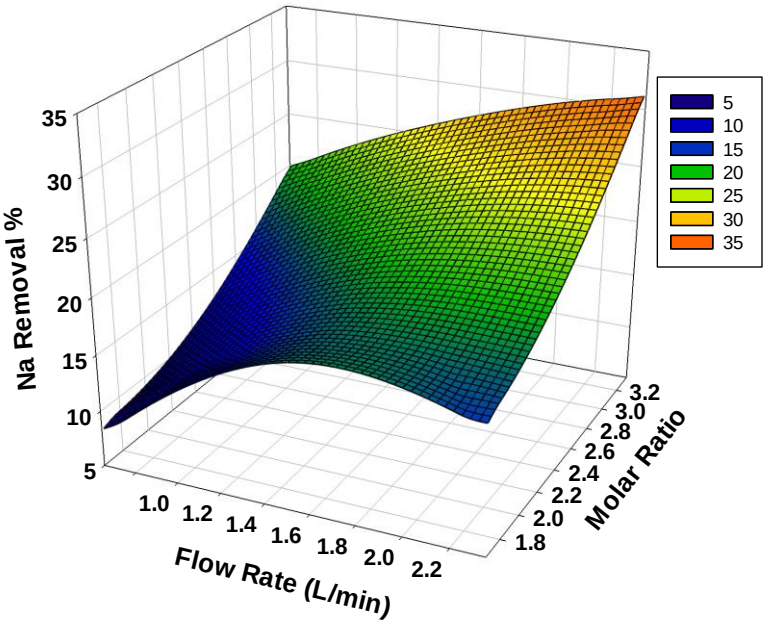

Figure 5.30: Na^+ removal % on 3-D graphics for response surface optimization versus gas flow rate and NH_3:NaCl molar ratio

5.2.6. Effect of NH_3: NaCl molar ratio.

Figures 5.31, 5.32, B.13, B.14 and B.15 present the maximum CO_2 capture efficiency and ions (Na^+, Mg^{+2}, K^+, Ca^{+2}) removal against molar ratio X_3 and flow rate X_2, while keeping the temperature X_1 constant. Increasing in ions removal and CO_2 capture efficiency could be achieved by increasing the molar ratio from 1.7 to 3.3 NH_3:1NaCl. The maximum CO_2 capture efficiency, and ions removal (Na^+, Mg^{+2}, K^+, Ca^{+2}) was 82.0, 26.8, 95.3, 39.2 and 88.4 % respectively, at molar ratio of 3.3NH_3:1NaCl. However high Mg and Ca removal were obtained at low NH_3:NaCl molar ratio. For magnesium it is clear that the major part of removal occurs before reaction with CO_2, since magnesium hydroxide precipitates directly after mixing with ammonia as discussed in Section (5.2.5); another reason is that magnesium has minimum solubility as bicarbonate product (0.106 g $Mg(HCO_3)_2$/1L in water at 20 ^oC). Regarding calcium ions which exist in low concentration in the feed brine, low molar ratio of ammonia is enough for complete forward reaction. However potassium removal was not as calcium removal even of the low initial concentration for both ions; this may be explained by the high solubility as bicarbonate product (337 g $KHCO_3$ /1L in water at 20 ^oC) comparing with (166 g $Ca(HCO_3)_2$ /1L in water at 20 ^oC). The minimum removal was observed for sodium even at high NH_3:NaCl molar ratio. This can be explained by the high volatility of NH_3, high initial sodium concentration and the relatively high solubility as bicarbonate product (Michael Clugston, 2000).

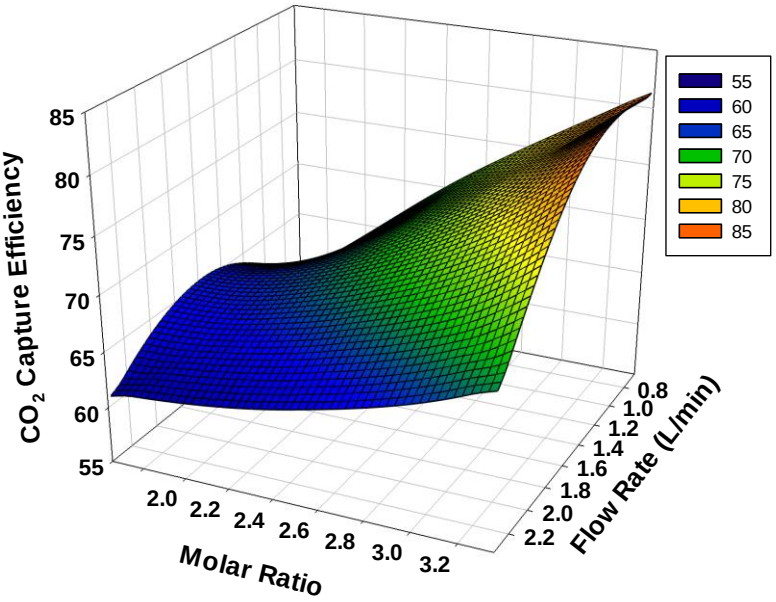

Figure 5.31: CO_2 capture efficiency on 3-D graphics for response surface optimization versus NH_3:NaCl molar ratio and gas flow rate**.**

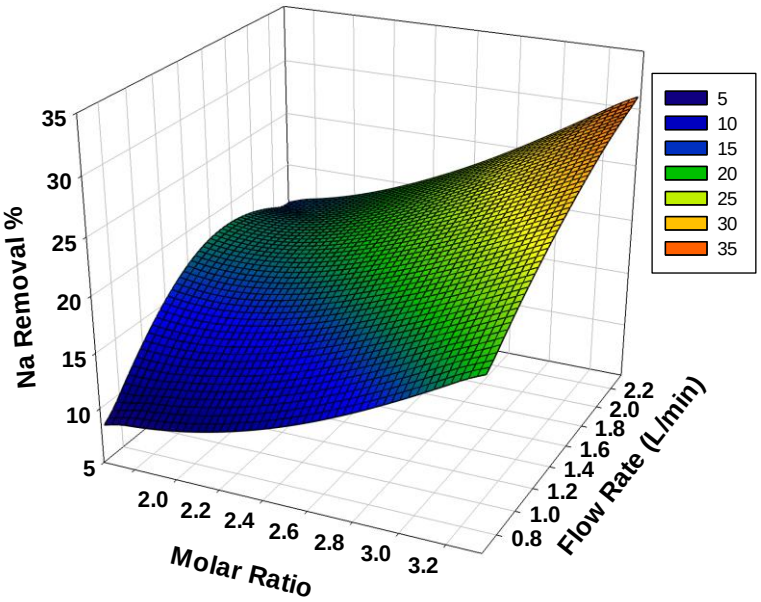

Figure 5.32: Na^+ removal on 3-D graphics for response surface optimization versus NH_3:NaCl molar ratio and gas flow rate.

5.3 Continuous Solvay process

5.3.1 Effect of liquid residence time on the ions removal

Continuous experiments were carried out at different liquid flow rate (50, 25, 16.7 and 12.5 ml/min); the results indicated that ions removal reached the maximum at the lowest liquid flow rate of 12.5 ml/min (4 hrs residence time). As expected, longer residence time results in higher removal since the gas will have more contact time with the ammoniated brine in the reactor. However the effect on the Na^+ and K^+ removal seemed to be more pronounced due to direct effect on the precipitation of sodium bicarbonate. At liquid flow rate of 12.5 ml/min, the increasing in the Na^+ and K^+ removals after one hour of reaction are 55% and 47% respectively. The Mg^{+2} removal seems to be not affected much by the liquid residence time, which can be explained by the precipitation of magnesium hydroxide as discussed in Section (5.2.5). The results are presented in Table A.29 and shown in Figures 5.33-5.36.

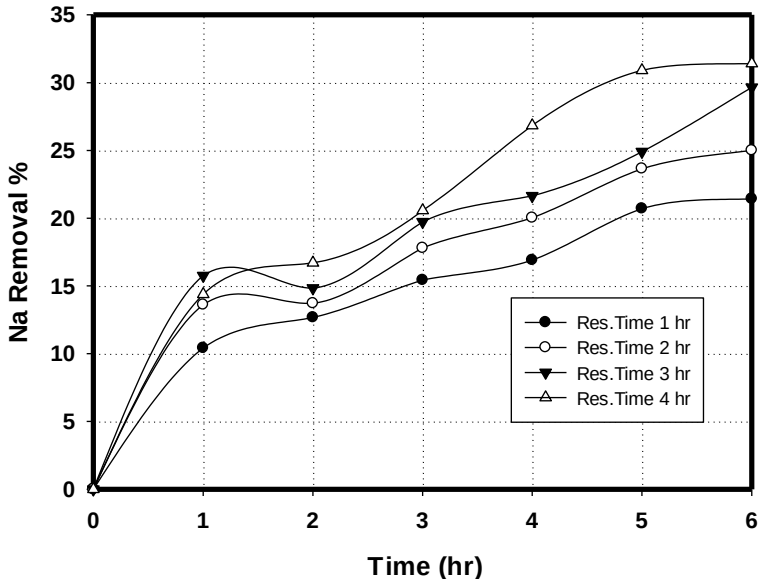

Figure 5.33: Na^+ removal versus reaction time for different liquid residence times at a temperature of 19.3 °C, molar ratio of $3.3NH_3$:1NaCl, and a gas flow rate of 1.544 L/min.

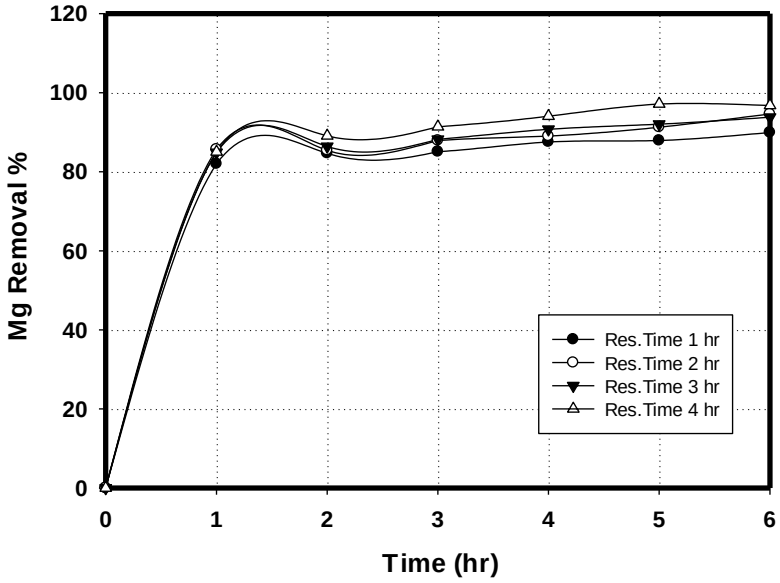

Figure 5.34: Mg^{+} removal versus reaction time for different liquid residence times at a temperature of 19.3 °C, molar ratio of $3.3NH_3$:1NaCl, and a gas flow rate of 1.544 L/min.

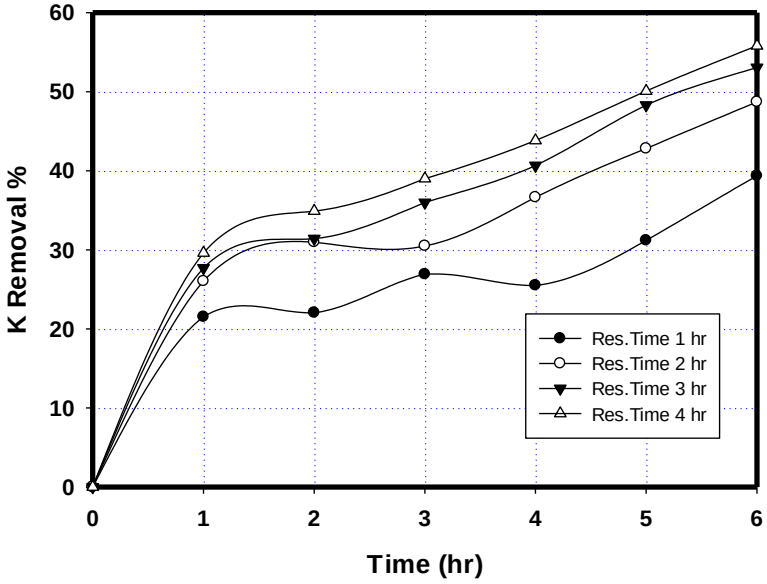

Figure 5.35: K^{+} removal versus reaction time for different liquid residence times at a temperature of 19.3 °C, molar ratio of $3.3NH_3$:1NaCl, and a gas flow rate of 1.544 L/min.

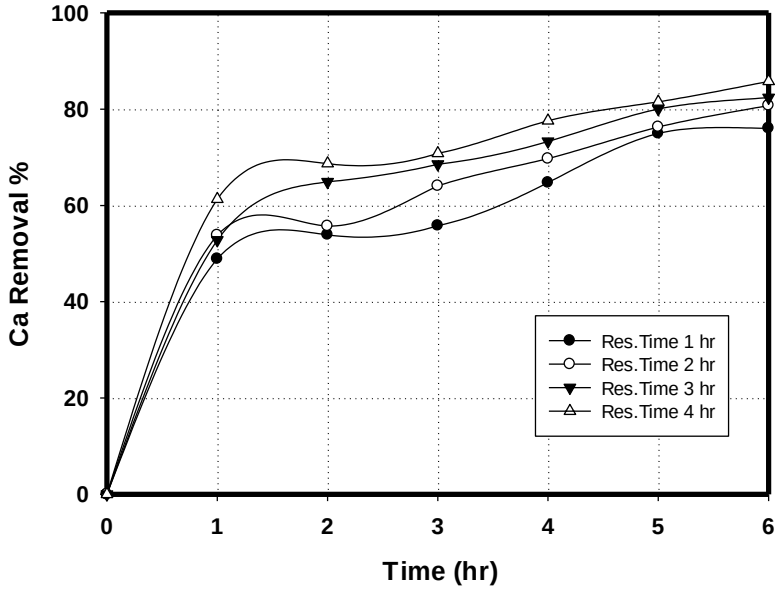

Figure 5.36: Ca^{+2} removal versus reaction time for different liquid residence times at a temperature of 19.3 °C, molar ratio of $3.3NH_3$:1NaCl, and a gas flow rate of 1.544 L/min.

5.3.2 Effect of liquid residence time on pH and CO_2 capture efficiency.

Contrary to the ions removal, the continuous experimental results indicated that the maximum CO_2 capture was obtained at the maximum liquid flow rate (1 hr liquid residence time), since lower liquid residence time resulted in higher pH level as more fresh ammoniated brine entered the reactor per unit time and hence more CO_2 would be captured. The results are presented in Tables A.30 and A.31 and shown in Figures 5.37-5.39.

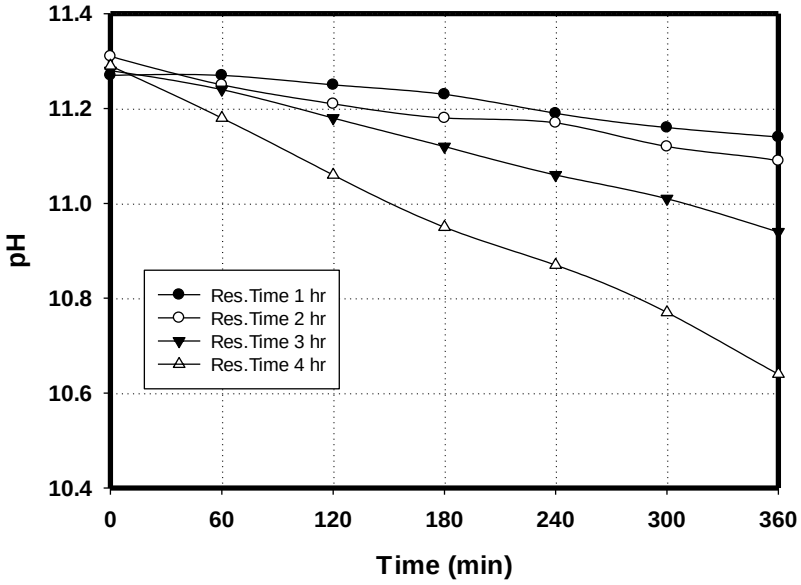

Figure 5.37: pH versus reaction time for different liquid residence times at a temperature of 19.3 °C, molar ratio of 3.3NH_3:1NaCl, and a gas flow rate of 1.544 L/min.

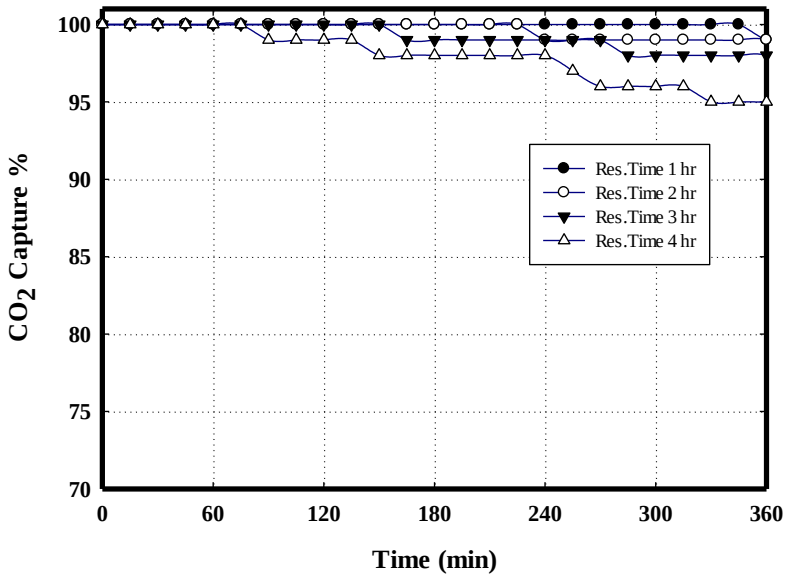

Figure 5.38: CO_2 capture versus reaction time for different liquid residence times at a temperature of 19.3 °C, molar ratio of 3.3NH_3:1NaCl, and a gas flow rate of 1.544 L/min.

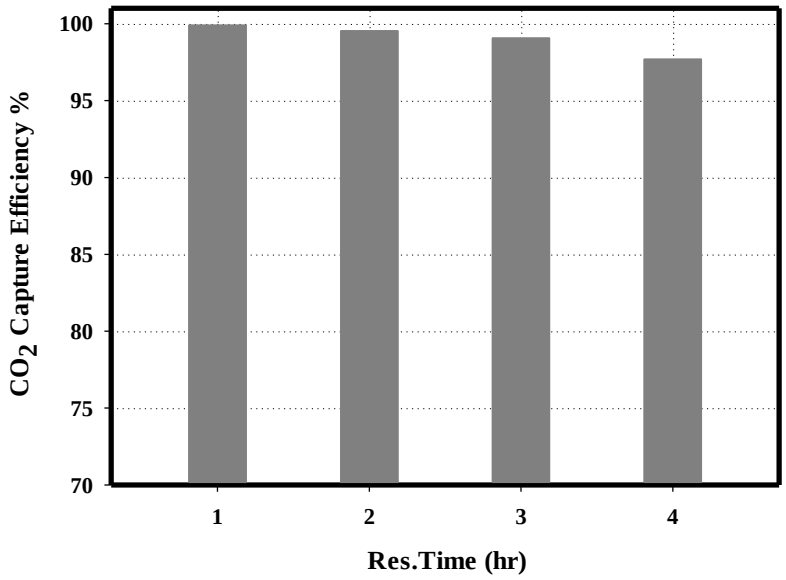

Figure 5.39: CO_2 capture efficiency versus liquid residence time at a temperature of 19.3 °C, molar ratio of 3.3NH_3:1NaCl, and a gas flow rate of 1.544 L/min.

5.3.3 Steady state in continuous Solvay process

Long continuous runs were carried out to assess the stability of the reactor and evaluate the steady state. The results indicated that the CO_2 capture and ions removal reached the maximum and stabilized after 240-300 minutes, at gas and liquid flow rates of 1.544 L/min and 12.5 ml/min, respectively, with a gas-to-liquid ratio of 123. Steady CO_2 capture and ions removal was recorded after this time for about three hours. The total CO_2 capture efficiency in 480 min was equal to 97.9% and maximum sodium removal was 32.45%. The results are presented in Tables A.32 and A.33 and shown in Figures 5.40 and 5.41.

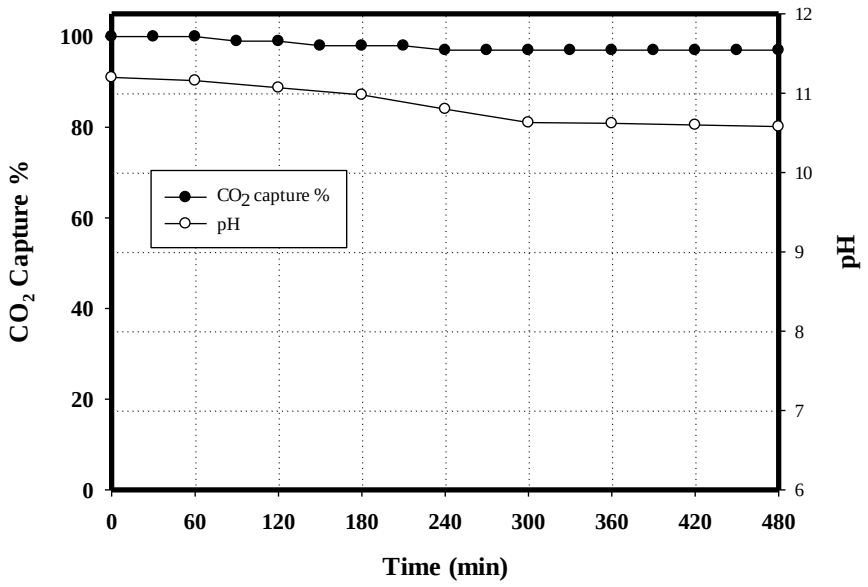

Figure 5.40: CO_2 capture and pH versus reaction time at a temperature of 19.3 °C, molar ratio of $3.3NH_3$:1NaCl, a gas flow rate of 1.544 L/min, and a liquid flow rate of 12.5 ml/min.

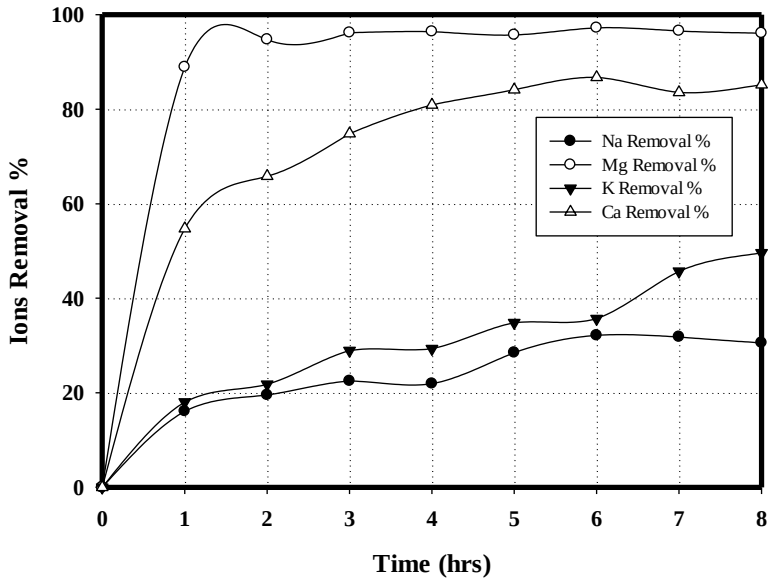

Figure 5.41: Ions removal versus reaction time at a temperature of 19.3 °C, molar ratio of $3.3NH_3$:1NaCl, a gas flow rate of 1.544 L/min and a liquid flow rate of 12.5 ml/min.

Chapter 6: *Conclusions & Recommended Future Work*

6.1. Conclusions

The Solvay process showed a feasible way to protect the environment by utilizing reject brine and industrial waste gases. This process has the dual benefit of decreasing sodium in the reject brine and reducing carbon dioxide emissions to the atmosphere. The objectives of the present work were to optimize the desalination of the reject brine and CO_2 capture based on the Solvay process in semi-batch and continuous mode. Process parameters were studied in semi-batch and continuous mode to determine their effect on CO_2 capture efficiency and ions removal. These parameters included: reaction time, temperature, gas flow rate, ammonia to sodium chloride molar ratio, pressure and ammonium bicarbonate to treated brine w/w%. The process yielded high CO_2 capture efficiency and low brine salinity. Below is a summary of the study's major conclusions:

1- Increasing ammonia to sodium chloride molar ratio increases the initial pH of brine mixture and consequently increases the CO_2 capture efficiency and ions removal.
2- The ions removal increased with increasing the reaction temperature reaching a maximum at temperature range of 20-30 ^{o}C; the reversibility of Solvay process reactions has been observed beyond this temperature range.
3- The CO_2 capture increased with decreasing the temperature due to increasing the CO_2 solubility in the brine.

4- By increasing the gas flow rate, the CO_2 loading increased, and hence the ions removal increased. However, flow rates higher than 2 L/min have a negative effect, since the residence time for CO_2 in the reactor will decrease.

5- The CO_2 capture increased with decreasing the gas flow rate due to the increase in the gas residence time.

6- CO_2 capture was improved by increasing the gauge pressure due to the increasing in CO_2 solubility.

7- The addition of ammonium bicarbonate to the treated brine effluent has a significant effect on the possibility of using the Solvay process, since it reduces the solubility of bicarbonate products and hence increases the ions removal.

8- Second order polynomial equations were adequate to predict the ions removal and CO_2 capture efficiency within three independent variables: ammonia to sodium chloride molar ratio, temperature and gas flow rate. All three variables indicated significant effect on the ions removal and CO_2 capture efficiency.

9- Analysis of variance for the sodium removal and CO_2 capture efficiency provides a determination coefficient (R^2) as 97.3% and 99.4% respectively. These values indicate that the model has an excellent fit.

10- The optimum CO_2 capture efficiency and ions removal was found to be at temperature of 19.3^oC, flow rate of 1.544 L/min, and molar ratio of $3.3NH_3$:1NaCl.

11- In the continuous Solvay process maximum ions removal were found at a liquid flow rate of 12.5 ml/min (4 hours residence time). The reaction reached

the steady state after four hours, the total CO_2 capture efficiency in 480 minutes equals to 97.9% and the maximum sodium removal was 32.5%.

6.2. Recommended Future Work

Based on the experimental results, the following future studies are recommended:

1. Carry out numerical modeling for the CO_2 capture and ions removal at different operating conditions

2. Expand the study into a pilot-scale to evaluate its performance at different operating conditions.

Bibliography

Abanades, J. C., 2013, 21 - Calcium looping for CO_2 capture in combustion systems, Fluidized Bed Technologies for Near-Zero Emission Combustion and Gasification, Woodhead Publishing, p. 931-970.

Adeosun, A., and M. R. M. Abu-Zahra, 2013, Evaluation of amine-blend solvent systems for CO2 post-combustion capture applications: Energy Procedia, v. 37, p. 211-218.

Afkhamipour, M., and M. Mofarahi, 2014, Sensitivity analysis of the rate-based CO_2 absorber model using amine solutions (MEA, MDEA and AMP) in packed columns: International Journal of Greenhouse Gas Control, v. 25, p. 9-22.

Ahmad, N., and R. E. Baddour, 2014, A review of sources, effects, disposal methods, and regulations of brine into marine environments: Ocean & Coastal Management, v. 87, p. 1-7.

Ahmed, M., W. H. Shayya, D. Hoey, A. Mahendran, R. Morris, and J. Al-Handaly, 2000, Use of evaporation ponds for brine disposal in desalination plants: Desalination, v. 130, p. 155-168.

Al-Faifi, H., A. M. Al-Omran, M. Nadeem, A. El-Eter, H. A. Khater, and S. E. El-Maghraby, 2010, Soil deterioration as influenced by land disposal of reject brine from Salbukh water desalination plant at Riyadh, Saudi Arabia: Desalination, v. 250, p. 479-484.

Al-Marzouqi, M., M. El-Naas, S. Marzouk, and N. Abdullatif, 2008, Modeling of chemical absorption of CO_2 in membrane contactors: Separation and Purification Technology, v. 62, p. 499-506.

Ali, E., M. K. Hadj-Kali, S. Mulyono, I. Alnashef, A. Fakeeha, F. Mjalli, and A. Hayyan, 2014, Solubility of CO_2 in deep eutectic solvents: experiments and modelling using the peng-robinson equation of state: Chemical Engineering Research and Design.

Anderson-Cook, C. M., C. M. Borror, and D. C. Montgomery, 2009a, Rejoinder for "Response surface design evaluation and comparison": Journal of Statistical Planning and Inference, v. 139, p. 671-674.

Anderson-Cook, C. M., C. M. Borror, and D. C. Montgomery, 2009b, Response surface design evaluation and comparison: Journal of Statistical Planning and Inference, v. 139, p. 629-641.

Antony, J., 2014, 6 - Full Factorial Designs, *in* J. Antony, ed., Design of Experiments for Engineers and Scientists (Second Edition): Oxford, Elsevier, p. 63-85.

Bai HL, Chin Y. A., 1997, Removal of CO_2 greenhouse gas by ammonia scrubbing: Ind Eng Chem Res 1997;36:2490–3.

Beecy, D. J., and S. Klara, 2003, The U.S. Department of Energy Carbon Sequestration Research, Development and Demonstration Program, *in* J. Gale, and Y. Kaya, eds., Greenhouse Gas Control Technologies - 6th International Conference: Oxford, Pergamon, p. 297-302.

Bennaceur, K., 2014, Chapter 26 - CO_2 Capture and Sequestration, *in* T. M. Letcher, ed., Future Energy (Second Edition): Boston, Elsevier, p. 583-611.

Breunig, H. M., J. T. Birkholzer, A. Borgia, C. M. Oldenburg, P. N. Price, and T. E. McKone, 2013, Regional evaluation of brine management for geologic carbon sequestration: International Journal of Greenhouse Gas Control, v. 14, p. 39-48.

Brunetti, A., F. Scura, G. Barbieri, and E. Drioli, 2010, Membrane technologies for CO2 separation: Journal of Membrane Science, v. 359, p. 115-125.

Bryngelsson, M., and M. Westermark, 2009, CO2 capture pilot test at a pressurized coal fired CHP plant: Energy Procedia, v. 1, p. 1403-1410.

Budd, P. M., K. J. Msayib, C. E. Tattershall, B. S. Ghanem, K. J. Reynolds, N. B. McKeown, and D. Fritsch, 2005, Gas separation membranes from polymers of intrinsic microporosity: Journal of Membrane Science, v. 251, p. 263-269.

Burchell, T. D., and R. R. Judkins, 1996, Passive CO_2 removal using a carbon fiber composite molecular sieve: Energy Conversion and Management, v. 37, p. 947-954.

Butler, J. N., 1982, Carbon dioxide equilibria and their applications, *in* Addison-Wesley, ed.

Calvo, L. M., and R. Domingo, 2014, Influence of process operating parameters on CO_2 emissions in continuous industrial plants: Journal of Cleaner Production.

Carroll, A. G., R. Przeslawski, L. C. Radke, J. R. Black, K. Picard, J. W. Moreau, R. R. Haese, and S. Nichol, 2013, Environmental considerations for subseabed geological storage of CO_2: A review: Continental Shelf Research.

Chacartegui, R., D. Sánchez, N. di Gregorio, F. J. Jiménez-Espadafor, A. Muñoz, and T. Sánchez, 2009, Feasibility analysis of a MED desalination plant in a combined cycle based cogeneration facility: Applied Thermal Engineering, v. 29, p. 412-417.

Chen, W.-H., Y.-L. Hou, and C.-I. Hung, 2012, Influence of droplet mutual interaction on carbon dioxide capture process in sprays: Applied Energy, v. 92, p. 185-193.

Choi, B. G., H. S. Park, G. H. Kim, Y. M. Jung, K. B. Yi, J.-N. Kim, and W. H. Hong, 2012, Analysis of CO2–NH3 reaction dynamics in an aqueous phase by PCA and 2D IR COS: Journal of Industrial and Engineering Chemistry, v. 18, p. 98-104.

Dave, N., T. Do, G. Puxty, R. Rowland, P. H. M. Feron, and M. I. Attalla, 2009, CO_2 capture by aqueous amines and aqueous ammonia–A Comparison: Energy Procedia, v. 1, p. 949-954.

den Elzen, M., M. Meinshausen, and D. van Vuuren, 2007, Multi-gas emission envelopes to meet greenhouse gas concentration targets: Costs versus certainty of limiting temperature increase: Global Environmental Change, v. 17, p. 260-280.

Diao, Y.-F., X.-Y. Zheng, B.-S. He, C.-H. Chen, and X.-C. Xu, 2004, Experimental study on capturing CO_2 greenhouse gas by ammonia scrubbing: Energy Conversion and Management, v. 45, p. 2283-2296.

El-Naas, M. H., Reject Brine Management, in Desalination, Trends and Technologies, Edited by: Michael Schorr, Publisher: InTech, February 2011; ISBN 978-953-307-311-8.

El-Naas, M. H., A. H. Al-Marzouqi, and O. Chaalal, 2010, A combined approach for the management of desalination reject brine and capture of CO2: Desalination, v. 251, p. 70-74.

Fahim, M. A., T. A. Alsahhaf, and A. Elkilani, 2010, Chapter 17 - Environmental Aspects in Refining, *in* M. A. Fahim, T. A. Alsahhaf, and A. Elkilani, eds., Fundamentals of Petroleum Refining: Amsterdam, Elsevier, p. 423-455.

Gaspar, J., and A.-M. Cormos, 2012, Dynamic modeling and absorption capacity assessment of CO_2 capture process: International Journal of Greenhouse Gas Control, v. 8, p. 45-55.

Gelowitz, D., W. Kritpiphat, and P. Tontiwachwuthikul, 1995, Cogeneration concepts for CO2 separation from power plants for enhanced oil recovery applications: Energy Conversion and Management, v. 36, p. 563-566.

Greenlee, L. F., D. F. Lawler, B. D. Freeman, B. Marrot, and P. Moulin, 2009, Reverse osmosis desalination: Water sources, technology, and today's challenges: Water Research, v. 43, p. 2317-2348.

Hashimoto, K., M. Yamasaki, K. Fujimura, T. Matsui, K. Izumiya, M. Komori, A. A. El-Moneim, E. Akiyama, H. Habazaki, N. Kumagai, A. Kawashima, and K. Asami, 1999, Global CO_2 recycling—novel materials and prospect for prevention of global warming and abundant energy supply: Materials Science and Engineering: A, v. 267, p. 200-206.

He, X., C. Fu, and M.-B. Hägg, 2015, Membrane system design and process feasibility analysis for CO2 capture from flue gas with a fixed-site-carrier membrane: Chemical Engineering Journal, v. 268, p. 1-9.

Hedin, N., L. Andersson, L. Bergström, and J. Yan, 2013, Adsorbents for the post-combustion capture of CO_2 using rapid temperature swing or vacuum swing adsorption: Applied Energy, v. 104, p. 418-433.

Herzog, H., K. Caldeira, and E. Adams, 2001, Carbon Sequestration Via Direct Injection, *in* J. H. Steele, ed., Encyclopedia of Ocean Sciences: Oxford, Academic Press, p. 408-414.

Herzog, H., and D. Golomb, 2004, Carbon Capture and Storage from Fossil Fuel Use, *in* C. J. Cleveland, ed., Encyclopedia of Energy: New York, Elsevier, p. 277-287.

Ho, S.-H., C.-Y. Chen, D.-J. Lee, and J.-S. Chang, 2011, Perspectives on microalgal CO_2-emission mitigation systems — A review: Biotechnology Advances, v. 29, p. 189-198.

Holtz-Eakin, D., and T. M. Selden, 1995, Stoking the fires? CO_2 emissions and economic growth: Journal of Public Economics, v. 57, p. 85-101.

Hossain, M. M., and H. I. de Lasa, 2008, Chemical-looping combustion (CLC) for inherent separations—a review: Chemical Engineering Science, v. 63, p. 4433-4451.

Hu, Y., J. Yan, and H. Li, 2012, Effects of flue gas recycle on oxy-coal power generation systems: Applied Energy, v. 97, p. 255-263.

Huijgen, W. J. J., R. N. J. Comans, and G.-J. Witkamp, 2007, Cost evaluation of CO_2 sequestration by aqueous mineral carbonation: Energy Conversion and Management, v. 48, p. 1923-1935.

Ishibashi, M., H. Ota, N. Akutsu, S. Umeda, M. Tajika, J. Izumi, A. Yasutake, T. Kabata, and Y. Kageyama, 1996, Technology for removing carbon dioxide from power plant flue gas by the physical adsorption method: Energy Conversion and Management, v. 37, p. 929-933.

Jayarathna, S. A., B. Lie, and M. C. Melaaen, 2011, NEQ rate based modeling of an absorption column for post combustion CO2 capturing: Energy Procedia, v. 4, p. 1797-1804.

John M. Prausnitz, R. N. L., Edmundo Gomes de Azevedo, 1998, Molecular Thermodynamics of Fluid-Phase Equilibria, Pearson Education.

Khaled Elsaid, N. B. a. A. A.-W. I. D. P. a. C., 2012, Advances in Chemical Engineering, Dr Zeeshan Nawaz (Ed.), ISBN: 978-953-51-0392-9, InTech, Available from: http://www.intechopen.com/books/advances-in-chemical-engineering/inland-desalinationpotentials-and-challenges.

Khawaji, A. D., I. K. Kutubkhanah, and J.-M. Wie, 2008, Advances in seawater desalination technologies: Desalination, v. 221, p. 47-69.

Khuri, A. I., 2003, Ch. 6. Current modeling and design issues in response surface methodology: GLMs and models with block effects, *in* R. K. a. C. R. Rao, ed., Handbook of Statistics, v. Volume 22, Elsevier, p. 209-229.

King, C., S. Coleman, S. Cohen, and G. Gülen, 2011, The economics of an integrated CO_2 capture and sequestration system: Texas Gulf Coast case study: Energy Procedia, v. 4, p. 2588-2595.

Kohl, A. L., and R. B. Nielsen, 1997, Chapter 15 - Membrane Permeation Processes, *in* A. L. Kohl, and R. B. Nielsen, eds., Gas Purification (Fifth Edition): Houston, Gulf Professional Publishing, p. 1238-1295.

Krishna, R., and J. M. van Baten, 2010, In silico screening of zeolite membranes for CO_2 capture: Journal of Membrane Science, v. 360, p. 323-333.

Kunze, C., and H. Spliethoff, 2012, Assessment of oxy-fuel, pre- and post-combustion-based carbon capture for future IGCC plants: Applied Energy, v. 94, p. 109-116.

Le Dirach, J., S. Nisan, and C. Poletiko, 2005, Extraction of strategic materials from the concentrated brine rejected by integrated nuclear desalination systems: Desalination, v. 182, p. 449-460.

Lee, J. W., and R. Li, 2003, Integration of fossil energy systems with CO_2 sequestration through NH4HCO3 production: Energy Conversion and Management, v. 44, p. 1535-1546.

Li, H., J. Yan, J. Yan, and M. Anheden, 2009, Impurity impacts on the purification process in oxy-fuel combustion based CO_2 capture and storage system: Applied Energy, v. 86, p. 202-213.

Liu, J., S. Wang, H. F. Svendsen, M. U. Idrees, I. Kim, and C. Chen, 2012, Heat of absorption of CO_2 in aqueous ammonia, piperazine solutions and their mixtures: International Journal of Greenhouse Gas Control, v. 9, p. 148-159.

Liu, Z.-K., J. Ågren, and M. Hillert, 1996, Application of the Le Chatelier principle on gas reactions: Fluid Phase Equilibria, v. 121, p. 167-177.

Mattisson, T., A. Lyngfelt, and P. Cho, 2001, The use of iron oxide as an oxygen carrier in chemical-looping combustion of methane with inherent separation of CO_2: Fuel, v. 80, p. 1953-1962.

Meier, W. M., 1984, 'The role of organic molecules in molecular sieve synthesis': Comment: Zeolites, v. 4, p. 402.

Michael Clugston, R. F., 2000, Advanced Chemistry: Oxford University Press.

Mohamed, A. M. O., M. Maraqa, and J. Al Handhaly, 2005, Impact of land disposal of reject brine from desalination plants on soil and groundwater: Desalination, v. 182, p. 411-433.

Mohapatra, D. P., S. K. Brar, R. D. Tyagi, and R. Y. Surampalli, 2011, Parameter optimization of ferro-sonication pre-treatment process for degradation of bisphenol A and biodegradation from wastewater sludge using response surface model: Journal of Hazardous Materials, v. 189, p. 100-107.

Molina, C. T., and C. Bouallou, Assessment of different methods of CO_2 capture in post-combustion using ammonia as solvent: Journal of Cleaner Production.

Morillo, J., J. Usero, D. Rosado, H. El Bakouri, A. Riaza, and F.-J. Bernaola, 2014, Comparative study of brine management technologies for desalination plants: Desalination, v. 336, p. 32-49.

Muniz, A., and S. Skehan, 1990, Disposal of concentrate from brackish water desalting plants by use of deep injection wells: Desalination, v. 78, p. 41-47.

Nancollas, G. H. a. M. M. R., 1974, Crystal growth kinetics of minerals encountered in water treatment processes."Environmental Chemistry of Metals, *in* A. J. Rubin, Ed., and A. A. Ann Arbor Science, MI, eds., p. 219-253.

Nicot, J.-P., and A. H. Chowdhury, 2005, Disposal of brackish water concentrate into depleted oil and gas fields: a texas study: Desalination, v. 181, p. 61-74.

Pelkie, J. E., Concannon, P.J., Manley, D.B., Poling, B.E., 1992, Product distributions in the CO_2–NH_3–H_2O system from liquid conductivity measurements, Industrialand Engineering Chemistry Research.

Plaza, M. G., A. S. González, C. Pevida, J. J. Pis, and F. Rubiera, 2012, Valorisation of spent coffee grounds as CO_2 adsorbents for postcombustion capture applications: Applied Energy, v. 99, p. 272-279.

Poling, B. E., 2000, The Properties of Gases and Liquids McGraw-Hill Professional.

Qiao, Z., Z. Wang, S. Yuan, J. Wang, and S. Wang, 2015, Preparation and characterization of small molecular amine modified PVAm membranes for CO_2/H_2 separation: Journal of Membrane Science, v. 475, p. 290-302.

Qin, F., S. Wang, A. Hartono, H. F. Svendsen, and C. Chen, 2010, Kinetics of CO_2 absorption in aqueous ammonia solution: International Journal of Greenhouse Gas Control, v. 4, p. 729-738.

Rai, K., R. T. Johns, M. Delshad, L. W. Lake, and A. Goudarzi, 2013, Oil-recovery predictions for surfactant polymer flooding: Journal of Petroleum Science and Engineering, v. 112, p. 341-350.

Ramachandran, K. M., and C. P. Tsokos, 2015, Chapter 9 - Design of Experiments, *in* K. M. R. P. Tsokos, ed., Mathematical Statistics with Applications in R (Second Edition): Boston, Academic Press, p. 459-494.

Rao, A. B., E. S. Rubin, D. W. Keith, and M. Granger Morgan, 2006, Evaluation of potential cost reductions from improved amine-based CO_2 capture systems: Energy Policy, v. 34, p. 3765-3772.

Rhoades, J. D., S. M. Lesch, R. D. LeMert, and W. J. Alves, 1997, Assessing irrigation/drainage/salinity management using spatially referenced salinity measurements: Agricultural Water Management, v. 35, p. 147-165.

Roine, A., 1989, HSC - SOFTWARE VER. 3.0 FOR THERMODYNAMIC CALCULATIONS, *in* W. T. Thompson, F. Ajersch, and G. Eriksson, eds., Proceedings of the International Symposium on Computer Software in Chemical and Extractive Metallurgy: Oxford, Pergamon, p. 15-29.

Sauvet-Goichon, B., 2007, Ashkelon desalination plant — A successful challenge: Desalination, v. 203, p. 75-81.

Sayyaadi, H., A. Saffari, and A. Mahmoodian, 2010, Various approaches in optimization of multi effects distillation desalination systems using a hybrid meta-heuristic optimization tool: Desalination, v. 254, p. 138-148.

Sema, T., A. Naami, K. Fu, M. Edali, H. Liu, H. Shi, Z. Liang, R. Idem, and P. Tontiwachwuthikul, 2012, Comprehensive mass transfer and reaction kinetics studies of CO_2 absorption into aqueous solutions of blended MDEA–MEA: Chemical Engineering Journal, v. 209, p. 501-512.

Shale, C. C., Simpson, D.G., Lewis, P.S., 1971, Removal of sulfur and nitrogen oxides from stack gases by ammonia, Chemical Engineering Progress Symposium Series 67, 52–57.

Shao, L., J. Samseth, and M.-B. Hägg, 2009, Crosslinking and stabilization of nanoparticle filled PMP nanocomposite membranes for gas separations: Journal of Membrane Science, v. 326, p. 285-292.

Shu, G., M. D. Webster, and H. J. Herzog, 2009, Scenario analysis of carbon capture and sequestration generation dispatch in the western U.S. electricity system: Energy Procedia, v. 1, p. 4119-4126.

Singh, R., and W. J. Koros, 2013, Carbon molecular sieve membrane performance tuning by dual temperature secondary oxygen doping (DTSOD): Journal of Membrane Science, v. 427, p. 472-478.

Sipöcz, N., A. Hernandez-Nogales, M. A. Gonzalez-Salazar, R. Shisler, and V. Lissianski, 2013, Low Temperature CO2 Capture for Near-term Applications: Energy Procedia, v. 37, p. 1228-1238.

Song, C., Y. Kitamura, and S. Li, 2014, Optimization of a novel cryogenic CO_2 capture process by response surface methodology (RSM): Journal of the Taiwan Institute of Chemical Engineers, v. 45, p. 1666-1676.

Song, C. F., Y. Kitamura, and S. H. Li, 2012, Evaluation of Stirling cooler system for cryogenic CO_2 capture: Applied Energy, v. 98, p. 491-501.

Stewart, C., and M.-A. Hessami, 2005, A study of methods of carbon dioxide capture and sequestration—the sustainability of a photosynthetic bioreactor approach: Energy Conversion and Management, v. 46, p. 403-420.

Tarun, C. B., E. Croiset, P. L. Douglas, M. Gupta, and M. H. M. Chowdhury, 2007, Techno-economic study of CO_2 capture from natural gas based hydrogen plants: International Journal of Greenhouse Gas Control, v. 1, p. 55-61.

Valenti, G., D. Bonalumi, and E. Macchi, 2009, Energy and exergy analyses for the carbon capture with the Chilled Ammonia Process (CAP): Energy Procedia, v. 1, p. 1059-1066.

Xia, G., Q. Sun, X. Cao, J. Wang, Y. Yu, and L. Wang, 2014, Thermodynamic analysis and optimization of a solar-powered transcritical CO_2 (carbon dioxide) power cycle for reverse osmosis desalination based on the recovery of cryogenic energy of LNG (liquefied natural gas): Energy, v. 66, p. 643-653.

Yeh, A. C., and H. Bai, 1999, Comparison of ammonia and monoethanolamine solvents to reduce CO_2 greenhouse gas emissions: Science of The Total Environment, v. 228, p. 121-133.

Yeh, J. T., K. P. Resnik, K. Rygle, and H. W. Pennline, 2005, Semi-batch absorption and regeneration studies for CO_2 capture by aqueous ammonia: Fuel Processing Technology, v. 86, p. 1533-1546.

Zapp, K.-H., K.-H. Wostbrock, M. Schäfer, K. Sato, H. Seiter, W. Zwick, R. Creutziger, and H. Leiter, Ammonium Compounds.

Zeng, Q., Y. Guo, Z. Niu, and W. Lin, 2013, The absorption rate of CO_2 by aqueous ammonia in a packed column: Fuel Processing Technology, v. 108, p. 76-81.

Zhang, M., and Y. Guo, 2013a, Process simulations of NH_3 abatement system for large-scale CO2 capture using aqueous ammonia solution: International Journal of Greenhouse Gas Control, v. 18, p. 114-127.

Zhang, M., and Y. Guo, 2013b, Rate based modeling of absorption and regeneration for CO_2 capture by aqueous ammonia solution: Applied Energy, v. 111, p. 142-152.

Zhao, B., Y. Su, W. Tao, L. Li, and Y. Peng, 2012, Post-combustion CO_2 capture by aqueous ammonia: A state-of-the-art review: International Journal of Greenhouse Gas Control, v. 9, p. 355-371.

Zhuang, Q., B. Clements, and Y. Li, 2012, From ammonium bicarbonate fertilizer production process to power plant CO_2 capture: International Journal of Greenhouse Gas Control, v. 10, p. 56-63.

Appendix A

Table A.1: Thermodynamic data for reaction (3.1.1).

Temperature (°C)	ΔH(kJ/kmol)	ΔS(kJ/kmol.°C)	ΔG(kJ/kmol)
0.0	-123.7	-332.4	-32.9
10.0	-129.4	-353.4	-29.3
20.0	-129.1	-352.4	-25.8
30.0	-128.8	-351.5	-22.3
40.0	-128.6	-350.6	-18.8
50.0	-128.3	-349.7	-15.3
60.0	-128.0	-348.9	-11.7
70.0	-127.7	-348.1	-8.3
80.0	-127.4	-347.2	-4.8
90.0	-127.1	-346.4	-1.3
100.0	-126.8	-345.6	2.1

Table A.2: Variation of the calculated equilibrium compositions with temperature for Reaction (3.1.1).

Temperature ºC	NH_4Cl kmol	$NaHCO_3$ kmol	CO_2(g) kmol	NH_3(g) kmol	NaCl kmol	H_2O kmol
10.0	1.96	1.96	0.04	0.04	0.04	0.04
14.0	1.95	1.95	0.05	0.05	0.05	0.05
18.0	1.94	1.94	0.06	0.06	0.06	0.06
22.0	1.92	1.92	0.08	0.08	0.08	0.08
26.0	1.90	1.90	0.10	0.10	0.10	0.10
30.0	1.87	1.87	0.13	0.13	0.13	0.13
34.0	1.84	1.84	0.16	0.16	0.16	0.16
38.0	1.81	1.81	0.20	0.20	0.20	0.20
42.0	1.76	1.76	0.24	0.24	0.24	0.24
46.0	1.71	1.71	0.29	0.29	0.29	0.29
50.0	1.66	1.66	0.34	0.34	0.34	0.34
54.0	1.59	1.59	0.41	0.41	0.41	0.41
58.0	1.52	1.52	0.48	0.48	0.48	0.48
62.0	1.44	1.44	0.56	0.56	0.56	0.56
66.0	1.35	1.35	0.65	0.65	0.65	0.65
70.0	1.26	1.26	0.74	0.74	0.74	0.74
74.0	1.16	1.16	0.84	0.84	0.84	0.84
78.0	1.06	1.06	0.94	0.94	0.94	0.94
82.0	0.96	0.96	1.05	1.05	1.05	1.05
86.0	0.85	0.85	1.15	1.15	1.15	1.15
90.0	0.76	0.76	1.24	1.24	1.24	1.24

Table A.3: Variation of the calculated equilibrium compositions with stoichiometric ratio of ammonia for Reaction (3.1.1).

$NH_3(g)$ kmol	$NH_3(g)$ kmol	NH_4Cl kmol	$NaHCO_3$ kmol	$CO_2(g)$ kmol	NaCl kmol	H_2O kmol
0.20	0.00	0.20	0.20	0.80	0.80	0.80
0.40	0.00	0.40	0.40	0.60	0.60	0.60
0.60	0.00	0.60	0.60	0.40	0.40	0.40
0.80	0.00	0.80	0.80	0.20	0.20	0.20
1.00	0.04	0.96	0.96	0.04	0.04	0.04
1.20	0.22	0.98	0.98	0.02	0.02	0.02
1.40	0.41	0.99	0.99	0.01	0.01	0.01
1.60	0.61	0.99	0.99	0.01	0.01	0.01
1.80	0.81	0.99	0.99	0.01	0.01	0.01
2.00	1.01	0.99	0.99	0.01	0.01	0.01
2.20	1.21	0.99	0.99	0.01	0.01	0.01
2.40	1.41	0.99	0.99	0.01	0.01	0.01
2.60	1.61	0.99	0.99	0.01	0.01	0.01
2.80	1.81	0.99	0.99	0.01	0.01	0.01
3.00	2.01	0.99	0.99	0.01	0.01	0.01
3.20	2.21	0.99	0.99	0.01	0.01	0.01
3.40	2.41	0.99	0.99	0.01	0.01	0.01
3.60	2.61	0.99	0.99	0.01	0.01	0.01
3.80	2.81	0.99	0.99	0.01	0.01	0.01
4.00	3.01	0.99	0.99	0.01	0.01	0.01
4.20	3.21	0.99	0.99	0.01	0.01	0.01

Table A.4: Variation of the calculated equilibrium compositions with pressure for Reaction (3.1.1).

Pressure bar	NH_3(g) kmol	NH_4Cl kmol	$NaHCO_3$ kmol	CO_2(g) kmol	NaCl kmol	H_2O kmol
1	1.93	1.93	0.07	0.07	0.07	0.07
1.2	1.94	1.94	0.06	0.06	0.06	0.06
1.4	1.94	1.94	0.06	0.06	0.06	0.06
1.6	1.95	1.95	0.05	0.05	0.05	0.05
1.8	1.95	1.95	0.05	0.05	0.05	0.05
2	1.95	1.95	0.05	0.05	0.05	0.05
2.2	1.96	1.96	0.04	0.04	0.04	0.04
2.4	1.96	1.96	0.04	0.04	0.04	0.04
2.6	1.96	1.96	0.04	0.04	0.04	0.04
2.8	1.96	1.96	0.04	0.04	0.04	0.04
3	1.96	1.96	0.04	0.04	0.04	0.04
3.2	1.97	1.97	0.03	0.03	0.03	0.03
3.4	1.97	1.97	0.03	0.03	0.03	0.03
3.6	1.97	1.97	0.03	0.03	0.03	0.03
3.8	1.97	1.97	0.03	0.03	0.03	0.03
4	1.97	1.97	0.03	0.03	0.03	0.03
4.2	1.97	1.97	0.03	0.03	0.03	0.03
4.4	1.97	1.97	0.03	0.03	0.03	0.03
4.6	1.97	1.97	0.03	0.03	0.03	0.03
4.8	1.97	1.97	0.03	0.03	0.03	0.03
5	1.97	1.97	0.03	0.03	0.03	0.03

Table A.5: Thermodynamic data for Reaction (3.5.1).

Temperture(°C)	ΔH (kJ/kmol. °C)	ΔS (kJ/kmol. C°)	ΔG (kJ/kmol)
0.0	-127.6	-241.6	-61.7
10.0	-129.6	-248.4	-59.2
20.0	-131.5	-255.1	-56.7
30.0	-133.4	-261.5	-54.1
40.0	-135.3	-267.8	-51.5
50.0	-137.2	-273.8	-48.8
60.0	-139.2	-279.7	-46.0
70.0	-141.1	-285.5	-43.2
80.0	-143.1	-291.1	-40.3
90.0	-145.0	-296.5	-37.3
100.0	-147.0	-301.8	-34.3

Table A.6: Thermodynamic data for Reaction (3.5.2).

Temperature (°C)	ΔH (kJ/kmol.°C)	ΔS (kJ/kmol.°C)	ΔG (kJ/kmol)
0.0	-6.3	-11.8	-3.1
10.0	-4.6	-5.5	-3.0
20.0	-2.8	0.6	-3.0
30.0	-1.1	6.5	-3.0
40.0	0.7	12.2	-3.1
50.0	2.5	17.8	-3.3
60.0	4.2	23.2	-3.5
70.0	6.0	28.6	-3.8
80.0	7.9	33.8	-4.1
90.0	9.7	38.9	-4.4
100.0	11.5	43.9	-4.8

Table A.7: Stainless Steel Reactor System (SSR) Specifications

Allowable Working Pressure	Atmospheric to 5 bar gauge
Allowable Working Temperature	10 to 90 ºC
Reactor Tube Dimensions	-Shell Dimensions : ID 77.9 mm x OD 88.9 mm x IL 700 mm -Jacket Dimensions : ID 108.2 mm x OD 114.3 mm -Annular Space Between shell & jacket : 9.65 mm
Material of Construction	SS 316

Table A.8: CO_2 gas analyzer (Model 600 NDIR) Specifications

IR analysis method	Non-Dispersive Infrared (NDIR)
NDIR components	CO_2
Detector type	Micro Flow
Range	0-3000ppm
Response time (IR)	T90 < 2 Seconds to 60 Seconds
IR sample cell	Stainless Steel with Replaceable Gold Cell Liner
Resolution	Displays Five Significant Digits
Repeatability	Better than 1.0% of Full Scale
Linearity	Better than 0.5% of Full Scale
Noise	Less than 1% of Full Scale
Zero & span drift	Less than 1% of Full Scale per 24 Hours
Sample flow rate	0.25 to 2.0 L/min

Table A.9: Ions removal in varying NH_3:NaCl molar ratio at gas flow rate of 1L/min and temperature of 20 ^oC.

NH_3:NaCl molar ratio	Na^+ removal %	Mg^{+2} removal %	K^+ removal %	Ca^{+2} removal %
1.0	3.5	88.3	3.5	59.9
1.5	5.6	85.3	11.4	75.8
2.0	13.1	87.6	16.8	91.2
2.5	17.6	88.5	28.1	87.6
3.0	**22.7**	**93.8**	**35.4**	**82.2**
3.5	19.1	94.8	32.2	89.7
with 20w/w% NH_4HCO_3				
1.0	23.6	89.0	12.6	65.6
1.5	25.7	87.4	13.6	77.1
2.0	29.7	82.2	28.4	95.4
2.5	33.9	88.5	30.1	89.7
3.0	**35.8**	**97.5**	**39.2**	**87.8**
3.5	36.5	96.4	45.2	82.9

Table A.10: pH and CO_2 capture through the reaction time in varying NH_3: NaCl molar ratio at gas flow rate of 1L/min and temperature of 20 ^oC.

	$1NH_3$:1NaCl		$1.5NH_3$:1NaCl		$2NH_3$:1NaCl		$2.5NH_3$:1NaCl		$3NH_3$:1NaCl		$3.5NH_3$:1NaCl	
Time (min)	pH	CO_2%	pH	CO_2%	pH	CO_2%	pH	CO_2%	pH	CO_2%	pH	CO_2%
0	10.36	100	10.5	100	10.67	100	10.78	100	10.93	100	10.94	100
15	10.36	96	10.49	95	10.65	96	10.76	96	10.81	95	10.83	96
30	10.35	92	10.47	91	10.63	92	10.72	91	10.76	88	10.78	89
45	10.36	83	10.43	85	10.6	86	10.68	87	10.6	82	10.64	83
60	10.37	71	10.38	75	10.53	78	10.51	81	10.48	81	10.5	82
75	10.3	68	10.36	70	10.4	71	10.43	78	10.44	79	10.48	81
90	10.28	61	10.32	66	10.36	70	10.38	76	10.4	77	10.42	78
105	10.17	55	10.22	58	10.23	66	10.3	72	10.32	73	10.37	74
120	10.07	48	10.17	50	10.2	62	10.28	71	10.23	71	10.29	72
135	10.01	44	10.12	49	10.18	60	10.23	68	10.19	67	10.21	69
150	9.94	40	10.09	43	10.13	56	10.19	63	10.16	65	10.19	68
165	9.89	38	9.98	41	10.09	51	10.17	56	10.1	63	10.17	66
180	9.87	36	9.96	39	9.97	46	10.08	53	10.03	61	10.15	64

Table A.11: CO_2 capture efficiency in varying NH_3: NaCl molar ratio at gas flow rate of 1L/min and temperature of 20 ^oC.

NH_3: NaCl molar ratio	Moles of CO_2 in	Moles of CO_2 captured	CO_2 capture efficiency %
1.0	0.804	0.513	63.7
1.5	0.804	0.531	66.0
2.0	0.804	0.577	71.8
2.5	0.804	0.613	76.3
3.0	0.804	0.617	76.8
3.5	**0.804**	**0.630**	**78.3**

Table A.12: Ions removal through the reaction time at $3NH_3$:1NaCl molar ratio, gas flow rate of 1L/min and temperature of 20 ^oC .

Time (min)	Na^+ removal %	Mg^{+2} removal %	K^+ removal %	Ca^{+2} removal %
60	6.5	83.7	28.2	50.1
120	11.9	88.0	29.5	62.9
180	**22.7**	**93.8**	**35.4**	**82.2**
240	20.8	93.4	37.4	75.5
300	21.2	97.2	32.6	80.4
with 20w/w% NH_4HCO_3				
60	12.4	87.7	35.4	62.2
120	19.3	93.4	34.6	72.9
180	**35.8**	**97.5**	**39.2**	**87.8**
240	34.9	95.5	37.1	82.5
300	36.1	96.9	38.4	88.4

Table A.13: pH and CO_2 capture % through the reaction time at $3NH_3$:1NaCl molar ratio, gas flow rate of 1L/min and temperature of 20 ^oC.

Time (min)	pH	CO_2 capture %
0	10.93	100
15	10.81	95
30	10.76	88
45	10.6	82
60	10.48	81
75	10.44	80
90	10.4	77
105	10.32	73
120	10.23	71
135	10.19	67
150	10.16	65
165	10.1	63
180	10.03	61
195	10.00	59
210	9.98	58
225	9.97	56
240	9.94	54
255	9.92	51
270	9.86	49
285	9.78	46
300	9.71	43

Table A.14: CO_2 capture efficiency through the reaction time at $3NH_3$:1NaCl molar ratio, gas flow rate of 1L/min and temperature of 20 ^oC.

Time (min)	Moles of CO_2 in	Moles of CO_2 captured	CO_2 capture efficiency %
60	**0.268**	**0.238**	**88.9**
120	0.536	0.443	82.7
180	0.804	0.618	76.9
240	1.071	0.772	72.1
300	1.339	0.902	67.4

Table A.15: Ions removal in varying temperature at $3NH_3$:1NaCl molar ratio and gas flow rate of 1L/min.

Temperature (^oC)	Na^+ removal %	Mg^{+2} removal %	K^+ removal %	Ca^{+2} removal %
10	14.8	85.0	23.5	99.9
20	**22.7**	**93.8**	**35.4**	**82.2**
30	21.4	92.6	31.4	79.5
40	18.7	86.9	22.2	72.8
50	12.5	82.4	23.1	65.1
with 20w/w% NH_4HCO_3				
10	17.8	97.1	25.8	97.5
20	**35.8**	**97.5**	**39.2**	**87.8**
30	32.9	97.1	38.1	85.1
40	29.8	95.7	39.1	89.9
50	22.8	90.1	28.5	82.4

Table A.16: pH and CO_2 capture through the reaction time in varying temperature at $3NH_3$:1NaCl molar ratio and gas flow rate of 1L/min.

	T=10^{o}C		T=20^{o}C		T=30^{o}C		T=40^{o}C		T=50^{o}C	
Time (min)	pH	CO_2%	pH	CO_2%	pH	CO_2%	pH	CO_2%	pH	CO_2%
0	10.84	100	10.93	100	10.79	100	10.87	100	10.87	100
15	10.84	96	10.81	95	10.74	96	10.76	95	10.88	96
30	10.84	91	10.76	88	10.68	91	10.64	89	10.73	87
45	10.84	88	10.6	82	10.58	83	10.53	79	10.61	76
60	10.83	85	10.48	81	10.42	73	10.41	70	10.51	64
75	10.82	81	10.44	89	10.39	71	10.35	66	10.23	52
90	10.79	79	10.4	77	10.35	68	10.27	61	10.01	48
105	10.73	76	10.32	73	10.29	65	10.18	59	9.93	44
120	10.69	72	10.23	71	10.2	62	10.01	56	9.89	41
135	10.62	70	10.19	67	10.15	60	9.98	51	9.85	32
150	10.58	67	10.16	65	10.1	58	9.93	48	9.81	26
165	10.51	66	10.1	63	10.08	57	9.89	44	9.79	22
180	10.47	68	10.03	61	9.91	56	9.87	41	9.74	17

Table A.17: CO_2 capture efficiency in varying temperature at $3NH_3$:1 NaCl molar ratio and gas flow rate of 1L/min.

Temperature (^oC)	Moles of CO_2 in	Moles of CO_2 captured	CO_2 capture efficiency %
10	**0.804**	**0.639**	**79.5**
20	0.804	0.617	76.9
30	0.804	0.577	71.8
40	0.804	0.528	65.7
50	0.804	0.433	53.9

Table A.18: Ions removal in varying gas flow rate at $3NH_3$:1NaCl molar ratio and temperature of 20^oC.

Gas flow rate (L/min)	Na^+ removal %	Mg^{+2} removal %	K^+ removal %	Ca^{+2} removal %
0.500	7.7	95.4	31.5	85.4
1.000	22.7	93.8	35.4	82.2
1.500	27.4	95.6	39.4	86.2
2.000	**32.4**	**98.8**	**52.4**	**92**
2.500	28.1	97.6	49.4	86.6
with 20w/w% NH_4HCO_3				
0.500	12.4	97.1	32.1	84.1
1.000	35.8	97.5	39.2	87.8
1.500	36.3	96.4	42.5	87.4
2.000	**37.1**	**98.0**	**63.4**	**83.1**
2.500	32.0	98.4	53.2	82.4

Table A.19: Sodium removal with reaction time in varying gas flow rate at $3NH_3$:1NaCl molar ratio and temperature of 20 ^oC.

Time (min)	Na^+ removal % at gas flow rate of 0.500 L/min	Na^+ removal % at gas flow rate of 1.000 L/min	Na^+ removal % at gas flow rate of 1.500 L/min	Na^+ removal % at gas flow rate of 2.000 L/min	Na^+ removal % at gas flow rate of 2.500 L/min
0	0	0	0	0	0
60	2.7	13.8	17.8	21.8	26.1
120	4.5	19.5	24.9	31.8	28.3
180	**7.7**	**22.7**	**27.4**	**32.4**	**28.1**

Table A.20: pH and CO_2 capture through the reaction time in varying gas flow rate at $3NH_3$:1NaC molar ratio and temperature of 20 ^oC.

	F= 0.500 L/min		F= 1.000 L/min		F= 1.500 L/min		F= 2.000 L/min		F= 2.500 L/min	
Time (min)	pH	CO_2%	pH	CO_2%	pH	CO_2%	pH	CO_2%	pH	CO_2%
0	11.05	100	10.93	100	11.01	100	10.94	100	11	100
15	10.98	98	10.81	95	10.87	93	10.81	95	10.8	89
30	10.91	97	10.76	88	10.64	86	10.6	91	10.6	76
45	10.85	97	10.6	82	10.53	79	10.52	86	10.5	69
60	10.75	96	10.48	81	10.43	76	10.45	82	10.4	55
75	10.74	94	10.44	80	10.4	71	10.38	71	10.3	50
90	10.7	91	10.4	77	10.35	69	10.31	55	10.3	46
105	10.69	89	10.32	73	10.2	66	10.18	50	10.1	39
120	10.65	88	10.23	71	10.19	62	10.1	44	10.0	32
135	10.64	87	10.19	67	10.15	60	10.07	40	9.98	29
150	10.64	86	10.16	65	10.04	56	10	36	9.92	23
165	10.63	85	10.1	63	9.95	54	9.9	30	9.86	18
180	10.61	84	10.13	61	9.91	50	9.83	26	9.8	11

Table A.21: CO_2 capture in varying gas flow rate at $3NH_3$:1NaCl molar ratio and temperature of 20°C.

Gas flow rate (L/min)	Moles of CO_2 in	Moles of CO_2 captured	CO_2 capture efficiency %
0.5	**0.402**	**0.368**	**91.7**
1	0.804	0.617	76.8
1.5	1.205	0.851	70.6
2	1.607	0.948	59.0
2.5	2.009	0.974	48.5

Table A.22: Ions removal in varying gauge pressure at $3NH_3$:1NaCl molar ratio, temperature of 20°C and gas flow rate of 1 L/min.

pressure (bar)	Na^+ removal %	Mg^{+2} removal %	K^+ removal %	Ca^{+2} removal %
0	**22.7**	**93.8**	**35.4**	**82.2**
1	21.8	95.2	34.3	83.8
2	22.7	99.8	44.3	75.7
3	17.5	93.6	17.2	53.8
4	15.4	89.5	19.4	52.4
with 20w/w% NH_4HCO_3				
0	**35.8**	**97.5**	**39.2**	**87.8**
1	33.5	96.4	40.2	82.5
2	34.8	99.7	45.4	76.2
3	21.4	92.9	23.3	69.8
4	20.5	93.4	31.5	70.3

Table A.23: pH and CO_2 capture through the reaction time in varying gauge pressure at $3NH_3$:1NaCl molar ratio, temperature of 20°C and gas flow rate of 1 L/min.

	P=0.0 bar		P=1.0 bar		P=2.0 bar		P=3.0 bar		P=4.0 bar	
Time (min)	pH	CO_2%	pH	CO_2%	pH	CO_2%	pH	CO_2%	pH	CO_2%
0	10.93	100	10.98	100	11.03	100	11.18	100	11.2	100
15		95		96		98		98		97
30		88		89		96		96		94
45		82		84		94		93		91
60	10.48	81	10.5	86	10.51	90	10.74	91	10.7	90
75		79		81		86		86		87
90		77		78		84		84		85
105		73		75		81		82		82
120	10.23	71	10.28	75	10.33	78	10.44	80	10.5	81
135		67		70		74		78		78
150		65		68		71		76		74
165		63		66		70		73		71
180	10.03	61	10.1	64	10.14	68	10.25	71	10.3	70

Table A.24: CO_2 capture efficiency in varying gauge pressure at $3NH_3$:1NaCl molar ratio, temperature of 20°C and gas flow rate of 1 L/min.

Pressure (bar)	Moles of CO_2 in	Moles of CO_2 captured	CO_2 capture efficiency %
0.0	0.804	0.617	76.8
1.0	0.804	0.634	78.8
2.0	0.804	0.674	83.8
3.0	**0.804**	**0.685**	**85.2**
4.0	0.804	0.680	84.6

Table A.25: Ions removal in varying ammonium bicarbonate to treated brine w/w% at $3NH_3$:1NaCl molar ratio, temperature of 20^{o}C and gas flow rate of 1 L/min.

NH_4HCO_3 to brine wt/wt %	Na^{+} removal %	Mg^{+2} removal %	K^{+} removal %	Ca^{+2} removal %
0	22.7	93.8	35.4	82.2
5	27.5	94.8	35.1	84.3
10	29.6	94.1	36.1	83.8
15	32.9	95.2	38.9	88.8
20	**35.8**	**97.5**	**39.2**	**87.8**
25	35.0	96.4	40.0	84.1
30	35.0	98.3	38.1	89.2

Table A.26: Response surface regression. Mg^{+2} removal % versus temperature, gas flow rate, and NH_3:NaCl molar ratio.

Analysis of Variance

Source	DF	Adj SS	Adj MS	F-Value	P-Value
Model	9	881.520	97.947	64.86	0.000
Linear	3	580.354	193.451	128.10	0.000
Temperature	1	420.986	420.986	278.77	0.000
Flow Rate	1	29.784	29.784	19.72	0.001
Molar Ratio	1	129.584	129.584	85.81	0.000
Square	3	224.229	74.743	49.49	0.000
Temperature*Temperature	1	110.875	110.875	73.42	0.000
Flow Rate*Flow Rate	1	19.613	19.613	12.99	0.005
Molar Ratio*Molar Ratio	1	71.945	71.945	47.64	0.000
2-Way Interaction	3	76.938	25.646	16.98	0.000
Temperature*Flow Rate	1	45.936	45.936	30.42	0.000
Temperature*Molar Ratio	1	1.702	1.702	1.13	0.313
Flow Rate*Molar Ratio	1	29.300	29.300	19.40	0.001
Error	10	15.101	1.510		
Lack-of-Fit	5	11.379	2.276	3.06	0.123
Pure Error	5	3.722	0.744		
Total	19	896.622			

Model Summary

S	R-sq	R-sq(adj)	R-sq(pred)
1.22888	98.32%	96.80%	89.61%

Table A.27: Response surface regression. K^{+} removal % versus temperature, gas flow rate, and NH_3:NaCl molar ratio.

Analysis of Variance

Source	DF	Adj SS	Adj MS	F-Value	P-Value
Model	9	1641.38	182.375	33.68	0.000
Linear	3	1136.94	378.979	69.99	0.000
Temperature	1	287.72	287.721	53.13	0.000
Flow Rate	1	277.94	277.944	51.33	0.000
Molar Ratio	1	571.27	571.272	105.50	0.000
Square	3	106.18	35.394	6.54	0.010
Temperature*Temperature	1	6.84	6.843	1.26	0.287
Flow Rate*Flow Rate	1	86.36	86.363	15.95	0.003
Molar Ratio*Molar Ratio	1	9.01	9.006	1.66	0.226
2-Way Interaction	3	398.26	132.752	24.52	0.000
Temperature*Flow Rate	1	75.15	75.154	13.88	0.004
Temperature*Molar Ratio	1	285.60	285.605	52.74	0.000
Flow Rate*Molar Ratio	1	37.50	37.498	6.92	0.025
Error	10	54.15	5.415		
Lack-of-Fit	5	44.96	8.992	4.89	0.053
Pure Error	5	9.19	1.839		
Total	19	1695.53			

Model Summary

S	R-sq	R-sq(adj)	R-sq(pred)
2.32704	96.81%	93.93%	79.09%

Table A.28: Response surface regression. Ca^{+2} removal % versus temperature, gas flow rate, and NH3:NaCl molar ratio.

Analysis of Variance

Source	DF	Adj SS	Adj MS	F-Value	P-Value
Model	9	1273.53	141.504	53.33	0.000
Linear	3	993.10	331.032	124.75	0.000
Temperature	1	700.67	700.672	264.05	0.000
Flow Rate	1	148.38	148.377	55.92	0.000
Molar Ratio	1	144.05	144.046	54.28	0.000
Square	3	237.53	79.176	29.84	0.000
Temperature*Temperature	1	182.15	182.150	68.64	0.000
Flow Rate*Flow Rate	1	34.00	33.999	12.81	0.005
Molar Ratio*Molar Ratio	1	1.32	1.315	0.50	0.498
2-Way Interaction	3	42.91	14.303	5.39	0.018
Temperature*Flow Rate	1	6.41	6.408	2.41	0.151
Temperature*Molar Ratio	1	0.04	0.036	0.01	0.909
Flow Rate*Molar Ratio	1	36.47	36.466	13.74	0.004
Error	10	26.54	2.654		
Lack-of-Fit	5	20.46	4.092	3.37	0.104
Pure Error	5	6.07	1.215		
Total	19	1300.07			

Model Summary

S	R-sq	R-sq(adj)	R-sq(pred)
1.62897	97.96%	96.12%	87.26%

Table A.29: Ions removal in varying liquid residence time at temperature of 19.3 °C, molar ratio of 3.3NH_3:1NaCl and gas flow rate of 1.544 L/min.

Residence time (hr)	Time (hr)	Na^+ removal %	Mg^{+2} removal %	K^+ removal %	Ca^{+2} removal %
1	1	10.4	82	21.5	48.9
	2	12.7	84.7	22	53.9
	3	15.4	85.1	26.9	53.8
	4	16.9	88.6	25.5	64.8
	5	20.7	87.9	31.2	75
	6	21.4	93.5	39.4	76
2	1	13.6	86.7	26	53.8
	2	13.7	85.4	31	55.7
	3	17.8	88.9	30.5	64.1
	4	20	89	36.7	69.7
	5	23.7	91.3	42.8	76.3
	6	25	94.6	48.7	83.8
3	1	15.8	84.9	27.7	52.8
	2	14.8	86.4	31.4	64.9
	3	19.7	88	36	68.6
	4	21.7	90.8	40.7	73.3
	5	24.9	92.1	48.3	80.1
	6	29.7	94.8	53.1	86.4
4	1	14.4	85	29.6	61.3
	2	16.7	89.1	34.9	72.7
	3	20.6	91.4	39	70.8
	4	26.8	94.1	43.8	77.6
	5	30.9	97.2	50.1	81.5
	6	**31.4**	**96.8**	**55.8**	**85.8**

Table A.30: pH and CO_2 capture through the continuous Solvay process in varying liquid residence time at temperature of 19.3 ℃, molar ratio of 3.3NH_3:1NaCl and gas flow rate of 1.544 L/min.

Residence time (hr)	1		2		3		4	
Liquid flow rate (ml/min)	50		25		16.66		12.5	
Time (min)	CO_2	pH	CO_2	pH	CO_2	pH	CO_2	pH
0	100	11.27	100	11.31	100	11.28	100	11.29
15	100		100		100		100	
30	100		100		100		100	
45	100		100		100		100	
60	100	11.27	100	11.25	100	11.24	100	11.18
75	100		100		100		100	
90	100		100		100		99	
105	100		100		100		99	
120	100	11.25	100	11.21	100	11.18	99	11.06
135	100		100		100		99	
150	100		100		100		98	
165	100		100		99		98	
180	100	11.23	100	11.18	99	11.12	98	10.95
195	100		100		99		98	
210	100		100		99		98	
225	100		100		99		98	
240	100	11.19	99	11.17	99	11.06	98	10.87
255	100		99		99		97	
270	100		99		99		96	
285	100		99		98		96	
300	100	11.16	99	11.12	98	11.01	96	10.77
315	100		99		98		96	
330	100		99		98		95	
345	100		99		98		95	
360	99	11.14	99	11.09	98	10.94	95	10.64

Table A.31: CO_2 capture efficiency in varying liquid residence time at temperature of 19.3 °C, molar ratio of 3.3NH_3:1NaCl and gas flow rate of 1.544 L/min.

Res. Time (hrs)	Moles of CO_2 in	Moles of CO_2 captured	CO_2 capture efficiency %
1	**2.685**	**2.682**	**99.9**
2	2.685	2.672	99.5
3	2.685	2.659	99.1
4	2.685	2.623	97.7

Table A.32: pH and CO_2 capture through continuous Solvay process at liquid residence time of 4 hrs (liquid flow rate 12.5 ml/min), temperature of 19.3 °C, molar ratio of 3.3NH_3:1NaCl and gas flow rate of 1.544 L/min.

Time	CO_2	pH
0	100	11.2
30	100	
60	100	11.16
90	99	
120	99	11.07
150	98	
180	98	10.98
210	98	
240	97	10.8
270	97	
300	97	10.63
330	97	
360	97	10.62
390	97	
420	97	10.6
450	97	
480	97	10.58

Table A.33: Ions removal in continuous Solvay process at liquid residence time of 4 hrs, temperature of 19.3 °C, molar ratio of 3.3NH_3:1NaCl and gas flow rate of 1.544 L/min.

Time (hr)	Na^+ removal %	Mg^{+2} removal %	K^+ removal %	Ca^{+2} removal %
1	16.1	88.9	18.0	54.7
2	19.5	94.7	21.8	65.8
3	22.5	96.2	28.9	74.8
4	21.9	96.4	29.3	80.9
5	28.5	95.7	34.8	84.1
6	**32.1**	**97.2**	**35.8**	**86.8**
7	31.8	96.6	45.7	83.6
8	30.6	96.1	49.6	85.2

Appendix B

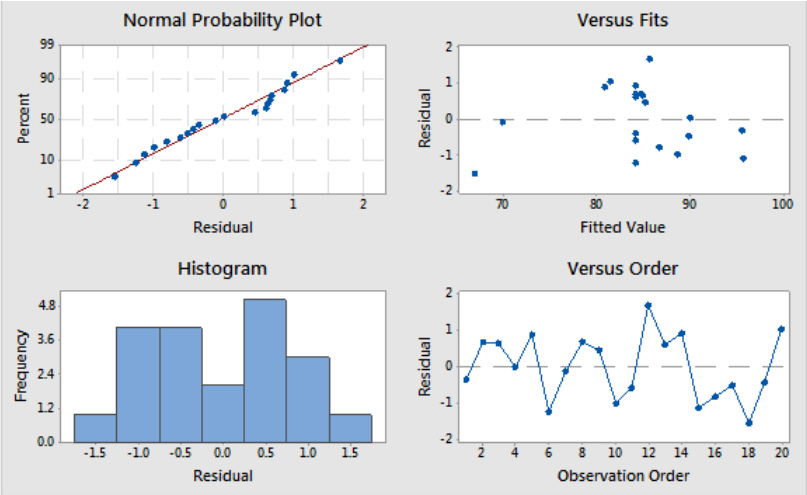

Figure B.1: Residual plots for Mg^{+2} removal %

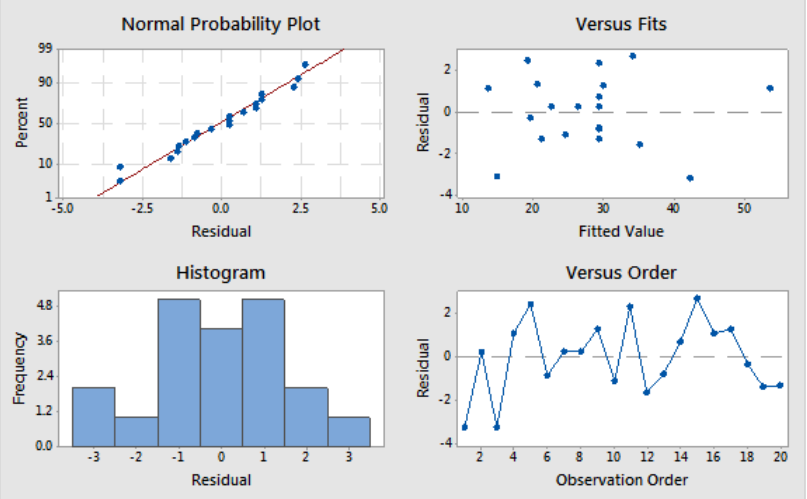

Figure B.2: Residual plots for K^{+} removal %

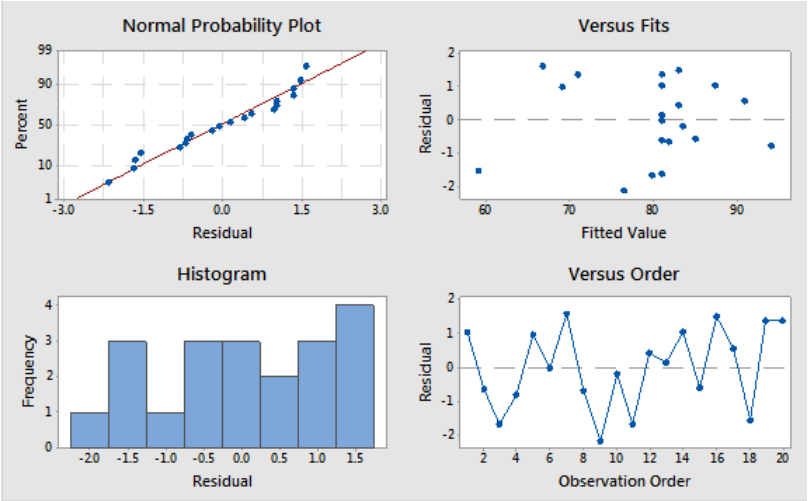

Figure B.3: Residual plots for Ca^{+2} removal %

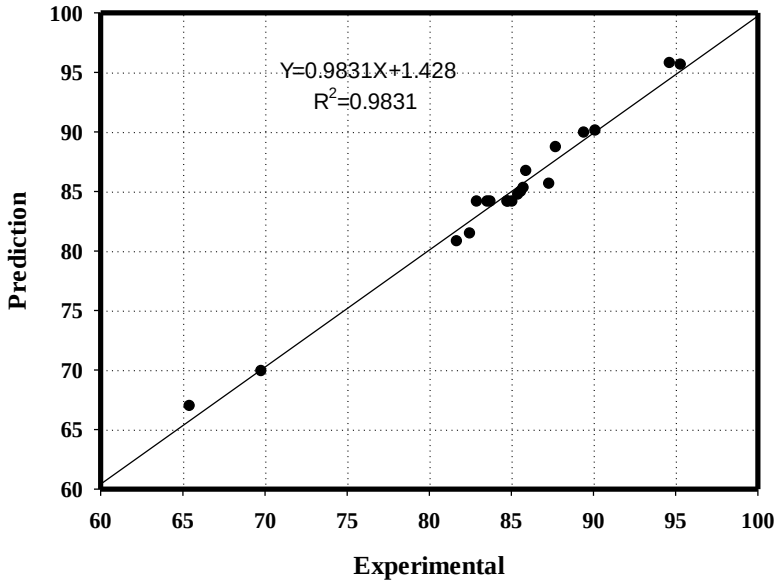

Figure B.4: Relationship between experimental and predicted values for Mg^{+2} removal.

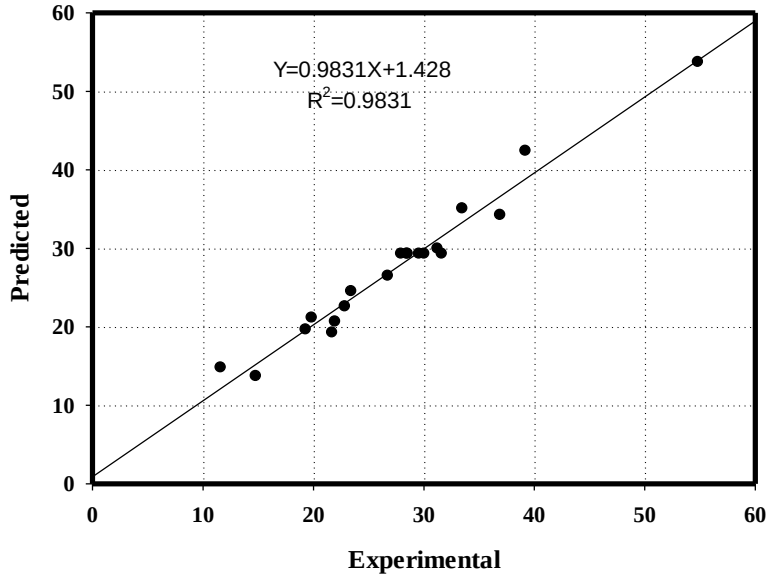

Figure B.5: Relationship between experimental and predicted values for K^+ removal.

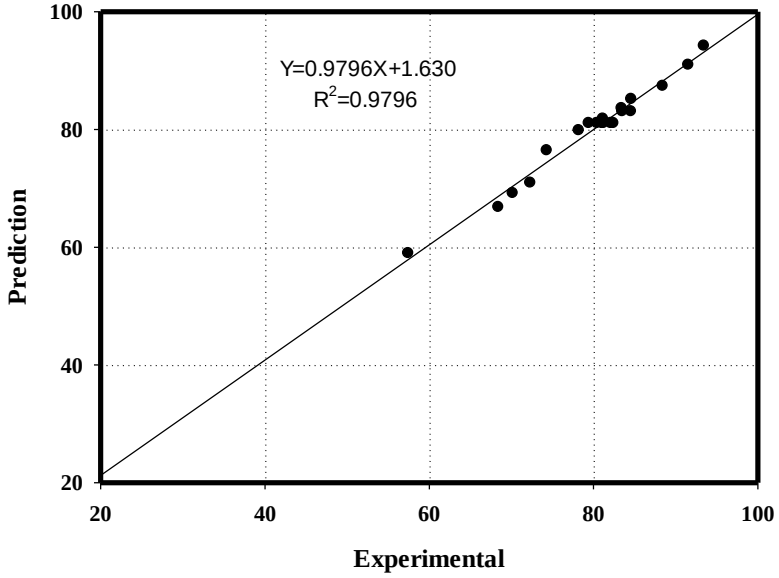

Figure B.6: Relationship between experimental and predicted values for Ca^{+2} removal.

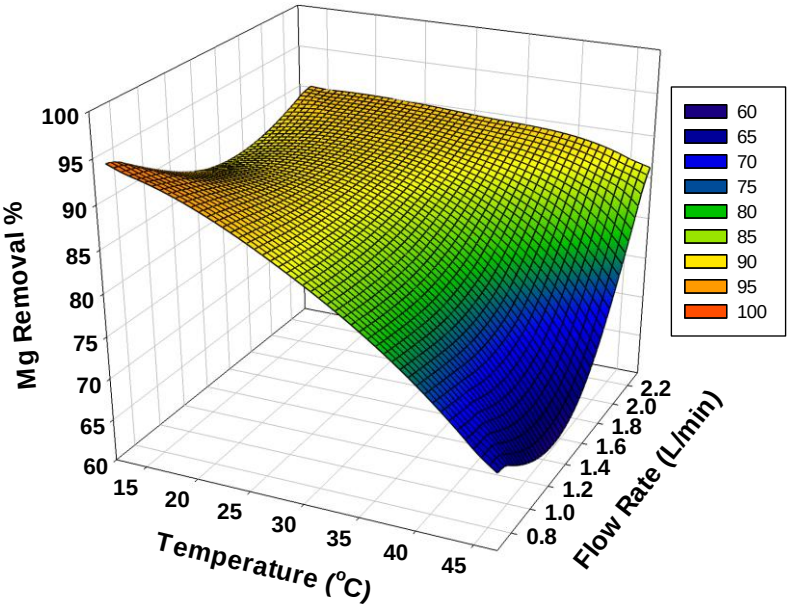

Figure B.7: Mg^{+2} removal % on 3-D graphics for response surface optimization versus temperature and gas flow rate.

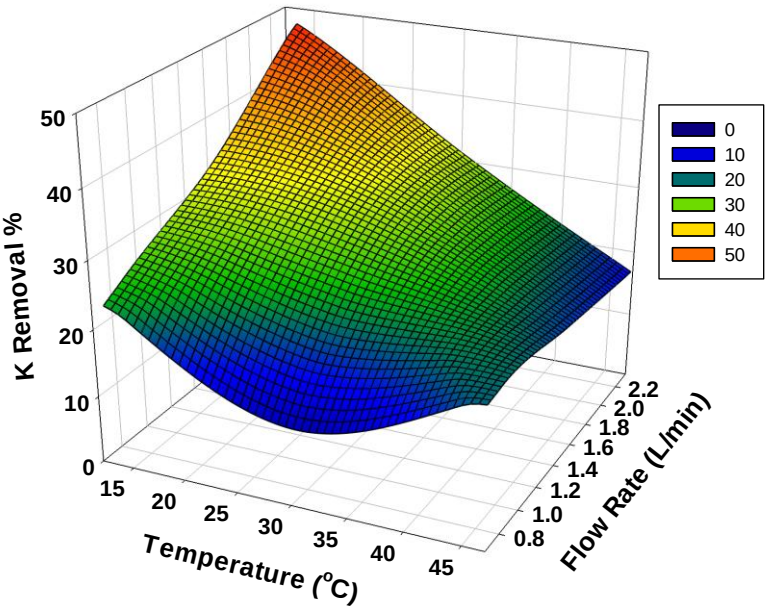

Figure B.8: K^{+} removal % on 3-D graphics for response surface optimization versus temperature and gas flow rate.

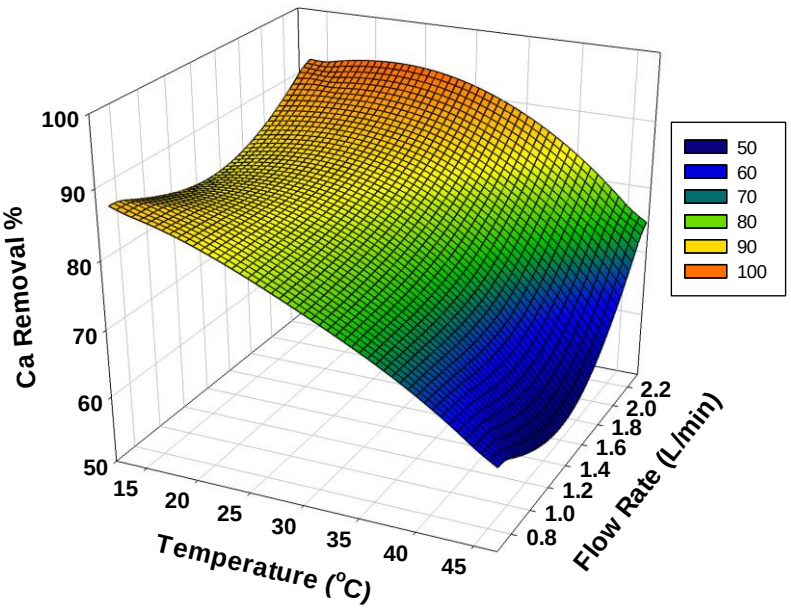

Figure B.9: Ca^{+2} removal % on 3-D graphics for response surface optimization versus temperature and gas flow rate.

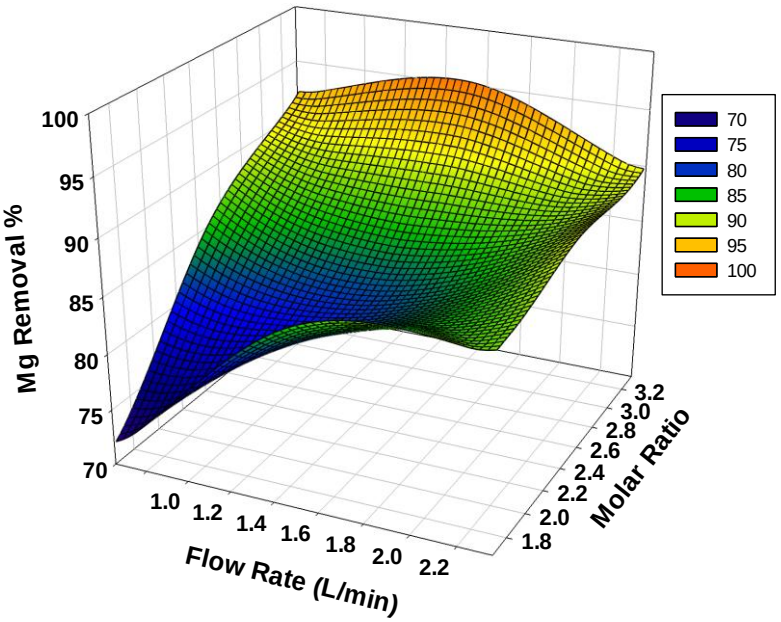

Figure B.10: Mg^{+2} removal % on 3-D graphics for response surface optimization versus gas flow rate and NH_3:NaCl molar ratio

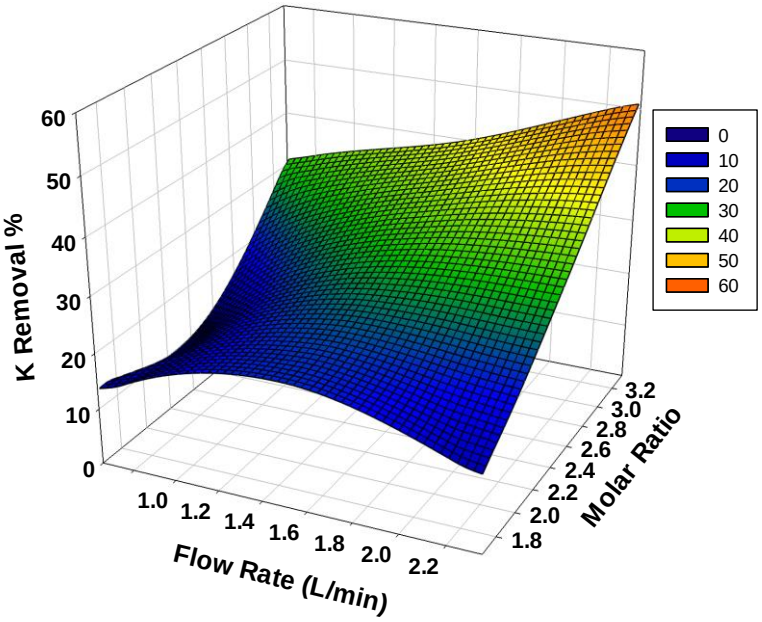

Figure B.11: K^{+} removal % on 3-D graphics for response surface optimization versus gas flow rate and NH_3:NaCl molar ratio

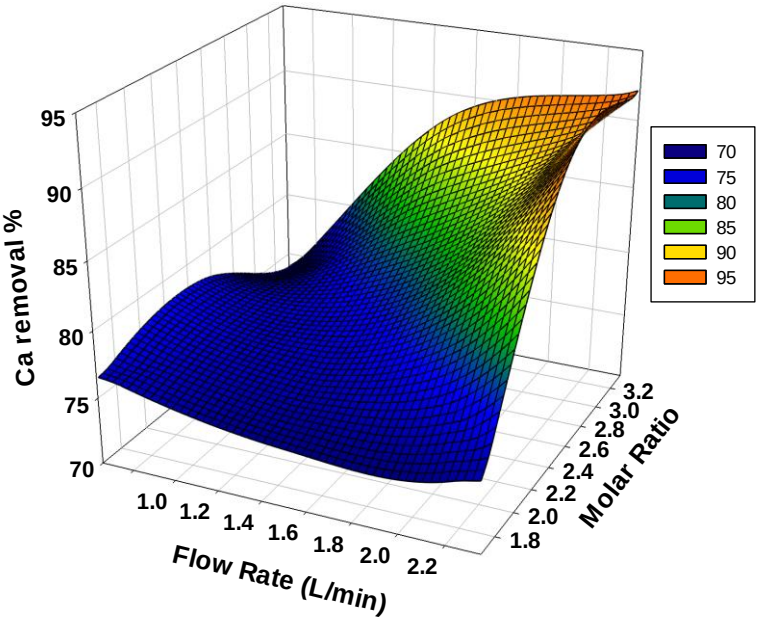

Figure B.12: Ca^{+2} removal % on 3-D graphics for response surface optimization versus gas flow rate and NH_3:NaCl molar ratio.

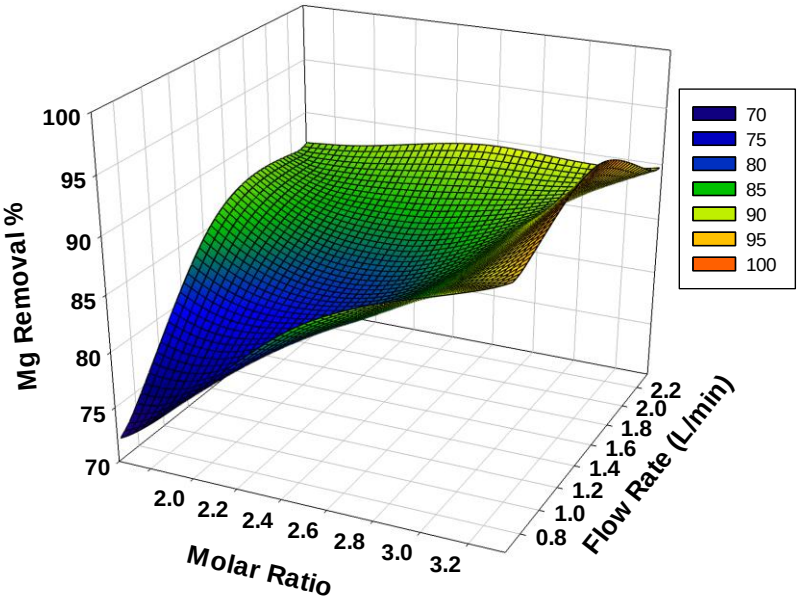

Figure B.13: Mg^{+2} removal % on 3-D graphics for response surface optimization versus NH_3:NaCl molar ratio and gas flow rate.

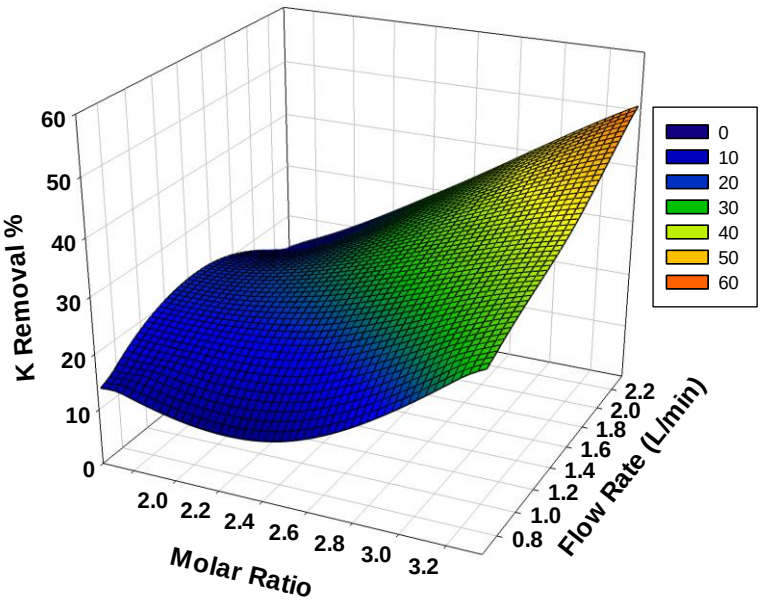

Figure B.14: K^{+} removal % on 3-D graphics for response surface optimization versus NH_3:NaCl molar ratio and gas flow rate.

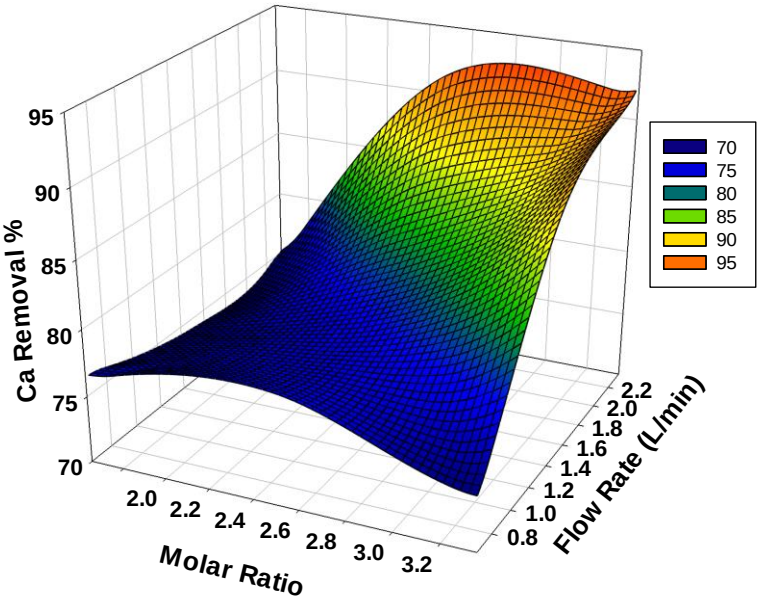

Figure B.15: Ca^{+2} removal % on 3-D graphics for response surface optimization versus NH_3:NaCl molar ratio and gas flow rate.